The matrix metalloproteinase-7 is involved in cellular senescence of human mammary epithelial cells

Von der naturwissenschaftlichen Fakultät
der Gottfried Wilhelm Leibniz Universität Hannover
zur Erlangung des Grades

Doktorin der Naturwissenschaften
Dr. rer. nat.

genehmigte Dissertation

von
Dipl.-Biochem. Catharina Bertram
geboren am 08.05.1982 in Göttingen

2009

Referent:	Prof. Dr. rer. nat. Ralf Hass
Koreferent:	Prof. Dr. rer. nat. Walter Müller
Tag der Promotion:	21.07.2009

Abstract

Besides typical characteristics of cellular senescence such as cell cycle arrest and increased SA β-gal (senescence-associated β-galactosidase) activity, the aging process of primary human mammary epithelial cells (HMEC) was accompanied by significant alterations of the extracellular environment, involving cell-cell and cell-matrix interactions. Expression of the cell surface-associated glycoproteins CD24, CD44 and CD227 (MUC1) was significantly reduced upon senescence, whereas these proteins were overexpressed in MCF-7 breast cancer cells. Analysis of different matrix metalloproteinases (MMPs) revealed a significant down-regulation of latent and active MMP-7 in senescent HMEC in contrast to the unchanged protein levels of MMP-1, MMP-2 and MMP-9. Down-modulation of MMP-7 by RNAi in young HMEC P12 implicated an accelerated aging and verified an essential role of MMP-7 for HMEC senescence, whereas no comparable effect was detectable in MCF-7 breast cancer cells.

Concomitant with an enhanced expression of the elastin precursor protein tropoelastin in senescent HMEC populations, the formation of elastin-like structures was observed. This was, moreover, paralleled by elevated lysyl oxidase-like 1 (LOXL1) levels and an increased lysyl oxidase (LO) activity. RNAi of MMP-7 identified a direct relation between reduced MMP-7 activity and an induction of tropoelastin expression, involving down-regulation of the transcription factor Fra-1. Similar effects were provoked upon impaired heparin-binding epidermal growth factor-like growth factor (HB-EGF) signaling, also causing a decline of Fra-1 levels followed by activation of tropoelastin synthesis. In addition, down-modulation of HB-EGF was associated with an elevated LOX activity as well as increased cell death and aberrant mitosis. Immunofluorescence studies revealed co-localization of MMP-7 and HB-EGF to be restricted to young HMEC, whereas their distribution differed significantly in senescent HMEC, and MMP-7 demonstrated a distinct nuclear localization.

Clearly, the extracellular proteinase MMP-7 is an important factor involved in an accelerated aging process of HMEC. It is suggested that the decreased activity of MMP-7 affects ectodomain shedding of HB-EGF in senescent HMEC and thereby inhibits intracellular signaling via Fra-1. As Fra-1 functions as a repressor of tropoelastin transcription, attenuated MMP-7 activity eventually initiates an increased tropoelastin synthesis and contributes to an enhanced extracellular formation of elastin-like structures during cellular senescence of HMEC.

Keywords: cellular senescence, HMEC, MMP-7

Zusammenfassung

Im Zuge der zellulären Seneszenz verlieren humane Mammaepithelzellen (HMEC) ihre Fähigkeit sich zu teilen, arretieren im Zellzyklus und zeigen eine erhöhte SA β-gal (senescence-associated β-galactosidase) Aktivität. Darüber hinaus war der Alterungsprozess der HMEC mit deutlichen Veränderungen ihrer extrazellulären Umgebung verbunden, die wiederum Einfluss auf Zell-Zell- sowie Zell-Matrix-Wechselwirkungen nimmt. So sank die Expression der Zelloberflächen-Glykoproteine CD24, CD44 und CD277 (MUC1) in seneszenten HMEC, während die Brustkrebszelllinie MCF-7 eine Überexpression dieser Proteine zeigte. Bei der Untersuchung verschiedener Matrixmetalloproteinasen während der HMEC-Alterung fiel eine drastische Reduktion von MMP-7 gegenüber einer gleichbleibenden Expression von MMP-1, MMP-2 und MMP-9 auf. Die Herunterregulation von MMP-7 in jungen HMEC P12 mittels siRNA induzierte eine stark beschleunigte Alterung, wohingegen keine vergleichbaren Effekte infolge MMP-7 RNAi in den immortalisierten MCF-7 festgestellt werden konnten. Dies ließ eine essentielle Rolle von MMP-7 während der zellulären Seneszenz primärer HMEC vermuten.

Des Weiteren wurde eine erhöhte Expression des Elastin-Vorläuferproteins Tropoelastin in gealterten HMEC nachgewiesen, die wiederum mit vermehrtem LOXL1 (lysyl oxidase-like-1) und einer gesteigerten Lysyloxidase-Aktivität sowie der extrazellulären Bildung Elastin-ähnlicher Fasern einherging. Ein weiterer siRNA-Ansatz bestätigte einen direkten Zusammenhang zwischen der verminderten MMP-7-Aktivität und einer Induktion der Tropoelastin-Synthese, wobei unter anderem der Transkriptionsfaktor Fra-1 involviert war. Eine vergleichbare Tropoelastin-Aktivierung, unter Einbezug reduzierter Fra-1-Level, wurde auch infolge einer siRNA-vermittelten Herunterregulation von HB-EGF (heparin-binding epidermal growth factor-like growth factor) in jungen HMEC bewirkt. Darüber hinaus wurde eine erhöhte LOX-Aktivität induziert und die verminderte HB-EGF-Expression war mit vermehrtem Zelltod bzw. unnatürlichen Mitosen ohne Zellteilung verbunden. Mittels Immunfluoreszenzanalysen wurde eine Co-Lokalisation von MMP-7 und HB-EGF in jungen HMEC festgestellt. In seneszenten HMEC unterschied sich die Verteilung der MMP-7 jedoch deutlich von der des HB-EGF und eine vorwiegend nukleäre MMP-7-Lokalisation fiel auf.

Diese Arbeit kennzeichnet MMP-7 als einen essentiellen Faktor im Rahmen der zellulären Seneszenz von HMEC und zeigt einen beschleunigten Alterungsprozess aufgrund verminderter MMP-7-Expression. Zudem vermag eine reduzierte MMP-7-Aktivität die extrazelluläre Spaltung von HB-EGF beeinflussen, was sich hingegen negativ auf die Aktivierung von Fra-1 auswirkt. Da Fra-1 als Repressor der Tropoelastin-Transkription fungiert, würde eine beeinträchtigte MMP-7-Aktivität die Induktion der Tropoelastin-Synthese bewirken und so zu einer verstärkten Bildung Elastin-ähnlicher Fasern durch die senezenten HMEC Populationen beitragen.

Schlüsselwörter: HMEC, MMP-7, zelluläre Seneszenz

The present study was carried out at the Biochemistry and Tumor Biology research unit of the Clinic of Obstetrics and Gynecology at the Medical School Hannover.

Parts of this study have already been published:

Bertram, C., Hass, R. (2008) MMP-7 is involved in the aging of primary human mammary epithelial cells (HMEC). Exp Gerontol 43, 209-217.

Bertram, C., Hass, R. (2008) Matrix metalloproteinase-7 and the 20S proteasome contribute to cellular senescence. Sci Signal 1, pt1.

Bertram, C., Hass, R. Cellular senescence of human mammary epithelial cells (HMEC) is associated with an altered MMP-7/HB-EGF signaling and increased formation of elastin-like structures.
Submitted

Table of contents

1 Introduction

1.1 Cell cycle regulation

Eukaryotic cellular proliferation, differentiation and development are controlled by the cell cycle. This complex mechanism can be divided into distinct phases: the M phase when cell division takes place and the interphase between two cell divisions, which is again subdivided in three precisely coordinated and regulated sections: G_1, S, and G_2 phase (Figure 1). Progression of cells through the cell division cycle is controlled by an extensive interplay of numerous molecules, including cyclin-dependent kinases (CDKs) as key regulatory enzymes (Pines, 1994). The balance between CDK activation and inactivation controls whether cells proceed through G_1 into S phase (G_1/S checkpoint), and thus, initiate DNA synthesis, and from G_2 to M phase (G_2/M checkpoint), allowing mitosis (Leake, 1996). Catalytic activation of CDKs requires specific dephosphorylation and binding to their regulatory subunit, the appropriate cyclin (Figure 1) (Morgan, 1995). Whereas CDKs are consistently expressed throughout the different cell cycle phases, cyclin levels are triggered by a precise coordination of synthesis and ubiquitin-dependent proteasomal degradation (Pines, 1994; Pagano, 1997). Expression of cyclins is tightly regulated and susceptible to a variety of environmental signals and numerous intracellular proteins that monitor the progress of events such as DNA replication or mitotic spindle-formation. Eventually, the cell decides about cyclin gene transcription in response to these signals (Arellano and Moreno, 1997). Binding of the specific cyclin to the appropriate CDK induces conformational changes and accessibility of the active center (Jeffrey et al., 1995). However, CDK activation additionally requires the phosphorylation of a distinct threonine residue in the active site T-loop by CDK-activating kinase (CAK, complex of CDK 7 with cyclin H) (Lolli et al., 2004) and the dephosphorylation of a tyrosine and threonine residue in the N-terminal region, which is mediated by Cdc25 (cell division cycle 25) dual-specificity phosphatases (Morgan, 1995; Nilsson and Hoffmann, 2000).

Cdc25A is required for progression from G_1 to S phase and activates CDK2 in complex with cyclin E and cyclin A (Figure 1) (Saha et al., 1997). Cdc25B is primarily activated during S phase and is responsible for CDK1/cyclin B dephosphorylation (Nilsson and Hoffmann, 2000). Recent studies identified Cdc25A and Cdc25C as additional regulators of CDK1 during G_2 phase, and thus, confirmed a crucial role for these phosphatases in G_2/M transition (Timofeev et al., 2009). Upon DNA damage a specific phosphorylation of Cdc25C on serine^{216} is mediated by CHK1 and CHK2 (checkpoint kinase 1 and 2), whereby a binding site for the negative cell cycle regulator 14-3-3-σ is disclosed (Sanchez et al., 1997; Matsuoka et al., 1998; Yang et al., 2003). Association of 14-3-3-σ with Cdc25C thus inhibits its dephosphorylation activity and impedes M phase entry (Sanchez et al., 1997). Moreover, hyperphosphorylation of Cdc25A and Cdc25C provokes ubiquitinylation and subsequent proteolysis of the Cdc25 phosphatases (Taylor and Stark, 2001; Timofeev et al., 2009).

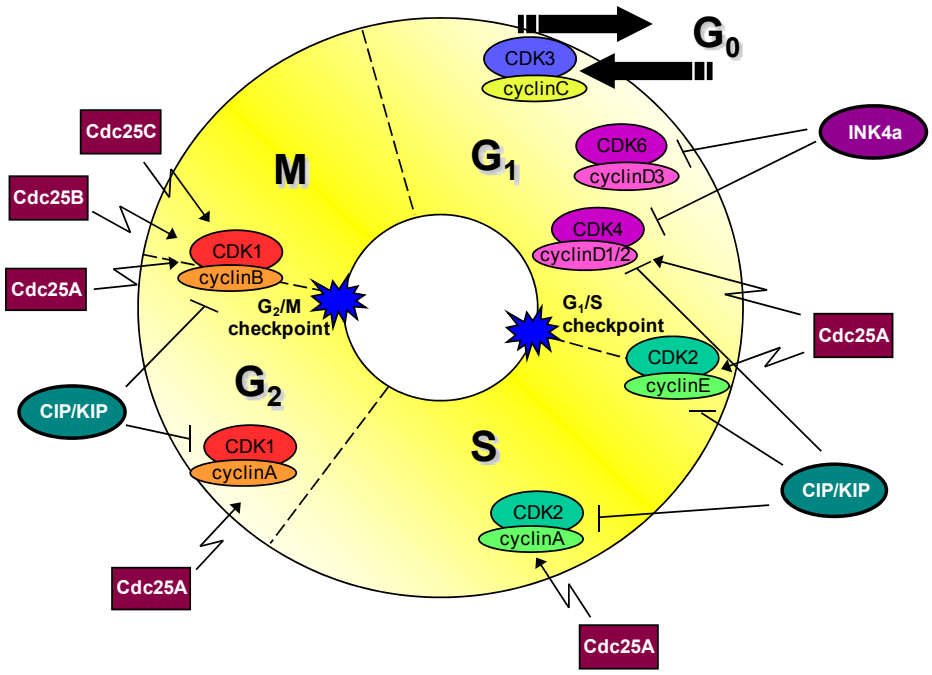

Figure 1: A schematic overview of essential steps in cell cycle regulation

Control of normal cell proliferation involves a multifaceted interplay of an enormous regulation-machinery. After mitosis (M phase), the cells can leave the cell cycle in G_0 phase for terminal differentiation or a transient cell cycle arrest and later re-entry in G_1, which is then controlled by CDK3/cyclin C (Ren and Rollins, 2004). Triggered for further cell divisions, the cells enter G_1 phase, grow and synthesize proteins essential for subsequent DNA-replication. Crucial effectors required for cell cycle progression are cyclin-dependent kinases (CDKs) in complex with their regulatory subunit, the cyclins. The group of D cyclins is predominantly expressed during G_1 phase and decides about the early cell cycle regulation. At the G_1/S checkpoint, cellular signaling determines, whether the cell complies with all requirements for later DNA synthesis (during S phase). Formation of the CDK2/cyclin E complex and activity of the phosphatase CdC25A allow transition into S phase and cyclin A is expressed to bind CDK2. Before mitosis, another restriction point (G_2/M checkpoint) controls that all preparations for a successful cell division are completed and binding of cyclin B to CDK1 with a simultaneous activation of the appropriate CdC25 phosphatase eventually facilitates mitosis. In addition, environmental alterations as well as endogenous stimuli can interfere with the cell cycle regulation, mediated by CDK-inhibitors (CIP/KIP family and INK4a family). Enhanced expression of a CDK-inhibitor and binding to the cyclin-CDK-complex abolishes further cell cycle progression. Underlying references are marked in the text. (Cdc25: cell division cycle 25, CDK: cyclin-dependent kinase, CIP: CDK-interacting protein, KIP: kinase inhibitor protein, INK4a: polypeptide inhibitors of CDK4 and CDK6)

CDK-activation is complemented by specific CDK-inhibitor proteins that underlie stimulation by both, factors sensing intrinsic defects (e.g. damaged DNA or insufficient replication) and those activated by extrinsic alterations (Figure 2). Binding of distinctive inhibitory proteins to cyclin-CDK-complexes prevents CDK-activation and triggers a cell cycle arrest. CDK-inhibitors can be distinguished into two families: proteins of the CIP/KIP family (including $p21^{Cip1,Sdi1,Waf1}$, p27, p57), which inhibit CDK2, CDK4 and CDK6 (He et al., 2005), and INK4a/ARF family members (including p16, P19), which abrogate the activity of CDK4 and CDK6 (Figure 1) (Villacanas et al., 2002).

These mechanisms and their complex regulation eventually determine cell proliferation and cell cycle progression; cell differentiation and an irreversible withdrawal from the cell cycle; quiescence and a transient cell cycle arrest; senescence and a permanent cell cycle arrest; or an elimination of the cell by apoptosis.

1.2 Cellular senescence

Somatic cells have a limited proliferative capacity and eventually enter a permanent growth arrest state, termed cellular senescence (Hayflick, 1965). However, senescent cells remain in a stable, viable and metabolically active form, but acquire a characteristic morphology of enlarged, flat, vacuolar cells (Goldstein, 1990). This phenomenon was first described in cultured human fibroblasts by Hayflick and colleagues (Hayflick and Moorhead, 1961; Hayflick, 1965). Further research has observed cellular senescence in numerous other cell types, such as epithelial or endothelial cells, derived from many species (Vojta and Barrett, 1995; Romanov et al., 2001; Hughes and Reynolds, 2005; Tsirpanlis, 2008).

Senescence can be induced by a variety of stimuli such as telomere attrition and DNA damage, chromatin perturbations, oxidative stress, oncogene overexpression or persistent signaling by anti-proliferative cytokines (Ferbeyre et al., 2002; Narita et al., 2003; Vijayachandra et al., 2003; d'Adda di Fagagna, 2008). On the other hand, senescent cells themselves produce high levels of reactive oxygen species (ROS), which in turn affect neighboring cells in the microenvironment (Song et al., 2005; Bertram and Hass, 2008b). Cellular senescence involves fundamental alterations in the regulation of gene expression and is accompanied by an interplay of multiple variations in cell signaling mechanisms (Cristofalo et al., 1998; Zhang et al., 2003; Campisi and d'Adda di Fagagna, 2007; Bertram and Hass, 2008b), whereof the most essential pathways and effectors are subsequently described in more detail.

1.2.1 Telomere-dependent senescence

Human telomeres comprise tandem repeats of a hexanucleotide sequence $(5'\text{-}TTAGGG\text{-}3')_n$ of approximately 10-15 kilo basepairs (kbp) in length (telomere restriction fragment) that cap and stabilize the ends of linear chromosomes to protect the genomic DNA from degradation and recombination (Blackburn, 1991; Aviv et al., 2003). Telomeres are synthesized and maintained by telomerase, a heterodimeric enzyme with an RNA template subunit (hTERC) and a catalytic protein component (hTERT) (Blackburn et al., 1989). A variety of telomere-interacting proteins have been identified and mammalian telomeres are thought to end in a large circular structure, termed the t-loop (Griffith et al., 1999).

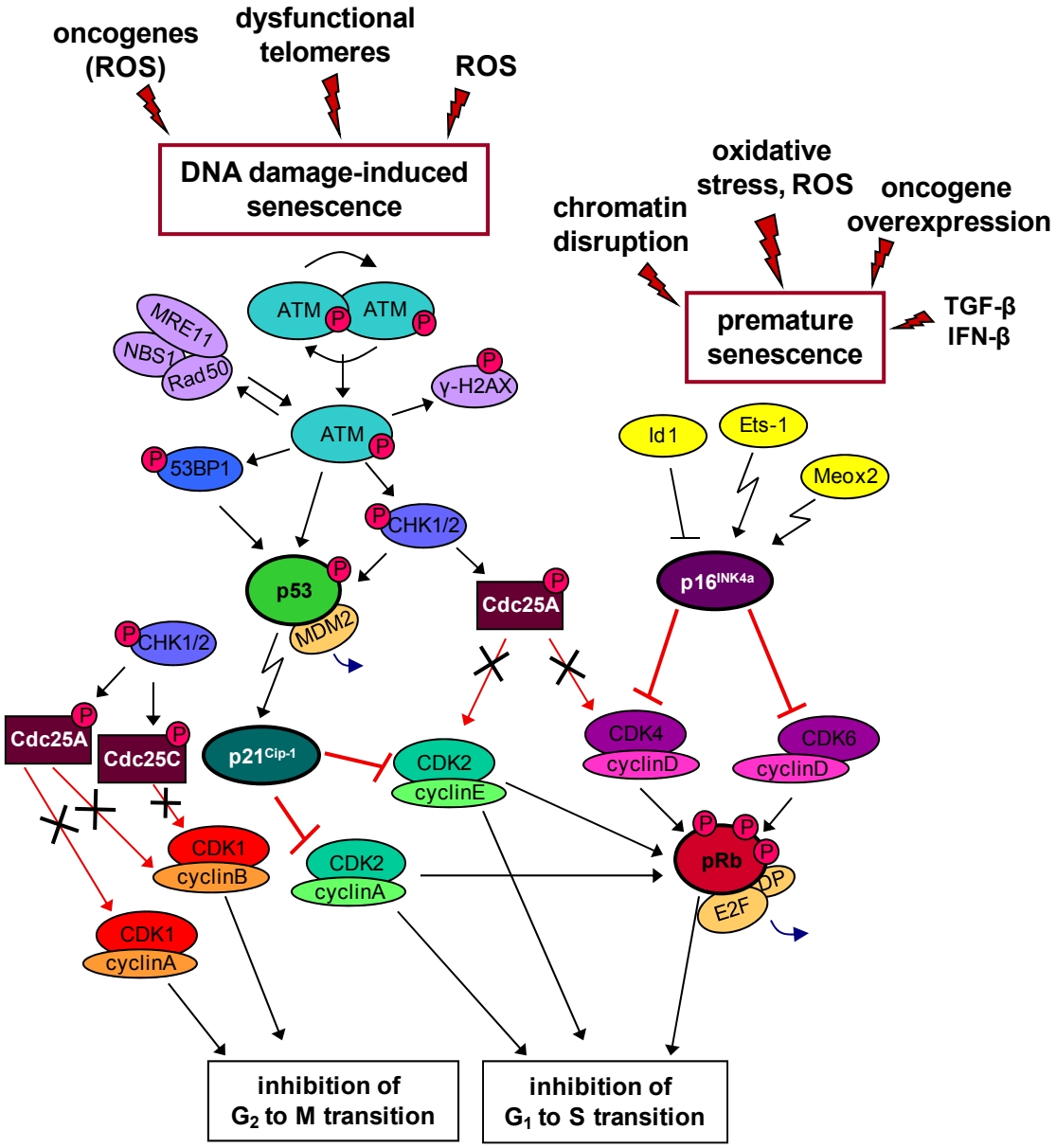

Figure 2: Molecular mechanisms involved in the induction of cellular senescence.

With increasing life span, continuous telomere erosion and finally short telomeres, resembling double stranded DNA breaks, induced p53-mediated DNA-damage response with subsequent activation of the CDK-inhibitor $p21^{Cip-1}$. Stress-associated signals, however, utilize activation of the CDK-inhibitor $p16^{INK4a}$, which in turn causes maintenance of hypophosphorylated pRb. Eventually, both the p53/$p21^{Cip1}$-pathway as well as $p^{16INK4a}$-mediated signaling function as transcriptional regulators and result in cell cycle arrest. Underlying references are marked in the text. (53BP1: p53 binding protein 1, ATM: Ataxia telangiectasia mutated, Cdc25: cell division cycle 25, CDK: cyclin-dependent kinase, CHK1/2: checkpoint kinase 1 and 2, DP: dimerization partner, Ets-1: erythroblastosis twenty six oncogene homolog 1, Id1: inhibitor of DNA binding 1, INF-β: interferon-β, MDM2: mouse double minute 2 homolog, MRE11: meiotic recombination 11, NBS1: Nijmegen breakage syndrome 1, P: phosphorylation, pRb: retinoblastoma protein, ROS: reactive oxygen species, TGF-β: transforming growth factor-β)

According to the end-replication problem, DNA polymerase is incapable of replicating the very ends of DNA. Thus, the telomeres progressively shorten and 50-200 bp are lost with each round of replication (Harley et al., 1990). Due to the lack of telomerase activity in normal somatic cells, continuous telomere erosion generates critically short telomeres, which lack the t-loop structure and resemble DNA after double-strand DNA breaks (DSB). Consequently, dysfunctional telomeres stimulate the DNA damage response machinery, which eventually signals the cell to cease proliferation (d'Adda di Fagagna et al., 2003; Shay and Wright, 2007).

The detection of DNA damage foci at sites of the telomeric ends characterizes an accumulation of proteins which are typically involved in the classical DNA damage response (e.g. RAD50, MRE11, γ-H2AX, ATM, 53BP1, CHK2) (Takai et al., 2003; Herbig et al., 2004) (Figure 2). DSB implicate an autophosphorylation of the Ser/Thr kinase ATM, and dissociation from homodimeric ATM-complexes relay phosphorylation signals downstream to CHK2, 53BP1 and p53 (Figure 2) (Bakkenist and Kastan, 2003). Activated CHK2 is capable of hyper-phosphorylating Cdc25A, thereby promoting its ubiquitylation and subsequent degradation, resulting in inefficient activation of CDKs and cell cycle arrest (cp. 1.1) (Busino et al., 2004). Likewise, Cdc25C, which is required for the activation of CDK1/cyclin B to enter mitosis, is inactivated by CHK1 and CHK2 kinase activity (Sanchez et al., 1997; Chaturvedi et al., 1999). Phosphorylation of the tumor suppressor protein p53 is followed by the release of its repressor MDM2 and subsequent p53 activation (Datta and Nicot, 2008). p53 subsequently activates the expression of several genes, including the one encoding for the CDK-inhibitor $p21^{Cip1}$ (Jackson and Pereira-Smith, 2006). $p21^{Cip1}$ impedes binding of CDK2 and CDK4 with their regulatory subunits cyclin E and cyclin A, respectively, and thus, inhibits CDK activity (Figure 2). However, this kinase activity is necessary for the activation of proteins required for the G_1/S transition, and consequently, the p53-mediated DNA damage response via $p21^{Cip1}$ induces a G_1 arrest in the cells (Harper et al., 1993).

Besides a direct activation of transcription factors, CDK2 and CDK4 regulate phosphorylation of the retinoblastoma protein (pRb). Governed by its phosphorylation state, pRb binds to and interacts with a variety of proteins and thereby modulates the activity of many transcription factors (Tamrakar et al., 2000). Thus, phosphorylation of pRb entails its inactivation and subsequent release of the transcription factor complex E2F/DP (Figure 2) (Connell-Crowley et al., 1997). Accordingly, free E2F/DP complexes ensure activation of genes necessary for DNA synthesis and cell cycle progression (Maiti et al., 2005). In contrast, hypophosphorylated, active pRb forms a tight complex with E2F/DP and thereby inhibits the G_1 to S phase transition (Figure 2) (Cooper et al., 1999).

The signaling mechanisms that determine whether $p21^{Cip1}$ provokes a transient growth arrest during the classical DNA damage response or a permanent withdrawal from the cell cycle associated with cellular senescence are still unknown.

1.2.2 The $p16^{INK4a}$-mediated senescence

A permanent cell cycle arrest and the induction of senescence can also be stimulated by the CDK-inhibitor $p16^{INK4a}$. Presence of $p16^{INK4a}$ inhibits the formation of complexes between D-type cyclins and CDK4 or CDK6, respectively, and likewise maintains the hypophosphorylated form of pRb, inhibiting the S phase entry (Figure 2) (Hara et al., 1996). However, the stimuli and the intracellular system that cause $p16^{INK4a}$ induction are poorly understood. Unlike $p21^{Cip1}$, $p16^{INK4a}$ activation is not directly related to DNA damage-induced senescence by telomere shortening (Herbig et al., 2004). Typically, the $p16^{INK4a}$-pathway is initiated by delayed kinetics when compared to p53-mediated DNA damage response, and thus, serves as a secondary mechanism to prevent cellular growth upon telomeric dysfunction (Jacobs and de Lange, 2005). Conversely, in the context of a premature stress-induced senescence there are stimuli such as oxidative stress and oncogene expression that primarily act through $p16^{INK4a}$ induction (Palmero and Serrano, 2001; Serrano and Blasco, 2001; Jacobs and de Lange, 2004). A potential molecular mechanism of $p16^{INKa4}$ activation is controlled by Id1, a transcriptional repressor of $p16^{INK4a}$. In senescent cells, Id1 expression is down-regulated and thus expression of the $p16^{INK4a}$ cell cycle inhibitor is enhanced (Alani et al., 2001). In contrast, it could be demonstrated that the transcription factor Ets-1 accumulates in senescent cells and functions as an activator of $p16^{INK4a}$ (Ohtani et al., 2001). Recently, binding experiments revealed the homeodomain protein Meox2 as an additional transcriptional activator of $p16^{INK4a}$ in association with the induction of premature senescence (Irelan et al., 2009). However, the detailed signaling pathways that contribute to the senescence-associated activation of $p16^{INK4a}$ still remain vague. Moreover, susceptibility to the CDK-inhibitor $p16^{INK4a}$ is largely cell type-dependent, and e.g. human mammary epithelial cells (HMEC) are more prone to the induction of a cell cycle arrest by $p16^{INK4a}$ than human fibroblasts (Stein et al., 1999; Romanov et al., 2001).

1.2.3 Cellular senescence in human mammary epithelial cells (HMEC)

Depending on the tissue and species of origin, cells underlying cellular senescence may differ in both their typical senescent phenotype and the importance of certain signaling pathways for the senescence response. Distinctive aspects characteristic for the process of cellular senescence in human mammary epithelial cells (HMEC) will be explained. Several stimuli and mechanisms are known to be involved in the prevention of infinite growth and an induction of senescence in HMEC (Shelton et al., 1999; Sandhu et al., 2000; Yaswen and Stampfer, 2002; Zhang et al., 2003). One early mechanism is associated with a dramatic increase in $p16^{INK4a}$ and is mediated by the pRb tumor suppressor protein, causing first a stress-associated senescence barrier, termed stasis (stress or aberrant signaling-inducing senescence) (Figure 3) (Yaswen and Stampfer, 2002; Narita et al., 2003). Accordingly, HMEC viably arrest in the G_1 cell cycle phase and reveal a reduced telomere restriction fragment length of about 6-8 kbp (cp. 1.2.1). Moreover, activity of the enzyme senescence-associated β-galactosidase (SA β-gal) is significantly enhanced in senescent HMEC (Dimri et al., 1995; Romanov et al., 2001).

SA β-gal was originally described as an aging biomarker by Dimri and colleagues in 1995 (Dimri et al., 1995). Per definition, this enzyme activity is histochemically detectable at pH 6 and should distinguish senescent cells from quiescent or terminally differentiated cells (Dimri et al., 1995). However, its function during cellular senescence and the suitability and validity of this enzyme activity in the context of senescence is controversial. Positive SA β-gal cells could also be detected upon inadequate culture conditions, serum starvation, cell confluence, H_2O_2 treatment and genetic manipulations (Severino et al., 2000; Yang and Hu, 2005; Lee et al., 2006). Thus, SA β-gal cannot be considered as a universal marker of senescence, and at most, is utilized in combination with the verification of other senescence-associated alterations such as cell cycle distribution, expression of $p21^{Cip-1}$ or $p16^{INK4a}$.

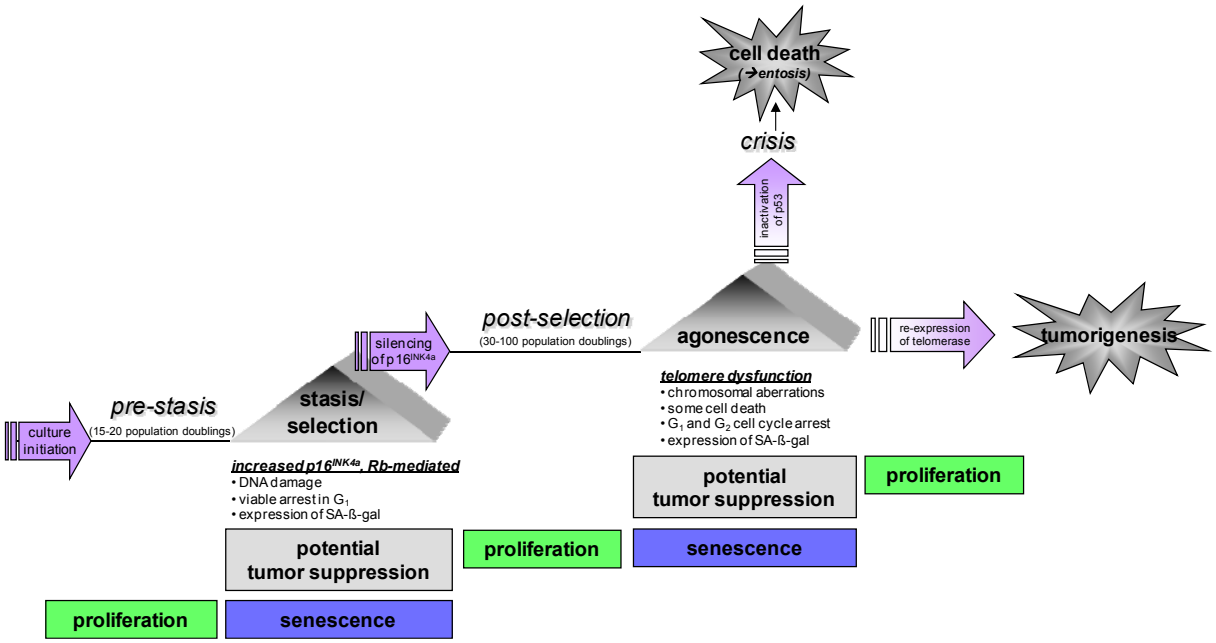

Figure 3: Cellular senescence in HMEC.

A dramatic increase in expression of the CDK-inhibitor $p16^{INK4a}$ in HMEC induces a state of stress-associated premature senescence, termed stasis. Some growth-arrested cells, however, underlie gene silencing of $p16^{INK4a}$ by post-translational hypermethylation of the p16 promoter and regain proliferative capacity. Continuous telomere erosion stimulates the DNA damage response and HMEC encounter a second growth arrest, termed agonescence. Further proliferation of agonescent HMEC due to inactivation of p53 entails a crisis-like state with extensive cell death. However, simultaneous reactivation of the enzyme telomerase in agonescent cells is associated with malignant cell transformation and potential tumor development. Underlying references are marked in the text.

Remarkably, some of these stasis-arrested HMEC are subjected to a self-selection process triggered by hypermethylation of the p16 promoter and subsequent loss of $p16^{INK4a}$ expression (Brenner et al., 1998; Huschtscha et al., 1998). Due to an improper G_1 checkpoint control, these post-selection HMEC escape from the growth plateau and resume proliferative capacity. However, the lack of telomerase activity in somatic cells causes continuous telomere erosion, eventually generating critically short telomeres and prevalent chromosomal aberrations (Harley et

al., 1990; Shay and Wright, 2007). The subsequent initiation of the DNA damage response (cp. 1.2.1) causes a withdrawal from the cell cycle and the post-selection HMEC encounter a second senescence barrier which is telomere length-dependent and termed agonescence (Figure 3) (Yaswen and Stampfer, 2002). The agonescent cells remain viable and metabolically active, but acquire characteristic morphological and functional changes of a senescent phenotype. They display a dramatic decrease in the mean telomeric length (about 4-5 kbp) and typically arrest in the G_1 and G_2 cell cycle phases, but retain long-term viability (Romanov et al., 2001; Tlsty et al., 2001). Inactivation of the tumor suppressor protein p53 and impaired cell cycle checkpoints in agonescent HMEC can partially restore cell divisions, which in combination with the telomeric dysfunctions induce massive cell death, a process termed crisis (Figure 3) (Garbe et al., 2007; Hornsby, 2007). Elimination of dying HMEC can be performed following internalization by neighboring cells, termed entosis (Overholtzer et al., 2007). In contrast, escape from these processes by reactivation of the telomerase activity in senescent post-selection HMEC can contribute to a malignant cell transformation, and thus, a potential breast cancer development (Kirkpatrick et al., 2003; Herbert et al., 2007).

1.2.4 Cellular senescence in relation to organismal aging

It has been hypothesized that cellular senescence, extensively investigated and defined using *in vitro* cell culture models, may reflect cellular aging *in vivo* and might contribute to the physiological processes of normal organismal aging (d'Adda di Fagagna, 2008; Jeyapalan and Sedivy, 2008). But the relationship between mechanisms inducing senescence and those that trigger aging of a multifaceted organism remains to be established. Whereas cellular senescence cannot be explained by a single distinct mechanism, but is rather an elaborated interaction of numerous signal transduction pathways, the complexity of organismal aging is additionally determined by intercellular processes and the interplay of the tissue system. Some of the senescence-associated alteration mentioned above could be observed to accumulate with age *in vivo*, but it has to be considered that none of these signals could be proven to be exclusively restricted to senescence *in vitro*. For example, in a variety of mammalian tissues such as skin, liver, ovary and uterus expression of the CDK-inhibitor $p16^{INK4a}$ and its transcriptional activator Ets-1 simultaneously increased with advancing age (Krishnamurthy et al., 2004; Jeyapalan et al., 2007). Normal breast epithelial cells displayed hypermethylation of the p16 promoter *in vivo* similarly to the post-selection process described for HMEC *in vitro* (Holst et al., 2003). In skin biopsies derived from aged baboons an accumulation of dermal fibroblasts was detected exhibiting cellular senescence-associated changes such as dysfunctional telomeres, enhanced ATM activation, elevated levels of proteins related to chromatin perturbations as well as increased expression of $p16^{INK4a}$ (Jeyapalan et al., 2007). An enrichment of senescent cells in the aging organism may reach a point that compromises the normal functionality of a particular tissue and may contribute to the development of age-associated diseases such as atherosclerosis, Alzheimer's or cardiovascular disease (Flanary et al., 2007; Golubnitschaja, 2007; Andreassi, 2008).

Data resulting from investigations based on *in vitro* cell culture systems might not entirely reflect the complex processes *in vivo*, but could partially provide new insights into organismal aging and might help in understanding the complex interplay of human aging and age-related disease.

1.2.5 The two faces of cellular senescence: tumor suppression and cancer-promotion

The growth inhibitory capacity of cellular senescence is accomplished by activation of the tumor suppressor proteins p53 and pRb, respectively, and subsequent induction of a permanent cell cycle arrest (cp. 1.2.1 and 1.2.2).

Besides the repression of cell cycle progression genes, senescent cells exhibit a marked up-regulation of genes encoding for secretion proteins (secretome) such as cytokines, growth factors and matrix-degrading enzymes (Millis et al., 1992; Shelton et al., 1999; Coppe et al., 2006). All these signaling molecules and enzymes confer an important function during embryonic development as well as in repair mechanisms such as wound healing in the adult organism. However, contemporary with an accumulation of senescent cells in the aging tissue, a deregulated senescence-associated secretome can significantly affect surrounding cells and may provoke severe consequences, including pathological developments and tumor growth (Krtolica et al., 2001; Parrinello et al., 2005; Liu and Hornsby, 2007). Thus, an increase in secreted growth factors may stimulate susceptible adjacent cells to proliferate, whereby inflammatory cytokines can induce local oxidative stress. Whereas the vascular endothelial growth factor (VEGF) is necessary for embryonic neovascularization, an enhanced expression of VEGF by senescent fibroblasts was also shown to promote tumor vascularization and to support higher proliferation of malignant cells in mice (Coppe et al., 2006). Activation of certain matrix metalloproteinases (MMPs) initiates extracellular remodeling and facilitates cell migration during wound healing (Kyriakides et al., 2009), but also improves the motility of tumor cells and contributes to metastatic development (Liu and Hornsby, 2007). In addition, MMP-induced alterations of the tissue environment such as extracellular matrix disruption or an increased capillary permeability implicate an enlarged release of active mitogens, cytokines and other plasma products (cp. 1.3.3.4) (Millis et al., 1992; Liu and Hornsby, 2007). The continuous exposure to a high concentration of growth promoting factors may reactivate proliferation of susceptible damaged cells and eventually favors a malignant transformation. On the other hand, matrix compounds such as laminin also directly affect activation of distinct precursor proteins and trigger intracellular signal transduction mechanisms whose deregulation supports proliferation and tumorigenicity of neighboring premalignant and malignant cells (Kang et al., 2008; Sprenger et al., 2008).

Early in life cellular senescence acts as a control system to prevent proliferation of damaged cells and represents an important tumor suppressive mechanism (Hornsby, 2007). However, altered gene expression and impaired function of senescent cells together with their continuous accumulation with increasing organismal age contribute to deleterious changes of the cell, eventually culminating in age-related disease and tumorigenic developments. These investigations

substantiate the theory of senescence as an antagonistic pleiotropic phenomenon, already hypothesized by Williams in 1957, claiming the existence of genes to be beneficial in young organisms but adopting harmful functions later in life (Williams, 1957).

1.3 The extracellular matrix (ECM)

The extracellular microenvironment is accredited with an increasing and influentially importance for physiological processes as well as pathological developments and tumorigenesis (Marastoni et al., 2008; Mbeunkui and Johann, 2009). The ECM represents an interacting network of scaffolding proteins, adhesive glycoproteins and proteoglycans that provide structural and mechanical support to cells and tissues. Moreover, as a storage system for numerous growth factors, chemokines and cytokines, the ECM holds an important function related to the activation and distribution of these signaling molecules (Taipale and Keski-Oja, 1997; Schonherr and Hausser, 2000). Thus, alterations in the composition and structure of the scaffolding matrix, disordered release of soluble signaling molecules, modified expression of proteoglycans and cell adhesion molecules or abnormal cell-matrix interactions play a crucial role for a variety of cellular signaling mechanisms, eventually deciding about proliferation, gene expression, differentiation or cell death and adhesion, migration or invasion, respectively (Pupa et al., 2002; Larsen et al., 2006; Huveneers et al., 2007; Kunz, 2007; Ghajar and Bissell, 2008).

1.3.1 The extracellular structural filament

The scaffolding fibers such as collagen and elastin provide biomechanical strength, shape and flexibility to the tissue (Ottani et al., 2001). This is supported by structural glycoproteins (e.g. fibronectin, laminin and vitronectin) and proteoglycans, which additionally provide an essential connective link between ECM and adjacent cells (Farhadian et al., 1995).

1.3.1.1 Collagen fibers and structural glycoproteins

Glycoproteins can adhere to the collagen and elastin scaffold and stabilize the extracellular network (Farhadian et al., 1995). On the other hand, these ECM proteins are able to interact with certain cell surface receptors, of which integrins constitute the most typical class, and play a crucial role in cell-matrix communication (Zhu et al., 1998). Hence, structural glycoproteins such as fibronectin or laminin ensure attachment of adjacent cells to the ECM and relate extracellular alterations to cellular signal transduction pathways and intracellular responses (Bosman and Stamenkovic, 2003). Fibronectin and other glycoproteins of this family present an essential binding factor for various secreted proteins, including collagen, tropoelastin, fibrillins and lysyl oxidases, and assist further processing and maturation on the cell surface (Fogelgren et al., 2005; Hinek et al., 2006; Kadler et al., 2008; Sabatier et al., 2009). The ability of fibronectin to bind both cell surface integrins and collagen represents an essential part of collagen fibril formation *in vivo*, however, the detailed mechanisms are still unknown (Kadler et al., 2008). More than 20

genetically distinct collagen molecules are known, but the most abundant are collagen I and II that are arranged in fibrils (also III, V, XI) (Kadler et al., 1996). Other collagens are associated with these fibrils (VI, IX, XII, XIV), form networks (IV, VIII, X) or repetitive beaded structures (VI) or represent transmembrane proteins (XIII, XVIII) (Bosman and Stamenkovic, 2003). Collagen is synthesized as precursor protein pro-collagen which undergoes extensive post-translational modifications requiring distinct chaperones and enzymes that assist folding and trimerization (Lamande and Bateman, 1999). Thus, conversion of proline residues in hydroxyproline by prolyl-4-hydroxylase is necessary for collagen packaging and the chaperone HSP47 carries an essential role for collagen folding and control of its aggregation (Smith et al., 1995; Myllyharju, 2003). Processing of pro-collagen, a key step during collagen fibril formation is mediated by two families of metalloproteinases. The N-terminus is truncated by ADAMTS (a desintegrin and metalloproteinase with thrombospondin motif) and the C-terminal pro-peptide is cleaved by members of the tolloid family of zinc metalloproteinases (e.g. bone morphogenetic protein-1 (BMP-1)) (Kessler et al., 1996; Fernandes et al., 2001). *In vitro* collagen fibril formation can occur in a self-assembly process, however, recent data verified that fibrillogenesis *in vivo* is dependent on the presence of fibronectin and fibronectin/collagen-binding integrins as well as collagen V as nucleator (Kadler et al., 2008). Maturation to strong, resistant collagen fibers, consisting of multiple fibrils, is strengthened by networking with small proteoglycans and formation of additional intra- and intermolecular cross-links by lysyl oxidases (Eyre et al., 1984; Danielson et al., 1997). Whereas the involvement of the lysyl oxidase LOX in the oxidation of mature collagen I fibrils was demonstrated (Siegel, 1974), the role of other LOX-like (LOXL) isoforms is rather tissue-specific and varies depending on the collagen type (Lucero and Kagan, 2006).

1.3.1.2 Elastic fiber formation and microfibrils

Whereas the processes, which contribute to the formation of collagen fibers, are widely clarified, little is known about the precise mechanisms of elastic fiber assembly. These fibers are the largest structure in the ECM and are comprised of two major compounds, an inner amorphous elastin core and an outer scaffold of microfibrils, endowing tissues such as lung, blood vessels, tendon and skin with the critical properties of elastic recoil and resilience (Mithieux and Weiss, 2005). Elastin is a highly stable, enzymatically resistant, hydrophobic polymer composed of cross-linked molecules of its precursor protein tropoelastin (Wagenseil and Mecham, 2007).

The tropoelastin protein demonstrates a characteristic alternating pattern of hydrophobic and hydrophilic, lysine-containing domains (Gray et al., 1973). These functional distinct elements are encoded in separate exons on the tropoelastin gene (Rosenbloom et al., 1995). However, the generated mRNAs are highly variable and about eleven protein isoforms in the range of 60-72 kDa are known that arise from multiple alternative splicing of the primary transcript (Wise and Weiss, 2009). The pattern and frequency of exon splicing is precisely regulated during development (Parks et al., 1988), but the specific conditions deciding about expression of individual isoforms are not known. Conversely, the C-terminal region is highly preserved. It

delineates cell- and ECM-interacting sites and is supposed to play a crucial role in assembly and cross-linking of the tropoelastin monomers (Broekelmann et al., 2008). The protein sequence is dominated by the hydrophobic amino acids valine, alanine, proline and glycine, generating the characteristic repetitive VGVAPG-hexapeptide (Price et al., 1993). Tropoelastin undergoes no post-translational modifications such as glycosylation, but due to the substantial amount of proline residues, the peptidyl-prolyl *cis-trans* isomerase FKBP65 confers the protein with essential restructuring (Davis et al., 1998; Patterson et al., 2005) (Figure 4). Additional folding is facilitated by interaction with the HSP70 molecular chaperone BiP in the endoplasmic reticulum (ER) (Davis et al., 1998). The tropoelastin protein follows the classical protein secretion pathway, traversing the Golgi apparatus and being packed into secretory vesicles (Davis and Mecham, 1998). Tropoelastin trafficking is supported by the elastin binding protein (EBP), which acts as recyclable chaperone and assists secretion of tropoelastin (Hinek et al., 1995). This process requires complex binding of EBP with the enzyme neuraminidase-1 (Neu-1) and protective protein/cathepsin A (PP) (Figure 4). Neu-1 activity ensures interaction of EBP with extracellular glycoproteins, which in turn induces release of tropoelastin at the cell surface (Hinek et al., 2006). Recent studies revealed Neu-1 to be essential for deposition of several other elastic fiber-associated proteins (e.g. fibrillin-2 and fibulin-5), and thus, represents a crucial factor involved in elastic fiber assembly (Starcher et al., 2008). Secreted tropoelastin is tethered to the cell surface, where it aggregates into small organized spheres and is bound by scaffolding microfibrils (Figure 4) (Kozel et al., 2006). The interaction with microfibrillar proteins is crucial for deposition and alignment of tropoelastin, which is required for the next phase of elastogenesis, the so-called coacervation (Broekelmann et al., 2005; Kozel et al., 2006). Multiple tropoelastin molecules grow into larger structures (Figure 4) dedicated by the precise patterning of mostly alternating hydrophobic and hydrophilic sequences in the protein (Toonkool et al., 2001; Wagenseil and Mecham, 2007). This characteristic organization is thought to be required for subsequent intermolecular cross-linking and eventual incorporation into growing elastic fibers (Mithieux and Weiss, 2005; Wagenseil and Mecham, 2007).

Microfibrils form the outer sheath of the mature elastic fiber and play a crucial role in elastogenesis, providing scaffold sites for depositing tropoelastin (Cleary and Gibson, 1983; Sherratt et al., 2001). Microfibrils are small structures composed of several glycoproteins, including fibrillins and MAGPs (microfibril-associated glycoproteins) (Kielty et al., 2005).

Fibrillin-1 and fibrillin-2 are the principal elements of microfibrils and represent large cysteine-rich glycoproteins (~350 kDa), whose primary structure is dominated by multiple repeated domains homologous to the Ca^{2+}-binding epidermal growth factor (cbEGF) module (Handford et al., 2000). Ca^{2+}-binding stabilizes contiguous cbEGF regions into a beaded rod-like structure, and thus, favors proper assembly of microfibrils (Downing et al., 1996; Wess et al., 1998). In addition, fibrillins possess several domains crucial for their interaction with distinct binding partners (Figure 5). Thus, heparin-binding domains contribute to proteoglycan (PG) interaction and Arg-Gly-Asp (RGD) sequences are related to cell surface integrin-binding, both imparting microfibrillar assembly (Tiedemann et al., 2001; Bax et al., 2003; Ritty et al., 2003). A TGF-β-

binding (TB) module confers fibrillins with an essential role in growth factor presentation and sequestering, and improper regulation causes severe pathological developments (e.g. Marfan syndrome) (Neptune et al., 2003). Furthermore, fibrillin-1 and fibrillin-2 bind to tropoelastin, confirming their function in elastic fiber maturation (Figure 4) (Trask et al., 2000).

Several other microfibril-associated proteins have been identified, including MAGPs (matrix-associated glycoproteins), fibulins and EMILINs (elastin-microfibril-interface located proteins) (Bressan et al., 1993; Henderson et al., 1996; Timpl et al., 2003). However, their distinct contribution to microfibrillar and elastic fiber assembly still remains vague. MAGPs are small glycoproteins of about 20 kDa that localize to the beaded structure of microfibrils (Henderson et al., 1996). MAGP-1 interacts with both fibrillin-1 as well as tropoelastin and is supposed to act as a bridge molecule in elastic fiber maturation (Figure 4 and Figure 5) (Brown-Augsburger et al., 1996; Jensen et al., 2001). MAGP-2 is a serine- and threonine-rich protein and contains RGD-sequences mediating integrin-binding (Gibson et al., 1999), and thus, may function in cellular signal transduction during microfibril assembly and elastogenesis. EMILIN-1 (~106 kDa) belongs to a family of glycoproteins which can associate with elastic fibers (Bressan et al., 1993). It binds tropoelastin as well as fibulin-5, but is also involved in cell attachment via interference with certain integrins and may entail both elastic fiber integrity as well as distinct cell-ECM adhesion properties (Figure 5) (Spessotto et al., 2003; Zanetti et al., 2004). Five members of the fibulin family are known so far (Timpl et al., 2003). They represent a structure dominated by a series of cbEGF domains and demonstrate different abilities to bind tropoelastin, fibrillin-1, fibronectin and PGs (Figure 5) (Timpl et al., 2003). Fibulin-1 (~77 kDa) associates with the elastin core but not with microfibrils (El-Hallous et al., 2007), whereas fibulin-2 (~127 kDa) strongly binds to tropoelastin and to fibrillin-1 in a Ca^{2+}-dependent manner (Reinhardt et al., 1996). Fibulin-2, fibulin-5 (~50 kDa) and to a less extent fibulin-4 (~50 kDa) are critical components for elastic fiber formation. As they provide binding sites for both tropoelastin as well as fibrillin-1, they may function as molecular bridge between microfibrils and elastin (Figure 4) (El-Hallous et al., 2007). Recent studies specified the function of fibulin-5 in elastin fiber assembly and demonstrated its requirement for activation of pro-lysyl oxidase-like-1 (proLOXL1) as well as elastin incorporation into the microfibrils (Choi et al., 2009). In addition, fibulin-5 interacts with cell surface integrins via its RGD motif, and thus, may anchor elastic fibers to the cells (Yanagisawa et al., 2002; Nonaka et al., 2009).

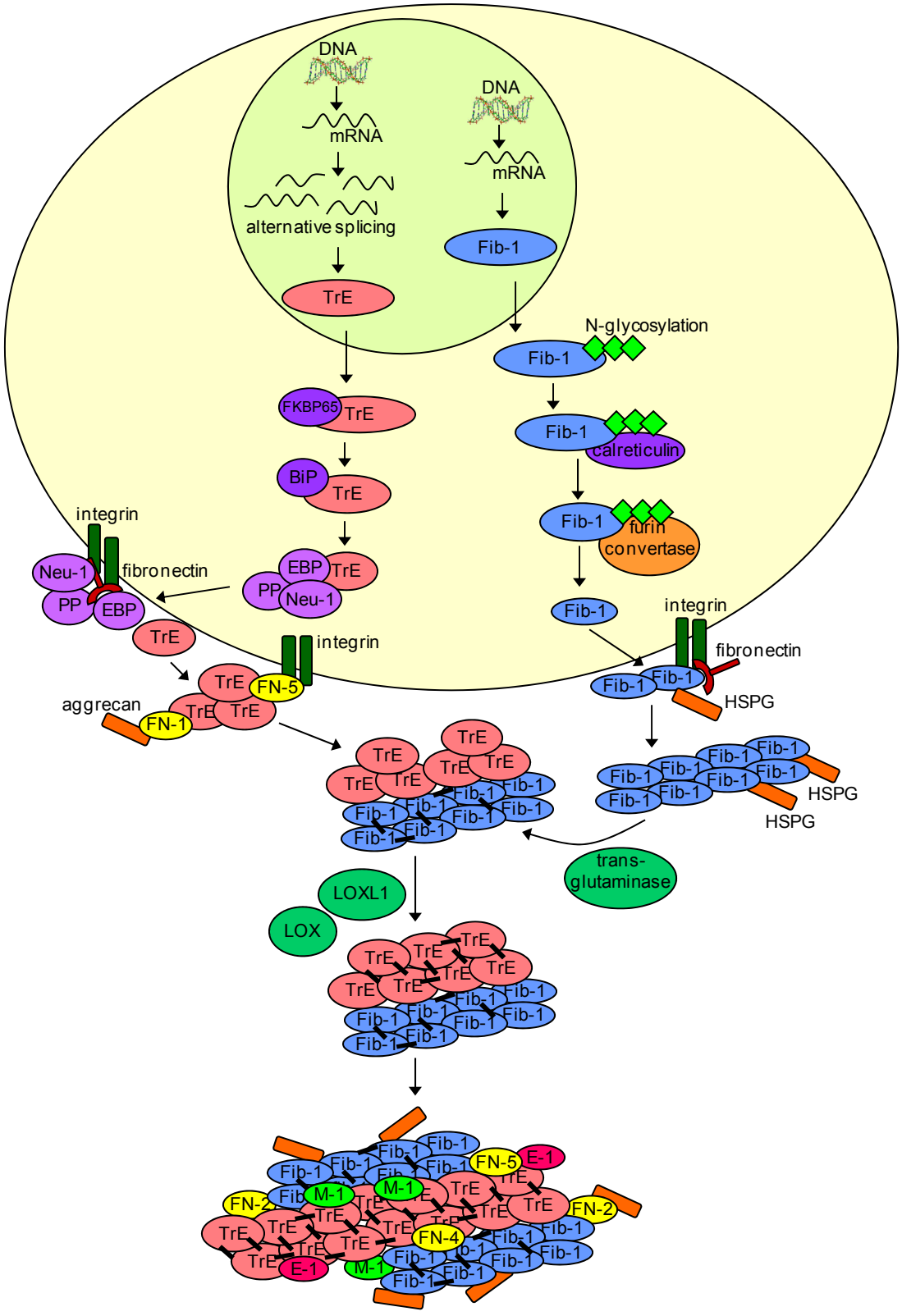

Figure 4: Formation of microfibrils and maturation of elastic fibers

A detailed description of the mechanism is given in the text. (BiP: heat shock 70kDa protein 5, E-1: EMILIN-1: elastin-microfibril-interface located protein-1, EBP: elastin binding protein, Fib-1: fibrillin-1, FKBP65: FK506 binding protein, FN: fibulin, HSPG: heparan sulfate proteoglycan, LOX: lysyl oxidase, LOXL1: lysyl oxidase-like 1, M-1: MAGP: matrix-associated glycoprotein-1, Neu-1: neuraminidase-1, PP: protective protein/cathepsin A)

The detailed mechanisms involved in the intracellular trafficking of proteins required for the formations of microfibrils are not yet understood. Fibrillins that form the major backbone of microfibrils interact in the ER with several chaperones e.g. calreticulin, facilitating folding and post-translational modifications such as N-glycosylation (Ashworth et al., 1999). Traversing the constitutive secretory pathway, fibrillin-1 undergoes initial assembly to form dimers and multimers and subsequent extracellular deposition requires cleavage of the C-terminal end by the serine protease furin convertase (Ritty et al., 1999). Microfibrils assemble close to the cell surface and recently, binding experiments revealed important interactions of fibrillins with the glycoprotein fibronectin (Sabatier et al., 2009). Moreover, latest studies substantiated that binding of fibrillins to cell surface integrins via their RGD domain as well as interactions with heparan sulfate PGs support fibrillogenesis (Tiedemann et al., 2001; Tsuruga et al., 2009). Maturation of microfibrils is associated with conformational changes and transglutaminase-catalyzed cross-links between fibrillin molecules as well as with MAGPs, which impart main stability to the microfibrils (Mecham et al., 1995; Qian and Glanville, 1997; Trask et al., 2001). Moreover, transglutaminase-dependent cross-linking of fibrillin-1 with tropoelastin molecules assists their deposition on the microfibrils and establishes eventual maturation of the complex elastic fiber (Rock et al., 2004).

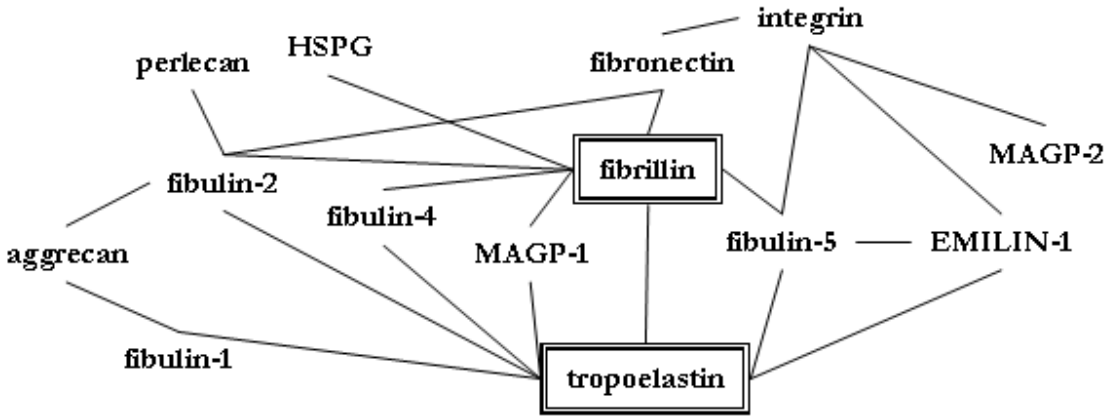

Figure 5: Protein interactions during elastic fiber maturation

1.3.1.3 Lysyl oxidases (LOs)

The family of lysyl oxidases includes at least five members, LOX and 4 LOX-like (LOXL) enzymes (Csiszar, 2001), whereof particularly LOX and LOXL1 are recognized as essential catalytic enzymes for oxidative cross-linking of lysine residues of the extracellular fiber proteins collagen and elastin, accounting for insolubilization and stabilization of the ECM (Smith-Mungo and Kagan, 1998; Wagenseil and Mecham, 2007). LOX and LOXL1 are most similar to each other, whereas LOXL2, LOXL3 and LOXL4 seem to build a second subfamily (Lucero and Kagan, 2006). LOs are secreted as N-glycosylated pro-enzymes, which enclose a N-terminal signal peptide followed by a variable region and a highly conserved C-terminus (Csiszar, 2001). Prior to activation, the secreted pro-enzyme is required to associate with the structural glycoprotein fibronectin on the extracellular cell surface (Fogelgren et al., 2005) and can then be cleaved by pro-collagen C-proteinase (BMP-1), resulting in loss of the glycosylated pro-peptide (Cronshaw et al., 1995; Panchenko et al., 1996). In addition, the activity of this redox enzyme family is dependent on two essential cofactors, a Cu^{2+} and a covalently bound lysyl tyrosine quinone (LTQ) (Figure 6a) (Wang et al., 1996).

The detailed mechanism involved in the oxidation of lysine residues in LO substrates that eventually permits intra- and intermolecular cross-links is shown in Figure 6b. It is suggested that in an intracellular self-processing reaction, Cu^{2+} initially catalyzes the oxidation of a specific tyrosine residue, resulting in a peptidyl dihydroxyphenylalanine quinone, which covalently binds to an adjoining lysyl ε-amino group. Final oxidation and transfer of the electrons to molecular oxygen generates the LTQ-cofactor as a transient electron sink (Figure 6a) (Bollinger et al., 2005). In the first step of the catalytic LO mechanism, one LTQ-carbonyl group reacts with the lysyl ε-amino group of the substrate, creating a Schiff base (1). A base-facilitated abstraction of the lysyl α-proton forms a reduced lysyl-tyrosyl-aminoquinol (2). Following hydrolysis of this imine intermediate, the release of the aldehyde product and the reduced LTQ is induced (3). Reoxidation of the cofactor is mediated by transferring two electrons on molecular oxygen producing hydrogen peroxide (4). Finally, the quinoneimine is hydrolyzed, resulting in regeneration of the original LTQ-cofactor and release of free ammonia (5) (Williamson and Kagan, 1986, 1987). The produced aldehyde then spontaneously interacts with unmodified lysyl ε-amino groups or with other aldehyde groups generating intra- and interpeptide chain cross-links (Lucero and Kagan, 2006). Spontaneous cross-linking of oxidized tropoelastin and elastin molecules results in the characteristic formation of the amino acid desmosine (Mecham et al., 1995). The production of hydrogen peroxide during this enzymatic reaction facilitates LOs activity measurements *in vitro* (Trackman et al., 1981).

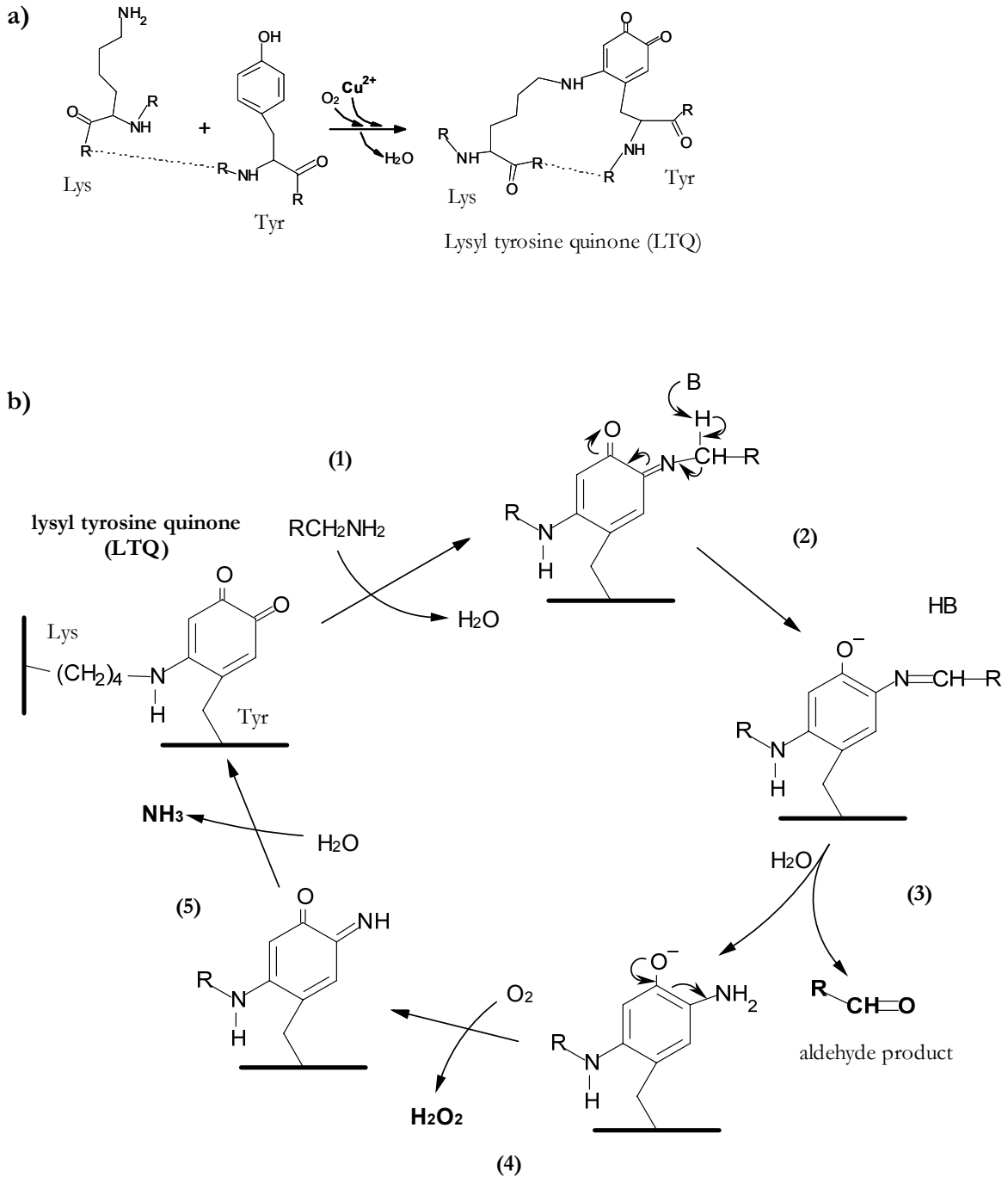

Figure 6: LO catalytic mechanism.

(a) LO activity is dependent on Cu^{2+} which catalyses the reaction of the ε-amino group of a lysine residue with an adjacent tyrosine residue generating the lysyl tyrosine quinone (LTQ)-cofactor. A detailed description is given in the text. (b) The enzymatic mechanism facilitating cross-links between lysine residues of tropoelastin molecules and matured collagen fibrils involves the carbonyl-groups of the LTQ-cofactor. Initially, one carbonyl-group reacts with the lysyl ε-amino group of the substrate (1). The essential basic environment (B) for this reaction mediates abstraction of the lysyl α-proton resulting in a reduced lysyl-tyrosyl-aminoquinol (2). Hydrolysis induces the release of the aldehyde product and a reduced LTQ-cofactor (3). Transfer of two electrons on molecular oxygen (4) and subsequent hydrolyzation of the quinoneimine (5) regenerates the original LTQ-cofactor under release of hydrogen peroxide and ammonia (4 and 5). The scheme is adapted from (Lucero and Kagan, 2006).

The electrostatic potential between the LO enzyme and its substrate plays an essential role in substrate specificity (Kagan et al., 1984). The particular preference of LOX and LOXL1 for cationic substrates might be explained by the LTQ-containing active site, which is surrounded by anionic amino acids (Lucero and Kagan, 2006). This is supported by the fact that LOX and LOXL1 are able to directly react with the elastin precursor tropoelastin, which possesses the appropriate electrostatic feature next to lysine residues, whereas oxidation of collagen does not happen before the generation of mature collagen fibers, possibly creating a more favorable environment (Gray et al., 1973; Lucero and Kagan, 2006).
Functionality of LO enzymes is of prime importance for the organism, demonstrated by numerous diseases associated with disordered LO activity such as lethal aortic aneurisms, dysfunction of the pulmonary system or skin disorders (Maki et al., 2005; Szauter et al., 2005; Rodriguez et al., 2008). Besides their extracellular activity, LOX and LOXL1 were detected in the cell nuclei (Nellaiappan et al., 2000) and might be involved in the modification of certain histones, implicating chromatin remodeling and altered transcriptional regulation (Giampuzzi et al., 2003). However, the detailed mechanisms involved in enzyme translocation and the precise function of nuclear LO are still obscure.

1.3.2 Proteoglycans (PGs)

Proteoglycans (PG) exist in the ECM, cell-associated and intracellular in secretory granules (Bajorath et al., 1998; Henningsson et al., 2006). These molecules are characteristically composed of a core protein and one or more covalently bound linear carbohydrate polymers, the glycosaminoglycans, consisting of repetitive, specifically sulfated disaccharides (Yanagishita et al., 2008). PGs appear as integral proteins or as extracellular cell surface proteins, covalently linked to glycosylphosphatidylinositol (GPI) anchors at the cell membrane (Ponta et al., 1998; Matsuda et al., 2001). Interference with a variety of factors is mediated either by charge interaction via the glycosaminoglycan chains or by specific domains within the core protein (Wight et al., 1992). PGs are involved in cell-cell adhesion as well as cell-matrix anchorage, and play a pivotal role in growth factor presentation and the induction of associated signaling pathways. However, the expression of particular PGs differs with cell type and tissue origin (Lories et al., 1992). As an extracellular reservoir for signaling molecules, PGs influence activation, localization and accessibility of growth factors and cytokines, which emphasizes the importance of these ECM compounds in the maintenance of regulated signal transduction (Bernfield et al., 1992; Ponta et al., 1998; Kresse and Schonherr, 2001). Thus, impaired expression levels or atypical post-translational modifications of PGs cause altered responses to mitogenic signals, involving influences of the cell homeostasis and growth, eventually favoring pathological and malignant transformations (Matsuda et al., 2001; Liu et al., 2003a). Previous work revealed down-regulated levels of syndecan-1 in various cancers and suppression of this heparan sulfate PG (HSPG) was associated with epithelial cell transformation and mammary tumor development (Lundin et al., 2005; Choi et al., 2007; Su et al., 2007). In contrast, glypican-1, which represents an essential

factor in heparin-binding growth factor-mediated signaling, demonstrated low levels in normal breast tissue, but was highly overexpressed in breast cancers, thus, rendering malignant cells more sensitive to mitogenic signals (Matsuda et al., 2001). As a major binding partner and effector of hyaluronic acid, the HSPG CD44 imparts extracellular alteration of hyaluronan to intracellular signaling mechanisms, thereby stimulating cell proliferation, differentiation and migration (Heldin et al., 2008). One possible mechanism is demonstrated by hyaluronan/CD44-mediated transactivation of downstream signals via ErbB1 involving the protein kinase C (PKC) family and Rac1. This causes activation of proteins involved in cytoskeleton reorganization and secretion of MMP-2, which eventually promotes cell migration (Kim et al., 2008). On the other hand, ectodomain shedding of CD44 by the transmembrane MT1-MMP (membrane type I matrix metalloproteinase) provokes the release of a soluble CD44-fragment which has also a cell motility-stimulating effect (Kajita et al., 2001). Furthermore, CD44 bears a crucial role in cytokine and growth factor presentation and the cell-specific presence of distinct CD44 variants enables specialized cellular functions (Mackay et al., 1994; Naor et al., 1997). The isoform CD44v3 (variant 3) is involved in extracellular presentation of the heparin-binding epidermal growth factor-like growth factor (HB-EGF). In addition, it binds the matrix metalloproteinase-7 (MMP-7) which subsequently facilitates proteolytic activation of HB-EGF. The ability of CD44v3 to simultaneously recruit the ErbB4 and ErbB1 receptor, respectively, ensures immediate signal transduction (Yu et al., 2002). The isoforms CD44v6 and CD44v9 were shown to interact with the Fas death receptor and thereby inhibit Fas-mediated signaling, which confers the cells with an important anti-apoptotic mechanism (Mielgo et al., 2006).
Impaired PG expression, structure and function, induced by transcriptional or post-translational alterations, may affect various intracellular signaling mechanisms and cellular adhesion processes, thereby contributing to disease progression and metastatic tumor developments.

1.3.3 Matrix metalloproteinases (MMPs)

1.3.3.1 The protein structure of MMPs – with particular emphasis on MMP-7

The family of human matrix metalloproteinases consists of currently 24 members and belongs to the metzincin group of proteases (Page-McCaw et al., 2007), which besides MMPs includes the bacterial serralysins, astacins (BMP-1 and tolloid/tolloid-like proteases) and ADAMs/ADAMTSs (Bode et al., 1993). This enzyme superfamily is characterized by an essential Zn^{2+} at the active site and a conserved methionine-turn beneath the catalytic metal (Bode et al., 1993).
MMPs are synthesized as prepro-proteins and contain a signal peptide at the N-terminus that directs the enzymes to the ER and is then removed, yielding the latent pro-enzymes (Lang et al., 2001). Most MMPs are secreted in the extracellular space, however, some have a transmembrane domain with a short cytoplasmic tail (pro-MT-MMPs including proMMP-14, -15, -16, -24) or are anchored to the cell surface via glycosylphosphatidylinositol (GPI) linkages (proMMP-17 and proMMP-25) (Figure 7) (Nagase and Woessner, 1999).

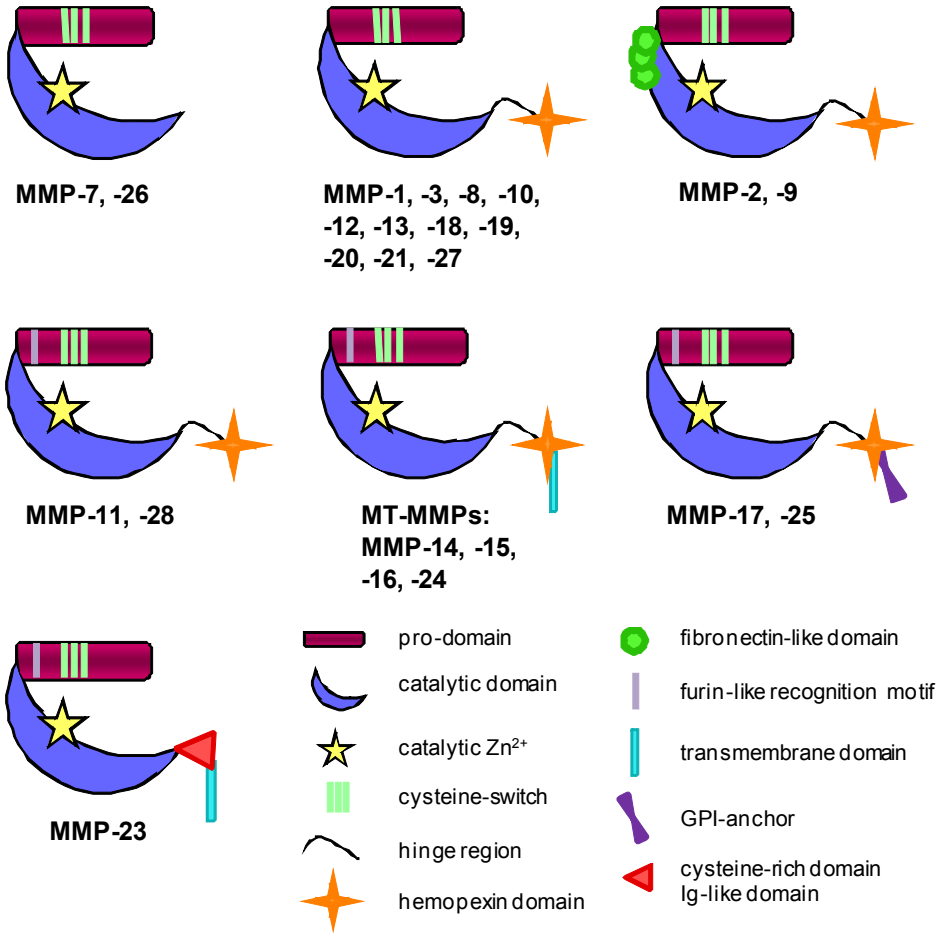

Figure 7: The MMP-family

The MMPs are expressed as pro-enzymes. The minimal domain MMPs (MMP-7 and MMP-26) are composed of the inhibitory pro-region and the catalytic domain. All other MMPs, except MMP-23, contain a hemopexin domain at the C-terminus, which is connected to the catalytic domain by a variable hinge region. MMP-23 has cysteine- and proline-rich regions instead of the hemopexin domain. The catalytic region of MMP-2 and MMP-9 additionally bears three fibronectin-like domains. The transmembrane and GPI-anchored MMPs as well as MMP-11 and MMP-28 provide a furin-like recognition motif and can be intracellularly activated. The scheme is adapted from (Bode and Maskos, 2003).

All MMPs possess an auto-inhibitory pro-domain, which maintains latency of MMPs, and a distinct adjacent catalytic domain (Massova et al., 1998). The pro-region holds a cysteine residue that forms a bridge with the Zn^{2+} at the active site and thereby prevents catalysis (Figure 7and Figure 8a) (Van Wart and Birkedal-Hansen, 1990). Enzymatic activity of MMPs requires the proteolytic cleavage of the pro-domain and subsequent access to the catalytically active center with the essential Zn^{2+} (Van Wart and Birkedal-Hansen, 1990). MMP-7 can be activated by MMP-3 and by several serine proteases such as trypsin, plasmin and leukocyte elastase which cleave at Glu^{94} (Figure 8a, highlighted in pink) and release a mature MMP-7 of approximately 19 kDa (Figure 8a) (Imai et al., 1995). MMP-7 (EC 3.4.24.23) together with MMP-26 represent minimal domain MMPs and their structure is restricted to the pro-domain and the catalytic region

(Massova et al., 1998). All other MMPs, except MMP-23, additionally contain the hemopexin domain, a C-terminal four-bladed β-propeller structure that is connected to the catalytic domain by a variable hinge region (Piccard et al., 2007). This domain mediates protein-protein interactions and significantly contributes to substrate specificity, MMP localization, activation, internalization and degradation (Piccard et al., 2007). Moreover, three fibronectin-like domains are inserted in the catalytic region of MMP-2 and MMP-9 (Morgunova et al., 1999).

The overall structure of the catalytic region is very similar among different MMPs and varies only in components framing the active site (Figure 8b, sV-hB loop and specificity loop) (Lang et al., 2001). MMPs catalytic domains share a common ellipsoid shape with a small active site cleft from left to right, which creates a lower and an upper subdomain (Figure 8b) (Bode and Maskos, 2003). The larger upper subdomain is dominated by a five-stranded β-sheet (sI-sV) and two long α-helices (hA and hB) connected by different loops (Figure 8b). Moreover, three Ca^{2+} and a second Zn^{2+} are involved in the structural organization (Figure 8b, blue and pink spheres). The active site region comprises the long horizontally extending α-helix B and the only antiparallel-running strand sIV as well as the specificity loop in the lower subdomain (Figure 8b). These elements influence substrate recognition and in the case of MMP-7 provide a particularly hydrophobic surface (Lang et al., 2001). The essential Zn^{2+} in the catalytic center is coordinated by three histidine residues as part of a Zn^{2+}-binding consensus sequence HEBXHXBGBXHZ (B: bulky hydrophobic amino acid, X: variable amino acid, Z: family specific amino acid), characteristic for the metzincin family, and a fixed water molecule that interacts in a hydrogen bond with the catalytic glutamate next to the first histidine (Lang et al., 2001). For most MMPs the last characteristic amino acid (Z) of the Zn^{2+}-binding motif is a serine residue (Bode et al., 1993) and the detailed sequence, representing this motif in the active site of MMP-7 is demonstrated in Figure 8a (turquoise). The α-helix B, which encompasses most of the Zn^{2+}-binding sequence, is followed by the highly conserved methionine-turn (Figure 8a and b). The protein chain runs through the specificity loop and then passes the α-helix C at the C-terminus in the lower subdomain (Figure 8b) (Lang et al., 2001).

Besides proteolytic control due to this structural organization, MMP activity is determined by a complex regulatory network involving diverse transcriptional, translational and post-translational events (Sternlicht and Werb, 2001).

a)

```
  1 mrltvlcavc llpgslalpl pqeaggmsel qweqaqdylk rfylydsetk nansleaklk
 61 emqkffglpi tgmlnsrvie imqkprdgvp dvaeyslfpn spkwtskvvt yrivsytrdl
121 phitvdrlvs kalnmwgkei plhfrkvvwg tadimigfar gahgdsypfd gpgntlahaf
181 apgtglggda hfdederwtd gsslginfly aathelghsl gmghssdpna vmyptygngd
241 pqnfklsqdd ikgiqklygk rsnsrkk
```

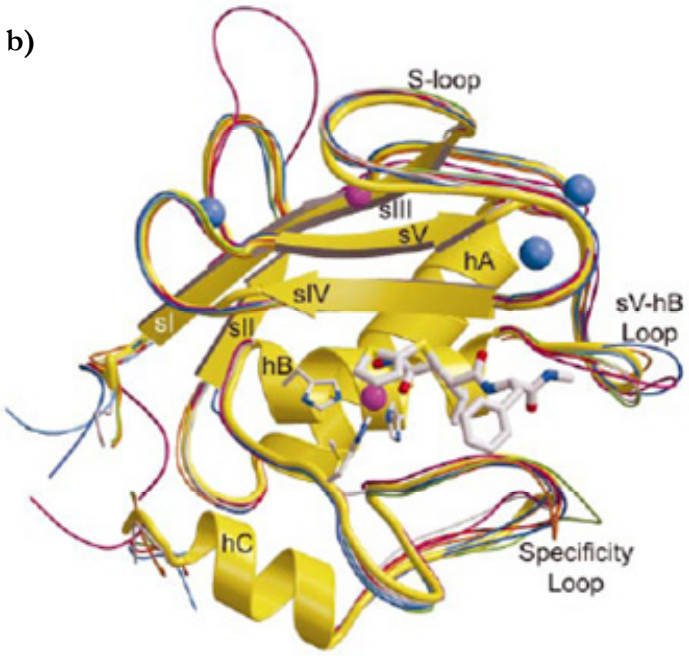

Figure 8: Amino acid sequence and tertiary structure of MMP-7.

(a) Amino acid sequence of MMP-7. The newly synthesized preproMMP-7 consists of 267 amino acids. The signal peptide (grey) is cleaved in the ER, releasing latent proMMP-7 (18-267). The auto-inhibitory feature of the pro-domain requires the cysteine residue (red) in the so-called cysteine-switch (85-92) (red letters) that coordinates the catalytic Zn^{2+} and thereby inhibits MMP activity. Moreover, the pro-domain contains a peptidoglycan binding domain (blue letters) that allows interaction with glycoproteins such as PGs. Proteolytic cleavage of MMP-7 at Glu^{94} (pink) yield the mature MMP-7 (95-267) (green letters). The characteristic Zn^{2+}-binding motif (turquoise) including three histidines (His^{214}, His^{218}, His^{224}) and the catalytic Glu^{215} is followed by the conserved Met^{232} (yellow) involved in the Met-turn (NCBI). **(b) Tertiary structure of MMP-7 catalytic domain together with a bound inhibitor.** The conserved secondary elements are demonstrated in yellow, whereas variations specific for MMP-7 are shown as orange ribbons. The active site cleft divides the catalytic domain in a small lower and a large upper subdomain. The upper subdomain is dominated by a five-stranded β-sheet (sI-sV) and two α-helices (hA and hB). After passing β-strand sI, the protein chain continues in α-helix hA. A small loop connects hA with the β-strand sII which is followed by a surface loop leading to sIII. The β-strands sIII and sIV are linked via the S-loop that involves the structural Zn^{2+} (pink sphere) as well as one of the Ca^{2+}-ions (blue sphere). The S-loop leads to the antiparallel-running β-strand sIV which is situated at the edge to the catalytic center. Another surface loop connects sIV and sV, and the second Ca^{2+} (blue sphere) is located between the sIV-sV loop and the sII-sIII bridge. After β-strand sV the protein chain passes the variable sV-hB loop and enters the active site α-helix hB. The α-helix hB contains most of the Zn^{2+}-binding motif and provides two histidine residues and the catalytic glutamate that interacts with the Zn^{2+}-coordinating water molecule. The third histidine is located beneath the helix and is followed by the methionine-turn. Finally, the chain runs through the MMP-dependent specificity loop into the C-terminal α-helix hC. Whereas the predominant structure elements are similar among different MMPs, they particularly differ in regions that frame the active site and ensure substrate specificity (e.g. sV-hB loop and specificity loop). Other MMPs are demonstrated by colored ribbons as follows: MMP-1 (red), MMP-2 (dark blue, lacking the fibronectin-like domain), MMP-3 (green), MMP-8 (grey), MMP-12 (yellow), MMP-13 (light blue) and MMP-14 (pink). The structure is adapted from (Lang et al., 2001).

1.3.3.2 Transcriptional regulation of MMP gene expression

Expression of MMPs is to a large extent regulated at the transcriptional level, substantiated by a variety of *cis*-elements in the MMP-promoter regions and the susceptibility to numerous *trans*-activators (Yan and Boyd, 2007). Besides categorization of MMPs according to their structural components, this enzyme family can also be subdivided on the basis of their promoters and the mechanisms involved in their gene expression. The majority of MMPs contains a TATA box as well as AP-1 and PEA3 binding sites in the promoter region completed by several other *cis*-regulatory elements. Gene expression of a smaller group, comprising MMP-8, MMP-11 and MMP-21, is simpler and determined by a TATA box but lack of an AP-1 site, whereas MMP-2, MMP-14 and MMP-28 have AP-1 binding sites but are deficient in a TATA box (Yan and Boyd, 2007). Expression regulation of the latter group is more susceptible to the family of SP-transcription factors, which act through GC-motifs (Suske, 1999). The diversity of *cis*-acting elements in the MMP-promoter regions illustrates the ability to act in response to a number of extra- and intracellular signaling molecules and conditions (Yan and Boyd, 2007). AP-1 binding sites and/or PEA3 motifs presented in most MMPs confer transcription of these proteinases with the crucial response to cytokines and growth factors (e.g. interleukins, interferons, EGF, KGF, basic FGF, VEGF, PDGF, TNF-α, TGF-β; plus EMMPRIN (extracellular matrix metalloproteinase inducer)) (Fini et al., 1998). *Trans*-activation of MMP-transcription through certain promoter elements can also be induced or repressed following cellular stimulation with glucocorticoids, hormones or ECM proteins or upon processes such as integrin-signaling, cell stress or altered cellular contacts and cell shape (Fini et al., 1998). These signals in turn are referred to intracellular factors, including MAPK, NF-κB, STATs and Smads that eventually lead to enhanced expression of distinct transcription factors (Vincenti and Brinckerhoff, 2007). The prominent AP-1 and PEA3 sites in the MMP-promoters are additionally supplemented by responsive elements for NF-κB, C/EBP-β, Ets, retinoic acid, p53 and β-catentin, respectively, facilitating a complex interplay and a strict regulation of MMP gene expression (Yan and Boyd, 2007).

Moreover, in a variety of MMP-promoters DNA polymorphisms have been detected which can dramatically interfere with the regulatory capacity of responsive elements (Ye, 2000). Thus, a single nucleotide polymorphism (SNP) in the promoter of MMP-1 creates a new Ets recognition site close to an AP-1 site. This causes a remarkably increased MMP-1 expression and bears cancer promoting effects (Zhu et al., 2001). On the other hand, SNPs can disrupt binding sites and reduce promoter activity. A nucleotide transition in the MMP-2 promoter impedes binding of estrogen receptor-α, and thus, causes a reduced MMP-2 transcriptional response upon estrogen stimulation in MCF-7 breast cancer cells (Harendza et al., 2003). Finally, epigenetic regulations such as DNA methylation and chromatin remodeling contributes to MMP gene transcription (Ma et al., 2004; Couillard et al., 2006). However, despite numerous advances in understanding of MMP gene regulation, the cross-talk between the many signaling pathways, nuclear factors and

responsive elements that regulate transcription and might govern cell- and tissue-specific MMP expression are still poorly understood.

1.3.3.3 Translational and post-translational MMP-regulation

The extensive and precise regulation of MMP activity on the transcriptional level is complemented by post-transcriptional alterations. Thus, distinct AU-rich sequences (ARE) at the 3'-untranslated region (UTR) recognize certain *trans*-acting proteins, thereby affecting mRNA stabilization (Huwiler et al., 2003; Rydziel et al., 2004). The 3'-UTR is additionally involved in recruitment of the mRNA to membrane-bound ribosomes and can mediate subsequent translation efficiency of a particular mRNA (Fahling et al., 2005). Once translated, the latent MMP proteins are usually constitutively secreted to the cell surface. Neutrophils, however, exhibited accumulation of MMP-8 and MMP-9 in intracellular vesicles and an induced secretion upon stimulation by inflammatory mediators (Sternlicht and Werb, 2001). As indicated above (cp. 1.3.3.1), latency of the secreted proteinases is maintained by the cysteine residue in the pro-domain of MMPs, which functions as a fourth ligand for the Zn^{2+}, and thus, blocks the catalytic center (Figure 7) (Van Wart and Birkedal-Hansen, 1990). Typically, MMPs become extracellularly activated by other MMPs or certain serine proteases and proMMP-2 represents the most complex mechanism involving MT1-MMP and TIMP-2 (tissue inhibitor of metalloproteinase-2) (Strongin et al., 1995). On the contrary, MT-MMPs as well as MMP-11 and MMP-28 provide a furin-like recognition motif and are already intracellularly processed and activated (Figure 7) (Pei and Weiss, 1995; Sternlicht and Werb, 2001).

The complex regulatory mechanisms of MMP activity are augmented by the interaction with endogenous MMP inhibitors such as TIMPs (tissue inhibitor of metalloproteinases) and α_2-macroglobulin. The α_2-macroglobulin is a strong inhibitor of MMPs, inducing an irreversible clearance of MMPs by receptor-mediated endocytosis (Woessner, 1991). Whereas α_2-macroglobulin is an abundant plasma protein, TIMPs act more locally in a cell- and tissue-specific manner. TIMPs comprise a family of so far four protease inhibitors of about 20-30 kDa that interact with active MMPs (except proMMP-2; (Strongin et al., 1995)) in a 1:1 stoichiometry (Edwards, 2001). Similar to MMPs, TIMPs underlie a tight gene regulation and exhibit a tissue-specific pattern of protein expression (Edwards, 2001). Moreover, TIMPs significantly differ in their ability to bind and inhibit diverse MMPs. Whereas the N-terminal domain bears the inhibitory function, the C-terminus influences substrate specificity (Willenbrock and Murphy, 1994). As already indicated by the function of α_2-macroglobulin, MMPs are finally influenced by catabolic mechanisms. Whereas α_2-macroglobulin induces MMP-clearance by receptor-mediated endocytosis, distinct cleavage can completely inactivate MMPs and signal their degradation, or interfere with normal enzyme features by alteration of their substrate specificity, cellular localization or TIMP-binding ability (Sternlicht and Werb, 2001).

Thus, MMP activity is controlled by an enormous regulatory machinery, indicating the importance of these enzymes and suggesting severe consequences of impaired signaling processes.

1.3.3.4 Matrix metalloproteinases are multifunctional proteins

Though MMPs were originally thought to be exclusively responsible for ECM degradation, a variety of additional mechanisms are now known that require MMPs (Sternlicht and Werb, 2001; Page-McCaw et al., 2007). Alteration of structural ECM compounds still represents a major task of MMPs, permitting ECM remodeling during physiological development and creating space for cells to migrate during wound healing (Vu et al., 1998; Kyriakides et al., 2009). But MMP activity also contributes to cellular migration and invasion during inflammation and pathological or metastatic events by degradation of the ECM and disruption of intercellular junctions or cell adhesion receptors (Page-McCaw et al., 2007). Thus, MMP-7 demonstrates strong proteolytic activity against elastin fibers *in vivo* and is known to contribute to atherosclerotic phenotypes (Filippov et al., 2003). Besides cleavage of the ECM, MT1-MMP is capable of degrading tissue transglutaminase and thereby impedes cellular adhesion on fibronectin (Belkin et al., 2001). Moreover, MMPs influence cell-cell and cell-ECM interactions by the generation of fragments with a different biologic activity (Noe et al., 2001). Proteolysis of E-cadherin by MMP-3 and MMP-7 creates a soluble protein fragment that affects E-cadherin function, looses cell aggregation and favors cellular invasion (Noe et al., 2001). Cleavage of fibrillar-associated collagen IV by MMP-2 reveals otherwise cryptic RGD domains, which are involved in integrin-binding and promote angiogenesis and tumor survival (Xu et al., 2001). Likewise, MMP-2 exposes a hidden signal on laminin-5 that acts promigratory for breast epithelial cells (Giannelli et al., 1997).

Moreover, MMPs play a key role in the regulation of activity and availability of diverse signaling molecules such as cytokines, chemokines, growth factors or hormones (Sternlicht and Werb, 2001). MMPs can provoke the release of growth factors and convert them into active molecules that in turn trigger intracellular signal transduction and cellular behavior (Fowlkes et al., 1995; Hao et al., 2004; Lee et al., 2005). Thus, MMP-9 is anchored by the HSPG CD44 to the cell surface and proteolytically activates latent TGF-β (Yu and Stamenkovic, 2000). Moreover, cleavage of a distinct matrix-bound isoform of the vascular endothelial growth factor (VEGF) by MMPs release a soluble fragment that triggers vascular dilation (Lee et al., 2005). An increase of functional insulin-like growth factors (IGF) is indirectly regulated by inactivation of their binding proteins (IGFBPs) through MMPs and results in an increased cell proliferation (Fowlkes et al., 1995). MMP-7 affects the generation of soluble ligand (sFasL) for the Fas death receptor and thereby increases apoptosis in the first place but finally favors selection for apoptotis-resistant cells, provoking mammary tumorigenesis (Vargo-Gogola et al., 2002b). MMP-cleavage can also inactivate certain chemoattractants and thereby has a great impact on wound healing and the inflammatory response (McQuibban et al., 2002).

Besides direct modification of signaling molecules, MMPs also act on the respective cell surface receptors e.g. growth factor receptors or cytokine receptors, and thereby alter cellular signal transduction pathways. Fibroblast growth factor (FGF) activities are affected by MMP-2-initiated ectodomain shedding of FGF receptor type 1 (FGFR1). The soluble extracellular domain still bears FGF binding capacity but is no longer capable of direct transactivation of intracellular mechanisms (Levi et al., 1996). MMP-9-mediated degradation of the interleukin-2 receptor α (IL-2Rα) impedes recruitment of functional T cells and provides cancer cells with an effective mechanism to suppress the immune response in tumor tissues (Sheu et al., 2001). As already mentioned above, MMPs are involved in activation of latent metalloproteinases and other pro-enzymes which may initiate proteolytic cascades that significantly intensify the initial signal (Mochizuki et al., 2004).

Moreover, interaction and/or direct cleavage of extracellular proteins such as PGs significantly influence the impact of MMPs on signaling molecules. Thus, proteolysis of decorin by MMPs abrogates the reservoir for TGF-β and consequentially induces TGF-β mediated processes (Imai et al., 1997). The HSPG CD44 indirectly influences cell signaling by facilitating localization of MMP-7 in close proximity to its substrate heparin-binding epidermal growth factor-like growth factor (HB-EGF) (Kajita et al., 2001; Yu et al., 2002). The recruitment of MMP-7 to the cell surface plays an essential role in ectodomain shedding of HB-EGF and emphasizes an important regulatory function of MMP-7 for HB-EGF signaling (Yu et al., 2002). The proteolytic cleavage of HB-EGF by MMP-7 results in the release of a soluble fragment (sHB-EGF) which in turn can transactivate intracellular signaling mechanisms via the EGF-receptors ErbB4 and ErbB1 (Lynch et al., 2007). Remarkably, CD44 not only anchors MMP-7 and HB-EGF to the cell surface but also associates with ErbB4 and ErbB1 to ensure an effective signal transduction (Yu et al., 2002).

In general, MMPs are less important for embryogenesis, but are crucial for postnatal development and in adult tissues, conferring the organism with essential tissue and ECM remodeling systems involved in bone formation, blood-vessel refinement or mammary gland development (Page-McCaw et al., 2007). MMP-7 predominantly bears crucial physiological functions in the matured organism and mediates ECM-restructuring and protein-processing related to wound healing and innate immunity (Page-McCaw et al., 2007). Moreover, several human tumors, including breast cancers, demonstrate significant overexpression of MMP-7, suggesting deregulated MMP-7 to be a crucial factor for tumorigenesis (Wilson and Matrisian, 1996). Several but definitely not all substrates of MMP-7 have been identified and the list of interacting proteins is growing. However, the detailed signal transduction pathways and their complex interplay are largely unknown and require further investigations.

1.4 Aim and concept of this study

Previous studies revealed that HMEC have a limited lifespan and underlie a process termed cellular senescence. Some fundamental aspects of the HMEC aging process such as a premature stress-associated senescence (stasis), cell cycle inhibition due to telomere erosion and the discrimination of these steps using $p16^{INK4a}$, respectively, were investigated. Besides considerable restructuring of the cell shape, senescence significantly interferes with cellular functionality. It is known that in senescent cells particularly extracellular secreted enzymes such as MMPs differ notably from those sequestered by young cells. Different effects of these enzymes on cancer cells have been described but the detailed mechanisms how the senescence-associated secretome may influence HMEC themselves remained obscure.

The focus of the present study will be on proteins involved in cell-cell and cell-matrix communications and their impact on the aging process of HMEC to verify a potential role of the extracellular microenvironment during cellular senescence.

An initial characterization of the HMEC cultures regarding $p16^{INK4a}$ expression, cell cycle regulation and SA β-gal activity will be required to identify the senescent state of the cells. Besides screening of distinct cell surface-associated glycoproteins, expression of extracellular MMPs will be analyzed to identify potential candidates that are affected by and may contribute to cellular senescence. Subsequent siRNA-targeting and down-modulation of the respective protein should reveal its function and potential relevance for the aging process of HMEC, while unraveling certain associated signal transduction mechanisms.

Taking into consideration that MMPs significantly contribute to ECM degradation and remodeling, potential alterations of ECM compounds should be examined. Protein levels of distinct ECM-precursor proteins as well as the expression and activity of certain enzymes involved in ECM maturation should be analyzed. A deregulation of these proteins could provide new insights in matrix-associated signaling mechanisms and their contribution to cellular senescence of HMEC.

2 Material and Methods

2.1 Material

2.1.1 Cell culture

Cell culture material	Manufacturer
Primary normal human mammary epithelial cells (HMEC)	BioWhittaker, Walkersviell, USA (Lot #1F1012)
MCF-7 mammary gland adenocarcinoma cells	American Type Culture Collection (ATCC), Manassas, USA
Mammary epithelial basal medium (MEBM)	PromoCell, Heidelberg, Germany
MEBM-Supplement	PromoCell, Heidelberg, Germany
Dulbecco's Modified Eagle Medium (DMEM)	Invitrogen, Karlsruhe, Germany
Fetal calf serum (FCS)	Biochrom, Hannover, Germany
Penicillin/streptomycin	Biochrom, Hannover, Germany
L-glutamine	PAA Laboratories, Cölbe, Germany
Sodium pyruvate	PAA Laboratories, Cölbe, Germany
Trypsin/EDTA (0.05%)	Invitrogen, Karlsruhe, Germany
Detach-Kit 2:	PromoCell, Heidelberg, Germany
HepesBSS-Buffer	
Trypsin/EDTA (0.025%/0.01%)	
Trypsin neutralization solution (0.05%)	

2.1.2 Kits

Kit	Manufacturer
BCA Protein Assay Reagent Kit	Pierce, Bonn, Germany
CINtec Cytology Kit	mtm Laboratories, Heidelberg, Germany
Cervatec $p16^{INK4a}$ ELISA	mtm Laboratories, Heidelberg, Germany
CyStain DNA 2 steps	Partec, Münster, Germany
HMEC Nucleofector Kit	Amaxa (Lonza), Köln, Germany
Roti Blue	Carl Roth, Karlsruhe, Germany
Senescence-associated β-Galactosidase Staining Kit	Cell Signaling, Danvers, USA
Western Lightning Chemiluminescence Reagent Plus	Perkin Elmer, Boston, USA

2.1.3 Antibodies

Antibody (Ab) (IF = immunofluorescence; WB = Western blot; F = Flow cytometry)	**Manufacturer**
Negative control FITC IgG_{2a} (F: 15µl/1x10^6 cells)	DakoCytomation, Glostrup, Denmark
Dual negative control FITC/R-PE IgG_1 (F: 15µl/1x10^6 cells)	DakoCytomation, Glostrup, Denmark
Monoclonal FITC-conjugated mouse IgG_{2a} anti-CD24 Ab. (F: 15µl/1x10^6 cells)	Becton Dickinson Pharmingen, Heidelberg, Germany
Monoclonal R-PE- conjugated mouse IgG_1 anti-CD29 Ab (F: 15µl/1x10^6 cells)	Becton Dickinson Pharmingen, Heidelberg, Germany
Monoclonal FITC- conjugated mouse IgG_1 anti-CD44 Ab (F: 15µl/1x10^6 cells)	Becton Dickinson Pharmingen, Heidelberg, Germany
Monoclonal FITC- conjugated mouse IgG_1 anti-CD227 Ab (F: 15µl/1x10^6 cells)	Becton Dickinson Pharmingen, Heidelberg, Germany
Monoclonal mouse anti-β-actin Ab (clone AC-15) (WB 1:15.000)	Sigma Aldrich, Taufkirchen, Germany
Monoclonal mouse anti-elastin Ab (clone BA-4) (IF: 1:15)	Santa Cruz Biotechnology, Santa Cruz, USA
Monoclonal mouse anti-fibrillin-1 Ab (clone 11C1.3) (IF: 1:15)	Thermo Fisher Scientific, Fremont, USA
Polyclonal rabbit anti-Fra-1 Ab (clone R-20) (WB: 1:1000)	Santa Cruz Biotechnology, Santa Cruz, USA
Monoclonal mouse anti-GAPDH Ab (clone 6C5) (WB 1:1.000)	Santa Cruz Biotechnology, Santa Cruz, USA
Monoclonal mouse anti-HB-EGF Ab (clone E-10) (WB: 1:100)	Santa Cruz Biotechnology, Santa Cruz, USA
Polyclonal goat anti-HB-EGF Ab (clone C-18) (IF: 1:10)	Santa Cruz Biotechnology, Santa Cruz, USA
Polyclonal rabbit anti-LOX Ab (ab31238) (WB: 1:200)	Abcam, Cambridge, USA
Polyclonal rabbit anti-LOXL1 Ab (clone H-165) (WB: 1:100)	Santa Cruz Biotechnology, Santa Cruz, USA
Polyclonal rabbit anti-MMP-1 Ab (SA-102) (WB: 1:2000)	Biomol, Hamburg, Germany
Monoclonal mouse anti-MMP-2 Ab (clone 2C1) (WB: 1:500)	Biomol, Hamburg, Germany

Antibody (Ab) (IF = immunofluorescence; WB = Western blot; F = Flow cytometry)	**Manufacturer**
Polyclonal rabbit anti-MMP-7 Ab (SA-105) (WB: 1:1000)	Novus Biologicals, Littleton, USA
Monoclonal mouse anti-MMP-7 Ab (clone 111433) (IF: 1:20; WB: 1:400)	RnD Systems, Minneapolis, USA
Polyclonal rabbit anti-MMP-9 Ab (SA-106) (WB: 1:1000)	Biomol, Hamburg, Germany
Polyclonal rabbit anti-tropoelastin Ab (PR398) (WB: 1:2000; IF: 1:20)	Elastin Products Company (EPC), Owensville, USA
Alexa Fluor 488 chicken anti-goat IgG (IF: 1:1000)	Invitrogen, Karlsruhe, Germany
Alexa Fluor 488 goat anti-rabbit IgG (IF: 1:1000)	Invitrogen, Karlsruhe, Germany
Alexa Fluor 568 goat anti-mouse IgG (IF 1:1000)	Invitrogen, Karlsruhe, Germany
Hoechst 33258 (IF: 1:200)	Invitrogen, Karlsruhe, Germany
HRP-conjugated sheep anti-mouse IgG (WB 1:10000)	GE Healthcare, Freiburg, Germany
HRP-conjugated donkey anti-rabbit IgG (WB 1:7500 - 1:15000)	GE Healthcare, Freiburg, Germany
HRP- conjugated donkey anti-goat IgG (WB 1:25.000)	Santa Cruz Biotechnology, Santa Cruz, USA

2.1.4 Small interfering RNAs (siRNAs)

siRNA	**Manufacturer**
AllStars Negative Control siRNA	Qiagen, Hilden, Germany
Negative Control siRNA-AF488	Qiagen, Hilden, Germany
Hs_MMP7_3_HP siRNA: TGG ACG GAT GGT AGC AGT CTA	Qiagen, Hilden, Germany
Hs_MMP7_4_HP siRNA: CTG CAT TTC AGG AAA GTT GTA	Qiagen, Hilden, Germany
Hs_ HBEGF_5_HP siRNA: AGC ACT GGC CAC ACC AAA CAA	Qiagen, Hilden, Germany
Hs_HBEGF_6_HP siRNA: GTG CTG GAT TTG ATG AGT TAA	Qiagen, Hilden, Germany

2.1.5 Chemicals

Industry standard chemicals were used as grade *'pro analysis'* and were obtained from the companies Merck (Darmstadt, Germany), J.T. Baker (Deventer, Netherlands), Sigma Aldrich (Taufkirchen, Germany) and Carl Roth (Karlsruhe, Germany), respectively. Specific reagents and chemicals were purchased from the following companies:

Chemical	**Manufacturer**
Albumin standard	Pierce, Rockford, USA
Ammonium persulfate (APS)	Serva, Heidelberg, Germany
Amplex Red Reagent	Invitrogen, Karlsruhe, Germany
β-aminopropionitrile (BAPN) fumarate salt	Sigma Aldrich, Taufkirchen, Germany
CHAPS	GE Healthcare, Freiburg, Germany
1,5-Diaminopentane	Sigma Aldrich, Taufkirchen, Germany
Dimethyl sulfoxide (DMSO)	Sigma Aldrich, Taufkirchen, Germany
Dithiothreitol	Carl Roth, Karlsruhe, Germany
Dried skimmed milk	Marvel, Dublin, Ireland
Horseradish peroxidase (HRP)	Sigma Aldrich, Taufkirchen, Germany
Hydrogen peroxide	Sigma Aldrich, Taufkirchen, Germany
Low-melting point agarose	Sigma Aldrich, Taufkirchen, Germany
Nonidet NP-40	Roche Diagnostics, Mannheim, Germany
Pharmalyte 3-10	GE Healthcare, Freiburg, Germany
Phenylmethansulfonyl fluoride (PMSF)	Sigma Aldrich, Taufkirchen, Germany
Precision Plus Protein all blue standard	BioRad, Munich, Germany
ProLong Gold Antifade	Invitrogen, Karlsruhe , Germany
Roti Blue	Carl Roth, Karlsruhe, Germany
Rotiphorese Gel 40 (37,5:1)	Carl Roth, Karlsruhe, Germany
Sodium tetraborate	Sigma Aldrich, Taufkirchen, Germany
N,N,N',N'-tetramethylethylendiamine (TEMED)	Sigma Aldrich, Taufkirchen, Germany
Tween 20	Carl Roth, Karlsruhe, Germany
Urea	Carl Roth, Karlsruhe, Germany

2.1.5.1 Sterile 1x phosphate buffered saline (PBS) pH 7.4

10x PBS pH 6.8

NaCl	1.37 M
KH_2PO_4	0.01 M
Na_2HPO_4	0.08 M
KCl	0.027 M

The 10-fold concentrated buffer solution (10x PBS) was diluted 1:10 with ddH_2O and portioned in 100ml-flasks. The buffer was subsequently autoclaved at 121°C for 20 min. After cooling down to room temperature, sterile 1x PBS was stored at 4°C.
In the following text PBS is always referred to 1x PBS.

2.1.6 Instruments and devices

Instruments and devices	Manufacturer
Autoclave LVSA 50/70	Zirbus, Bad Grund, Germany
Autoclave HST 6x6x6	Zirbus, Bad Grund, Germany
Centrifuge 5415 C, 5415 D, 5415 R, 5810 R	Eppendorf, Hamburg, Germany
Electrophoresis Power Supply EPS301	GE Healthcare, Freiburg, Germany
Fluoroskan Ascent Fl	Thermo Fisher Scientific, Dreieich, Germany
Freezing container	(Nalgene) Thermo Fisher Scientific, Langenselbold, Germany
Galaxy Flow cytometer	Dako, Hamburg, Germany
Glassware pipettes	Brand, Wertheim, Germany
Incubator	Heraeus, Hannover, Germany
Laboratory device cleaner G7883 CD	Miele, Gütersloh, Germany
Microscope Leica AF6000	Leica, Wetzlar, Germany
Microscope Keyence BZ-8100	Keyence, Neu-Isenburg, Germany
Microscope Olympus IX50	Olympus, Hamburg, Germany
Mini-Protean 3 Electrophoresis System	Bio-Rad, Munich, Germany
Mixer Reax Top	Heidolph Instruments, Schwabach, Germany
Multiscan EX	Thermo Fisher Scientific, Dreieich, Germany
Neubauer chamber	Brand, Wertheim, Germany
Nucleofector	Amaxa (Lonza), Cologne, Germany
pH-meter 766 Calimatic	Knick, Berlin, Germany
Pipette cleaner	Hölzel, Hörkofen, Germany
Power supply PAC200	Bio-Rad, Munich, Germany
Rotation device	GfL, Burgwedel, Germany
Sterile workbench	Heraeus, Hannover, Germany

Instruments and devices	Manufacturer
Sterilizer, model 440	Memmert, Schwabach, Germany
Shaker Duomax 1030	Heidolph Instruments, Schwabach, Germany
TE 22 Mini Tank Transfer Unit	GE Healthcare, Freiburg, Germany
TE 62 Tank Transfer Unit	GE Healthcare, Freiburg, Germany
Thermo mixer 546 plus	Eppendorf, Hamburg, Germany
Vertical electrophoresis system	PEQLAB Biotechnologie, Erlangen, Germany
Vi-Cell	Beckman Coulter, Krefeld, Germany
X-ray Processor XP505	3M, Neuss, Germany

2.1.7 Consumable supplies

Consumable supplies	Manufacturer
Blotting paper	Omnilab, Bremen, Germany
Cell culture dishes, flasks, microtiterplates	(Nunc) Thermo Fisher Scientific, Langenselbold, Germany
Centrifugal filter devices (Amicon Ultra-4 Centrifugal Filter Units with an Ultracel-10 membrane)	Millipore, Schwalbach, Germany
Cryo.S vials	Greiner Bio-One, Frickenhausen, Germany
Cover slips	Thermo Fisher Scientific, Dreieich, Germany
Disposable syringe Omnifix 40 Solo	Braun Petzold, Melsungen, Germany
Hybond-C Extra	GE Healthcare, Freiburg, Germany
Hyperfilm	GE Healthcare, Freiburg, Germany
Needles (0.4, 0.6, 0.8)	Becton Dickinson, Heidelberg, Germany
Microscope slides superfrost plus	Thermo Fisher Scientific, Dreieich, Germany
Tubes (0.5 ml, 1.5 ml, 2.0 ml)	Eppendorf, Hamburg, Germany
Silanized slides	Dako, Hamburg, Germany

2.1.8 Software

Software	Manufacturer
Adobe Photoshop	Adobe Systems, Munich, Germany
Ascent Software v.2.6	Thermo Electron Corporation, Dreieich, Germany
Endnote	Thomson Reuters, Carlsbad, USA
FloMax Flow Cytometry Software	Partec, Münster, Germany
ImageJ	NIH, Bethesda, USA
Keyence BZ-8100 Software	Keyence, Neu-Isenburg, Germany
LAS AF	Leica, Wetzlar, Germany
Microsoft Office	Microsoft Deutschland, Unterschleißheim, Germany
MultiCycle Software	Phoenix Flow Systems, San Diego, USA
NCBI	National Center for Biotechnology Information, Bethesda, MD, USA

2.2 Methods

2.2.1 Cell biology

2.2.1.1 Cell culture of primary human mammary epithelial cells (HMEC)

Primary cultures of human mammary epithelial cells (HMEC) were isolated from a 50 year old Caucasian female and commercially provided by BioWhittaker Inc. as culture passage 7 (Lot #1F1012). HMEC were tested positive for cytokeratins 14 and 18 and negative for cytokeratin 19 and vimentin, respectively. They were performance tested and tested negative for HIV-1, hepatitis B & C, mycoplasma, bacteria, yeast and fungi.
HMEC were seeded at 2,500 cells/cm^2 and cultured in mammary epithelial cell basal medium (PromoCell). The HMEC medium (500 ml) was supplemented with 2 ml of bovine pituitary extract (13 mg/ml), 0.5 ml of hydrocortisone (0.5 µg/ml), 0.5 ml of human recombinant epidermal growth factor (10 µg/ml), 0.5 ml insulin (5 mg/ml), and 0.5 ml gentamycin (50 µg/ml)/amphotericin-B (50 µg/ml). The cells were cultured at 37°C in a humidified atmosphere with 5 % CO_2 and the appropriate medium of each culture was replaced every two to three days.

2.2.1.2 Subculture of primary HMEC

At subconfluent conditions, residual medium was removed from the cells by washing with HepesBSS buffer (PromoCell) and HMEC were incubated with 0.025 %/0.01 % trypsin/EDTA (PromoCell) for about 7 min/37°C until they detached. Thereafter, immediate addition of trypsin neutralization solution (TNS) from soybean was required to inactivate the trypsin followed by subsequent centrifugation (220 g/6 min). The pelleted cells were resuspended in new medium at about 10^4 cells/ml and cultured further on in the next passage number.

2.2.1.3 Stimulation of HMEC with β-aminopropionitrile (BAPN)

HMEC populations during cellular senescence were cultured in the presence and absence of the LO-inhibitor BAPN for 12 days. HMEC were seeded in passage 16 on cover slips in a cell culture dish. After two days of culture, the cells were stimulated with 2 mM BAPN, whereas the appropriate control populations were cultured without BAPN. The respective medium (with or without BAPN) was changed every two days. After 12 days of culture, the control populations and BAPN-treated HMEC were fixed with 4% paraformaldehyde and processed for immunofluorescence detection as described below (2.2.2.2).

2.2.1.4 Cell culture of MCF-7 mammary gland adenocarcinoma cells

Human MCF-7 mammary gland adenocarcinoma cells originally isolated from a 69 year old Caucasian woman with several characteristics of differentiated mammary epithelium (Soule et al., 1973) were derived from the American Type Culture Collection (ATCC #HTB-22) as passage 146 or earlier and cultured in DMEM-medium (Invitrogen), including 10% (v/v) heat-

inactivated fetal calf serum (FCS) (Biochrom), 2 mM L-glutamine (Invitrogen), 1 mM sodium pyruvate (Invitrogen) and 1 mM penicillin/streptomycin (Invitrogen). The cells were cultured at 37°C in a humidified atmosphere with 5 % CO_2 and the appropriate medium of each culture was replaced every two to three days.

2.2.1.5 Subculture of MCF-7 cell line

At subconfluent conditions, the conditioned medium was collected and residual medium was removed from the cells by washing with PBS. MCF-7 cells were incubated with 0.05 % trypsin/EDTA (Invitrogen) for about 5 min/37°C until they detached. Thereafter, immediate addition of conditioned medium, containing 10 % FCS, was required to inactivate the trypsin followed by subsequent centrifugation (350 g/6 min). The pelleted cells were resuspended in new DMEM medium at about 5×10^4 cells/ml and cultured further on in the next passage number.

2.2.1.6 Cryostorage of cells in liquid nitrogen

HMEC and MCF-7 were harvested by trypsinization. After determination of the cell number, about 1×10^6 HMEC and 3×10^6 MCF-7 cells, respectively, were transferred in a 2 ml-cryogenic vial (Greiner) and supplemented with 10 % (v/v) FCS and 10 % (v/v) DMSO. Vials were placed in a freezing container (Nalgene) and cooled at a rate of 1°C/min in the -80°C freezer to ensure optimal cryopreservation. Finally, the vials were transferred in a liquid nitrogen tank for long term storage.

2.2.1.7 Determination of cell number and viability

After trypsinization, cell number and viability were determined by trypan blue exclusion either using the Neubauer chamber or by automatic measurement in the Vi-Cell (Beckman Coulter).

2.2.1.8 Determination of population doublings

The proliferative capacity of a cell population can be determined by calculating the population doublings (PD) per day according to the formula:

$$PD/day = \left(\frac{\log N_h - \log N_i}{\log 2} \right) * \frac{1}{t}$$

N_i = initial cell number

N_h = cell number harvested

t = time of cell culture in days

2.2.1.9 Senescence-associated β-galactosidase assay (SA β-gal)

About 1×10^4 HMEC were seeded in a 24-well plate (nunc, Thermo Fisher Scientific) and cultured for the appropriate time. The cells were fixed with 1x Fixative Solution, containing 20% formaldehyde and 2% glutaraldehyde (Cell Signaling Technology), and stained against senescence-associated β-galactosidase (SA β-gal) (Cell Signaling Technology) for 24 h/37°C in the dark according to the manufacturer's protocol and recommendations. The staining was proportional to the amount of substrate (5-bromo-4-chloro-3-indolyl-beta-D-galactopyranoside) enzymatically transformed. Following two washes with PBS the differentially-stained cell cultures were documented by phase contrast microscopy using the Olympus imaging software cell^B (Olympus) and quantified by counting.

2.2.1.10 Cell cycle analysis

Cell cycle analysis by flow cytometry is based on the fluorescent staining of nuclear DNA. After trypsinization, about 1×10^5 HMEC were fixed in 70% (v/v) ice-cold ethanol at 4°C for 24 h. Thereafter, the fixed cells were washed twice with PBS, stained with CyStain DNA 2 step kit according to the manufacturer's protocol (Partec) and filtered through a 50 µm filter. The samples were analyzed in a Galaxy flow cytometer (Dako) using FloMax analysis software (Partec) and the MultiCycle cell cycle software (Phoenix Flow Systems). Subsequently, the particular cell cycle phases were quantified using FloMax analysis software. The population with degenerated DNA was defined as the rate of dying or dead cells, whereby 8N DNA represented aberrant mitosis.

2.2.1.11 Analysis of surface marker expression by flow cytometry

HMEC P12 to P16 and the cancer cell line MCF-7 were trypsinized and fixed in 70% (v/v) ice-cold ethanol at 4°C for 24 h. Thereafter, the cells were washed twice with PBS and incubated with the appropriate fluorescence-labeled antibodies, CD24, CD29, CD44, CD227 (all from BD Biosciences) and the isotype-specific negative controls (DakoCytomation), for 30 min at room temperature. After two additional washing steps, the cells were measured with a Galaxy flow cytometer (Dako) using FloMax analysis software (Partec). The amount of cell surface marker expression was proportional to the fluorescence intensity.

2.2.1.12 siRNA-transfection

Transfection of HMEC and MCF-7, respectively, was performed according to the manufacturer's protocol (amaxa). Briefly, 1×10^6 HMEC P11 or 2×10^6 MCF-7 were harvested by trypsinization and resuspended in 100 µl HMEC Nucleofector Solution (amaxa). The cell suspension was mixed with 1 µg siRNA and 2 µg pmaxGFP, respectively, placed in a sterile electroporation cuvette and subjected to program X-005 using the Nucleofector II (amaxa). For MMP-7 gene silencing the following sequences were targeted: TGG ACG GAT GGT AGC AGT CTA (Hs_MMP7_3_HP siRNA) and CTG CAT TTC AGG AAA GTT GTA (Hs_MMP7_4_HP siRNA). Moreover,

HB-EGF was targeted using: AGC ACT GGC CAC ACC AAA CAA (Hs_ HBEGF_5_HP siRNA) and GTG CTG GAT TTG ATG AGT TAA (Hs_HBEGF_6_HP siRNA). AllStars Negative Control siRNA was used as a negative control and Negative Control siRNA-AF488 as a green fluorescence-labeled negative control (all from Qiagen), respectively. Both negative siRNAs have no homology to any known mammalian gene. pmaxGFP was provided with the HMEC Nucleofector Kit (amaxa) and served as a positive control. After transfection, the cells were immediately transferred into pre-warmed culture medium. To evaluate the transfection efficiency, HMEC controls and cells transfected with Negative Control siRNA-AF488 were harvested after 5 h, washed twice with PBS and subjected to the Galaxy flow cytometer (Dako) using FloMax analysis software (Partec). HMEC transfected with pmaxGFP (amaxa) were analyzed by fluorescence microscopy (Olympus) after 48 h.
To prolong the transient down-modulation of MMP-7 and HB-EGF, additional transfections with the particular siRNA were performed after 48 h. Therefore, the MMP-7 and HB-EGF transfected HMEC were harvested by trypsinization, transfected again with 1 μg siRNA as described above and incubated for another 48 h. For Western blot and cell cycle analysis, the transfected cells were harvested at the indicated time points post transfection. At the same time, cells were fixed for SA β-gal staining (Cell Signaling Technology) (2.2.1.9).

2.2.1.13 Cell lysis

Lysis buffer pH 7.5

Tris	20 mM
NaCl	150 mM
EDTA	1 mM
EGTA	1 mM
Sodium pyrophosphate	2.5 mM
β-glycerolphosphate	1 mM
Sodium metavanadate	1 mM
Leupeptin	1 μg/ml
Triton X-100	1 % (v/v)
Nonidet P-40	0.5 % (v/v)
PMSF	1 mM

HMEC and MCF-7 populations were harvested by trypsinization and the cell number was determined by trypan blue exclusion. Cells were washed with PBS and collected by centrifugation (220g/6 min). The cell pellets were either shock frozen in liquid nitrogen and stored at -80°C or immediately processed. Cell pellets which were stored at -80°C were thawed on ice and homogenized in the appropriate volume of ice-cold lysis buffer pH 7.5. After centrifugation (14,000 g/10 min/4°C), the resulting supernatant with the appropriate protein homogenate was subjected to a protein quantification measurement using the BCA protein assay (Pierce).

2.2.2 Immunocytochemical methods

2.2.2.1 $p16^{INK4a}$ assay

The $p16^{INK4a}$ assay is based on the qualitative immunocytochemistry method and was performed according to the CINtec Cytology Kit protocol (mtm laboratories). Briefly, about 1×10^4 HMEC were seeded on glass slides and cultured in mammary epithelial cell basal medium (PromoCell). The cells were fixed in 96 % (v/v) ethanol, rehydrated and initially incubated for 15 min at 95°C in the epitope retrieval solution provided with the kit. Including several washing steps with wash buffer (mtm laboratories), the cells were incubated with peroxidase blocking reagent, primary anti-human $p16^{INK4a}$ antibody and a HRP-conjugated secondary antibody. The chromogen solution was based on 3,3'-diaminobenzidine (DAB) and indicated the over-expression of $p16^{INK4a}$ by a brown staining of the cells. Haematoxylin was used as a counterstain. Phase contrast microscopy was performed with an Olympus IX50 microscope using the Olympus imaging software cell^B (Olympus).

2.2.2.2 Immunofluorescence detection of MMP-7 and HB-EGF

For immunofluorescence, $1x10^4$ HMEC were seeded on cover slips. The cells were fixed with 4 % (v/v) paraformaldehyde for 5 min at room temperature. After neutralization with 1x TBS and permeabilization with 0.1 % (v/v) Triton X-100 in PBS, unspecific binding sites were blocked with 3 % BSA/PBS for 30 min at 37°C. Then the slides were incubated with a monoclonal mouse anti-MMP-7 (RnD Systems) and a polyclonal goat anti-HB-EGF (Santa Cruz Biotechnology) antibody, respectively, in 3 % BSA/PBS for 1 h at 37°C. After washing with PBS, the slides were incubated for 1 h at 37°C with an AlexaFluor488-labeled chicken anti-goat antibody and a AlexaFluor568-labeled goat anti-mouse antibody (both Invitrogen), respectively. Control staining with the secondary antibodies alone revealed no detectable fluorescence. Co-localization of MMP-7 and HB-EGF was investigated by a double staining for these proteins. Therefore, the anti-HB-EGF stained HMEC were fixed again, blocked with 10 % (v/v) goat serum and were subsequently incubated with monoclonal mouse anti-MMP-7 antibody and the appropriate secondary antibody. Following an additional washing step, further incubation was performed with the DNA-intercalating dye Hoechst 33258 (Invitrogen) for detection of the nuclei. After two final washing steps with PBS and ddH_2O, the slides were mounted using ProLong Gold Antifade (Invitrogen). Epifluorescence microscopy was performed with a Keyence BZ-8100 using the appropriate Keyence software (Keyence).

2.2.2.3 Immunofluorescence detection of fibrillin-1 and elastin

For immunofluorescence detection of cell-associated elastin-like fiber formation, HMEC P16 control populations and BAPN-treated HMEC P16 were fixed with 4% paraformaldehyde for 10 min at room temperature and processed as described above. The slides were incubated with a monoclonal mouse anti-fibrillin-1 antibody (Thermo Fisher Scientific) and an AlexaFluor488-labeled goat anti-mouse antibody (Invitrogen). An additional blocking step with 10 % (v/v)

mouse serum for 1 h at 37°C was followed by the incubation with a monoclonal mouse anti-elastin antibody (Santa Cruz Biotechnology) and an AlexaFluor568-labeled goat anti-mouse antibody (Invitrogen). Control staining with the secondary antibodies alone revealed no detectable fluorescence. Further incubation was performed with the DNA-intercalating dye Hoechst 33258 (Invitrogen) for detection of the nuclei. After two final washing steps with PBS and ddH_2O, the slides were mounted using ProLong Gold Antifade (Invitrogen). Epifluorescence microscopy was performed with a Leica AF-6000 using the appropriate Leica LAS software (Leica).

2.2.2.4 Immunofluorescence of extracellular matrix fibers

For immunofluorescence of extracellular matrix, the extracellular filaments were harvested, plated on silanized slides (Dako) and fixed with 4% (v/v) paraformaldehyde for 10 min at room temperature. For a better visualization of matrix proteins, the fibers were incubated with 6 M guanidine hydrochloride, 50 mM DTT in 20 mM Tris pH 8 for 15 min at room temperature. After careful washing with 20 mM Tris pH 8, an incubation in the dark followed with 100 mM iodacetamide in 20 mM Tris pH 8 for 15 min at room temperature to alkylate free sulfhydryl groups. An additional washing step with 20 mM Tris pH 8 is then followed by the incubation with 3% BSA/PBS for 30 min at 37°C. Thereafter, the fibers were incubated with a monoclonal mouse anti-fibrillin-1 antibody for 1 h at 37°C. After washing with PBS, the slides were incubated for 1 h at 37°C with an AlexaFluor488-labeled goat anti-mouse antibody (Invitrogen). An additional blocking step with 10% (v/v) mouse serum for 1 h at 37°C was followed by the incubation with a monoclonal mouse anti-elastin antibody (Santa Cruz Biotechnology) (1 h; 37°C) and an AlexaFluor568-labeled goat anti-mouse antibody (Invitrogen) for 1 h at 37°C. After two final washing steps with PBS and ddH_2O, the slides were mounted using ProLong Gold Antifade (Invitrogen). Epifluorescence microscopy was performed with a Leica AF-6000 using the appropriate Leica LAS software (Leica). Control staining with the secondary antibodies alone revealed no detectable fluorescence.

2.2.3 Biochemical methods

2.2.3.1 Protein quantification by BCA protein assay

Protein quantification measurement was performed in microtiterplates using the BCA Protein Assay Reagent Kit according to the manufacturer's recommendations (Pierce). The method combines the biuret reaction, known as the reduction of Cu^{2+} to Cu^{+} by protein in an alkaline medium, with the calorimetric detection based on the chelation of Cu^{+} by two bicinchoninic acid (BCA) molecules. The calibration curve was prepared with defined concentrations of bovine serum albumin (BSA, Pierce) and absorption was read at 562 nm using a Multiscan EX with the Ascent Software version 2.6 (Thermo Fisher Scientific).

2.2.3.2 Protein separation by SDS-polyacrylamide gel electrophoresis

Glycine gel electrophoresis

Glycine gel electrophoresis was performed according to the Laemmli protocol (Laemmli, 1970). Resolving and stacking gel demonstrate discontinuities in pH value and ionic strength.

Loading buffer pH 6.8 (5x)	
Tris	2.5 M
Glycine	40% (w/v)
SDS	2.5 % (w/v)
DTT	25 mM
Bromphenol blue	0.005 % (w/v)

10x electrophoresis buffer	
Tris base	0.25 M
Glycine	1.92 M
SDS	1 % (w/v)

Resolving gel (10 %)	
ddH_2O	4.5 ml
1.5 M Tris-Base pH 8,8	2.5 ml
37.5 % Acrylamide (w/v)	2.7 ml
10 % SDS (w/v)	100 µl
10 % APS (w/v)	50 µl
TEMED	50 µl

Resolving gel (7.5 %)	
ddH_2O	5.2 ml
1.5 M Tris-Base pH 8,8	2.5 ml
37.5 % Acrylamide (w/v)	2 ml
10 % SDS (w/v)	100 µl
10 % APS (w/v)	50 µl
TEMED	50 µl

Stacking gel (4%)	
ddH_2O	3 ml
0.5 M Tris/HCl pH 6,8	1.25 ml
37.5% Acrylamide (w/v)	540 µl
10% SDS (w/v)	50 µl
10% APS (w/v)	38 µl
TEMED	13 µl

Tricine gel electrophoresis

For a better resolution of low molecular weight peptides and proteins, the tricine buffer system was used according to the Schagger protocol (Schagger, 2006).

Loading buffer pH 6.8 (3x)	
Tris	2.5 M
Glycine	40%(w/v)
SDS	2.5%(w/v)
DTT	25 mM
Bromphenol blue	0.005%(w/v)

Gel buffer pH 8.45 (3x)	
Tris base	3 M
SDS	0.3%(w/v)

Resolving gel (10 %)		Stacking gel (4 %)	
3x Gel buffer pH 8.45	5 ml	3x Gel buffer pH 8.45	1.5 ml
37.5 % Acrylamide (w/v)	3 ml	37.5 % Acrylamide (w/v)	0.5 ml
Glycerol	1.5 g	ad ddH_2O	ad 6 ml
ad ddH_2O	ad 15 ml	10 % APS (w/v)	40 µl
10 % APS (w/v)	75 µl	TEMED	15 µl
TEMED	75 µl		

Anode buffer pH 8.9 (10x)		Cathode buffer (10x)	
Tris base	2 M	Tris base	1 M
		Tricine	1 M
		SDS (w/v)	1%

Equal amounts of protein lysate were mixed with loading buffer pH 6.8, denatured at 95°C for 5 min and cooled on ice before loading. The samples were separated using glycine- and tricine gels (10 % and 7.5 %), respectively, in the Mini-Protean 3 Electrophoresis Systems (BioRad), starting with 60 V for 30 min and increasing to 80 V for about 2 h until the bromphenol blue reached the lower end of the gel matrix. Standardization was performed using pre-stained low-molecular-weight markers (BioRad).

2.2.3.3 Coomassie stain of SDS-polyacrylamide gels

Fixative Solution		Stain solution	
Ethanol	40 % (v/v)	5x Roti Blue (Roth)	20 % (v/v)
Acetic acid	10 % (v/v)	Methanol	20 % (v/v)

Destain solution	
Methanol	25 % (v/v)

For visualization of the separated proteins, the gels were stained with Coomassie brilliant blue after electrophoresis (2.2.3.2). The detection limit for Coomassie stain is about 200-400 ng protein. Proteins were fixed in the gel by incubation with fixative solution for 1h at room temperature followed by the incubation in staining solution for 12 h. Thereafter, the gel was washed several times with destain solution to reduce the background.
The Coomassie-stained gels were shrink-wrapped in ddH_2O and stored at 4°C.

2.2.3.4 Western blot: protein transfer on nitrocellulose membranes

Transfer buffer

Glycine	39 mM
Tris	48 mM
SDS	1.2 mM
Methanol	20 % (v/v)

After gel electrophoresis, the separated proteins were transferred to a nitrocellulose membrane (Hybond-C Extra, Amersham) using the tank blot systems TE 22 Mini and the TE 62 Tank Transfer Unit, respectively (Amersham). Therefore, both the gel as well as the nitrocellulose membrane were equilibrated in transfer buffer for 10 min. The sponge and the blotting paper were soaked in the buffer. All components were layered in the transfer cassette according to the transfer direction, placed in the chilled transfer tank and the proteins were blotted for 1-1.5 h at 100 V.

2.2.3.5 Immunoblot analysis

PBST

1x PBS

0.05 % Tween 20

Storage buffer

Glycerine	87 % (w/v)
Sodium acid	0.02 % (w/v)

Blocking buffers

- 5 % FCS in 1x PBST
- 5 % non-fat dry milk in 1x PBST

After a successful protein transfer on the nitrocellulose membrane, unspecific binding was prevented by incubation with blocking buffer. Usually, 5 % FCS/PBST was used as blocking solution. However, for the detection of extracellular matrix proteins 5 % non-fat dry milk/PBST served as a better blocking reagent. Subsequently, the membranes were incubated with the distinct polyclonal or monoclonal primary antibodies for 2 h at room temperature or over night at 4°C, respectively, diluted in the particular blocking solution. Excessive antibody solution was removed by several washing steps with PBST. Following incubation with the appropriate peroxidase-conjugated secondary antibody for 1 h at room temperature and additional washing steps, the blots were developed using the ECL detection kit (Perkin Elmer) followed by exposure to a Hyperfilm (GE Healthcare). Eventually, the exposed film was developed in the X-ray Processor XP505 (3M).
Afterwards, the membrane was shrink-wrapped with storage buffer and kept at 4°C.

2.2.3.6 Stripping: removal of the bound antibody complex from the membrane

Stripping buffer pH 6.8

Tris	62.5 mM
SDS	2 % (w/v)
DTT	100 mM

The membranes could be used for detection of further proteins. Therefore, the original bound antibody complex was removed from the membrane by shaking it in stripping buffer pH 6.8 for 30 min in a 60°C-water bath. Subsequent washing in PBST removed the stripping solution and the membrane could be utilized in another immunoassay, starting with the blocking buffer (2.2.3.5). Subsequent incubation with a specific antibody allowed the detection of a distinct protein.

2.2.3.7 Cervatec $p16^{INK4a}$ ELISA

This assay was used for the quantitative determination of human $p16^{INK4a}$ protein in the different HMEC populations during cellular senescence and was performed according to the manufacturer's recommendations (mtm laboratories). Briefly, 1×10^6 HMEC of passages 12 to 16 were collected in the appropriate Cervatec sampling vial (mtm laboratories) and incubated in the associated heating block (mtm laboratories). After incubating the samples in the particular microtiter stripes, the absorbance was measured at 450 nm using the Multiskan Ascent FL with Ascent software version 2.6 (Thermo Fisher Scientific).

2.2.3.8 Lysyl oxidase (LO) activity assay

4x LO-buffer pH 8.2

Urea	4.8 M
Sodium borate	200 mM

Stock solutions

Amplex red	10 mM
Horseradish peroxidase	1000 U/ml
1,5-diaminopentane	8.54 M
β-aminopropionitrile (BAPN)	50 mM

The LO activity assay is based on an indirect fluorescent method described by Palamakumbura and Trackman (Palamakumbura and Trackman, 2002). LO activity was determined in conditioned cell culture media as well as in whole cell lysates of HMEC. Conditioned media of young HMEC P12 and senescent HMEC P16 were collected after a 72 h culture period and concentrated about 25-fold using Amicon Ultra-4 Centrifugal Filter Units with an Ultracel-10 membrane (Millipore). Alternatively, HMEC P12 to P16 were harvested by trypsinization and

$1x10^6$ cells were homogenized in 4x LO-buffer pH 8.2. Both the concentrated media as well as the cell homogenates were subjected to a protein quantification measurement using the BCA protein assay (Pierce) (2.2.3.1).

For the fluorescent-based LO activity assay, samples were prepared in a final volume of 2 ml, containing 1.2 M urea, 50 mM sodium borate (pH 8.2), 1 U/ml horseradish peroxidase, 10 mM 1,5-diaminopentane (all from Sigma-Aldrich) and 10 µM Amplex red (Invitrogen). While LOs can oxidatively deaminate peptidyl lysine residues *in vivo*, these enzymes can also deaminate non-peptidyl amines *in vitro*, and thus, previous work has demonstrated that the 1,5-diaminopentane provides an optimal enzyme substrate in this assay (Trackman et al., 1981). The amine oxidation is accompanied by the release of hydrogen peroxide, which in turn reacts with Amplex red in the presence of horseradish peroxidase in a 1:1 stoichiometry to form the fluorescent product 7-hydroxy-3H-phenoxazine-3-one (resorufin).

Inhibitor samples were similarly prepared, but additionally contained the specific LO-inhibitor β-aminopropionitrile (BAPN) (500 µM) (Sigma-Aldrich) to completely abolish LO activity. The calibration curve was set up in the same buffer system using different amounts of hydrogen peroxide ranging from 0.025 ng to 1 ng. All samples were incubated for 1.5 h at 37°C. Finally, the fluorescent product was excited at 544 nm, and the emission was detected at 590 nm using the Fluoroskan Ascent FL with the appropriate Ascent software version 2.6 (Thermo Scientific). The resulting difference in fluorescence intensity between the control sample and the appropriate BAPN sample was recorded and normalized to the cell number.

2.2.4 Statistical analysis

All assays were performed in triplicate and experiments were repeated at least twice to confirm the results. Data represent mean ± SD and were statistically analyzed using the unpaired T-test (Microsoft Excel). Results were considered as statistically significant when P value was < 0.05 ($^*P < 0.05$; $^{**}P < 0.01$; $^{***}P < 0.001$).

3 Results

3.1 Cellular senescence in human mammary epithelial cells (HMEC)

3.1.1 Proliferation and morphology of HMEC during long term culture

Cellular senescence of primary HMEC is associated with significant morphological and functional changes. Young HMEC exhibited small, adherent cells which grew as a monolayer with frequent cell divisions (Figure 9a). But long term culture of these cells, and thus, the advanced senescence implicated considerable changes in cell morphology. The cells progressively increased in cell size and during passage 14 (P14) the enlarged HMEC formed long cytoplasmic processes spread across several neighbor cells. Finally, senescent HMEC after P16 developed enormous giant cells, exhibiting several fold the size of young P12 HMEC (Figure 9a). Consistent with the enlarged morphology of senescent HMEC, determination of the total protein amount in HMEC P12 compared to HMEC P16 demonstrated a significant increase in the protein quantity per cell during cellular senescence (Figure 9b).

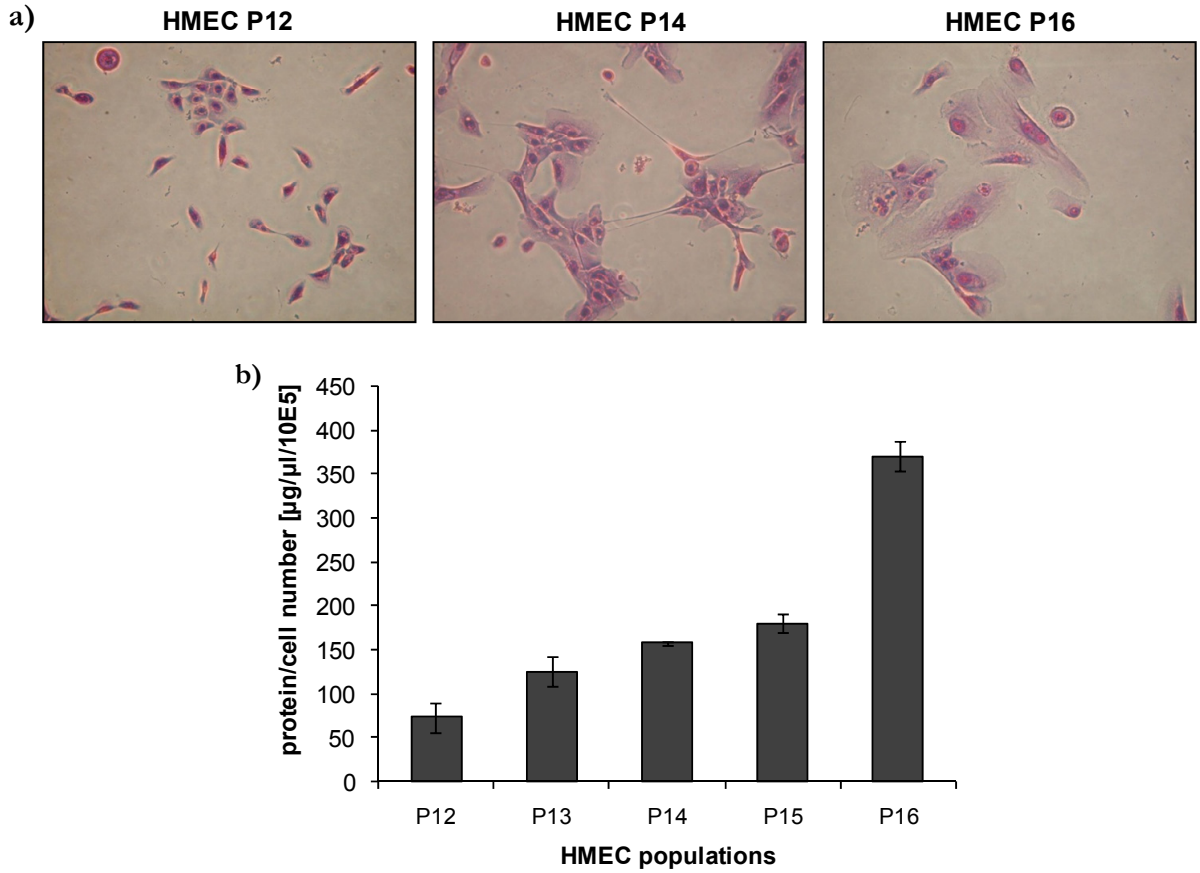

Figure 9: Morphological changes and the total protein amount per cell following senescence of HMEC.

(a) The morphology of HMEC cultures in passage 12, 14 and 16 was visualized by Pappenheim-staining. The initially young small HMEC in P12 increased in size and grew up to giant cells in P16 (magnification 200x) (Bertram and Hass, 2008a). (b) The total amount of proteins per cell was determined in the different HMEC populations, revealing a progressive increase during cellular senescence. Data represent mean ± SD of three independent experiments.

Whereas young small HMEC until P13 possessed strong proliferative capacity, demonstrated by population doublings per day (Figure 10a), cell growth was gradually reduced with increasing culture period and advanced cellular senescence. While young HMEC P12 doubled approximately every 1.5 days, HMEC P14 had a doubling time of about 5 days and, finally, in senescent HMEC P16 little if any cell division could be detected (Figure 10a). However, this was not associated with an increase in cell death. Both the young proliferative HMEC populations and the senescent populations demonstrated a cell viability of about 92 % to 85 %, respectively (Figure 10b). Thus, senescent cells cease proliferation but remain in a viable and metabolically active state.

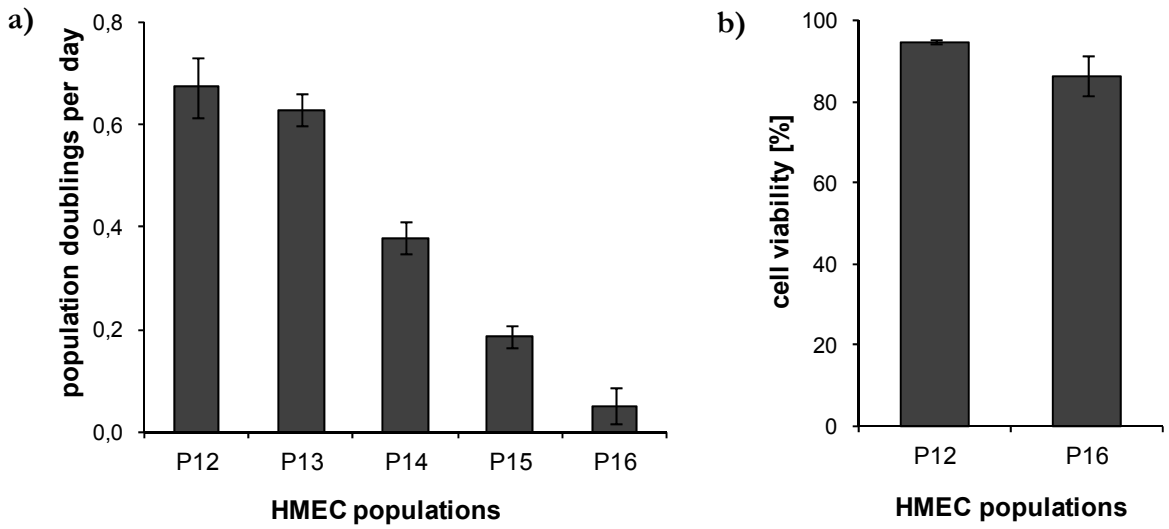

Figure 10: Analysis of proliferative capacity and cell viability in HMEC cultures.
(a) Within the appropriate passages, cell number and cell viability were determined by trypan exclusion. Proliferative capacity, represented by population doublings per day, significantly decreased during cellular senescence of HMEC. Error bars represent the mean ± SD of five independent experiments. (b) However, cell viability was not affected by the aging process and both young and senescent HMEC demonstrated about 92% to 85% viable cells. Error bars represent the mean ± SD of five independent experiments. (Bertram and Hass, 2008a)

3.1.2 HMEC cell cycle distribution during cellular senescence

As exemplified by the proliferation data (Figure 10), cellular senescence of HMEC was accompanied by a remarkable decrease in cell growth. This was substantiated by flow cytometry analysis of the cell cycle distribution in HMEC populations between passage 12 and 16 (Figure 11). Cell cycle histograms exemplarily represented the cell cycle pattern of HMEC P12, P14 and P16, respectively (Figure 11a) and quantitative evaluation of the distinct cell cycle phases is shown in the bar diagram (Figure 11b). With increasing culture period, cell cycle analysis of the different stages during senescence revealed a continuously decreasing amount of cells with 2N DNA (from 73% ± 1.1% in P12 to 32% ± 1.0% in P16) and S phase cells (from 7 % ± 0.3 % in P12 to 2% ± 0.2% in P16), respectively. On the contrary, markedly elevated

levels could be detected for the 4N DNA population with progressing senescence (from 17 % ± 0.5 % in P12 to 44 % ± 0.5 % in P16). Moreover, this was paralleled by the appearance of a peak in the range of 8N DNA, probably representing aberrant mitosis with DNA doubling but no subsequent cell division. In conformity with the viability data, no massive cell death could be discovered by flow cytometry during cellular senescence of HMEC and the amount of dying cells indicated by the degraded DNA remained below 5 % (Figure 11b). These findings suggested senescence to be initiated following passage 13 and finalized after passage 15.

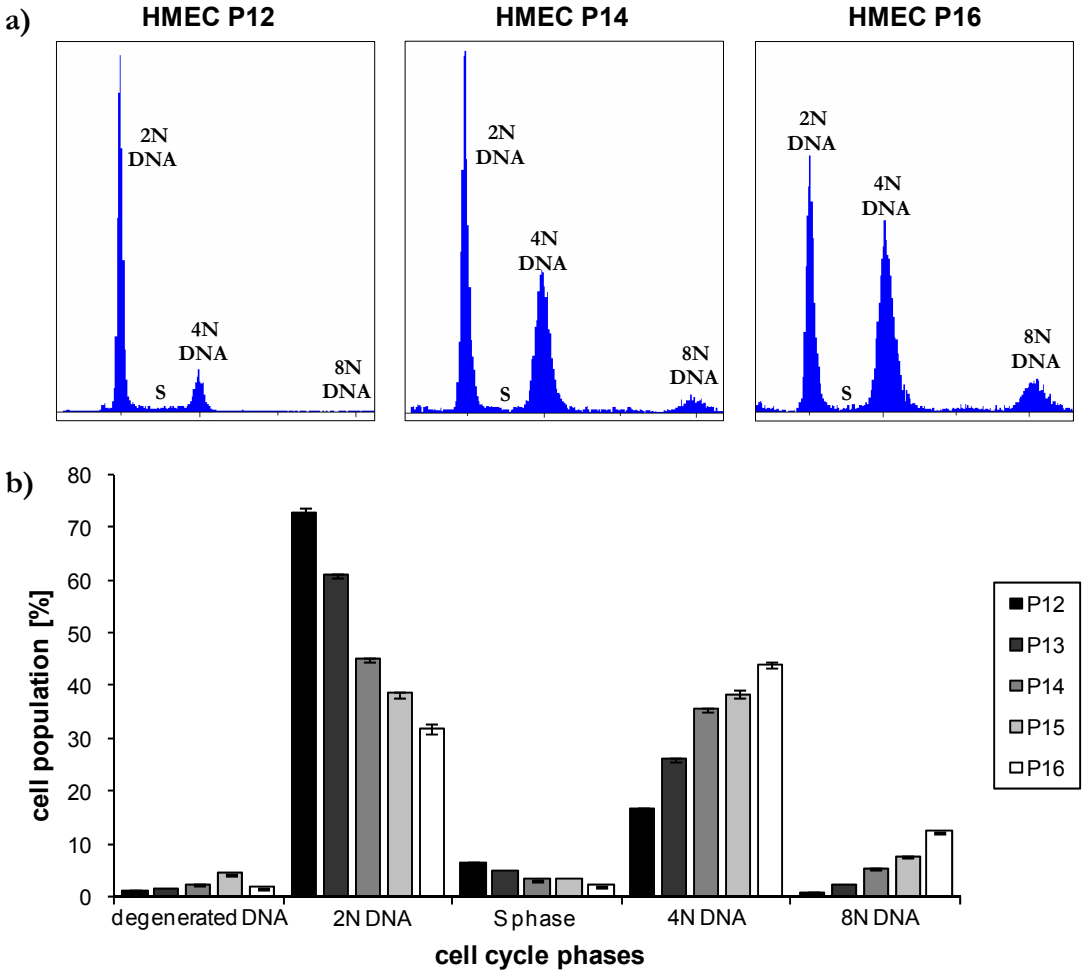

Figure 11: Cell cycle analysis of HMEC cultures during cellular senescence.

(a) The cell cycle distribution of HMEC P12, P14 and P16 is represented by flow cytometric histograms and (b) quantitative determination of each particular cell cycle phase was evaluated using FlowMax software. A progressively decreasing level of cells with 2N DNA was paralleled by an accumulation of 4N DNA cells during the aging process of HMEC. HMEC populations after P15 ceased to divide. Following aberrant mitosis by DNA doubling without cell division a population with 8N DNA arose. Data represent mean ± SD of three independent experiments. (Bertram and Hass, 2008a)

3.1.3 Senescence-associated marker proteins

To further characterize the senescent status of the different HMEC populations, expression and activity of distinct senescence-associated proteins was investigated. It was previously demonstrated that the activity of the enzyme senescence-associated β-galactosidase (SA β-gal) markedly increased in certain senescent cells, including HMEC (Romanov et al., 2001). Determination of SA β-gal activity was performed using a cytological assay which allows the visualization of substrate turnover. The synthetic substrate X-gal, composed of a galactoside linked to indole, is cleaved by SA β-gal and subsequent oxidation results in the development of a blue color. Images of the cytological staining of young and senescent HMEC are exemplarily shown in passage 12, 14 and 16 demonstrating the missing activity in HMEC P12 in contrast to the high SA β-gal activity and the predominant staining in HMEC P16 (Figure 12a). Quantification revealed only 6 ± 1.4 % positive cells in the HMEC P12 population, whereas the amount of SA β-gal-active cells gradually increased with succeeding culture period and the P16 cell population demonstrated SA β-gal activity in 81 ± 2.5 % of the cells (Figure 12b).

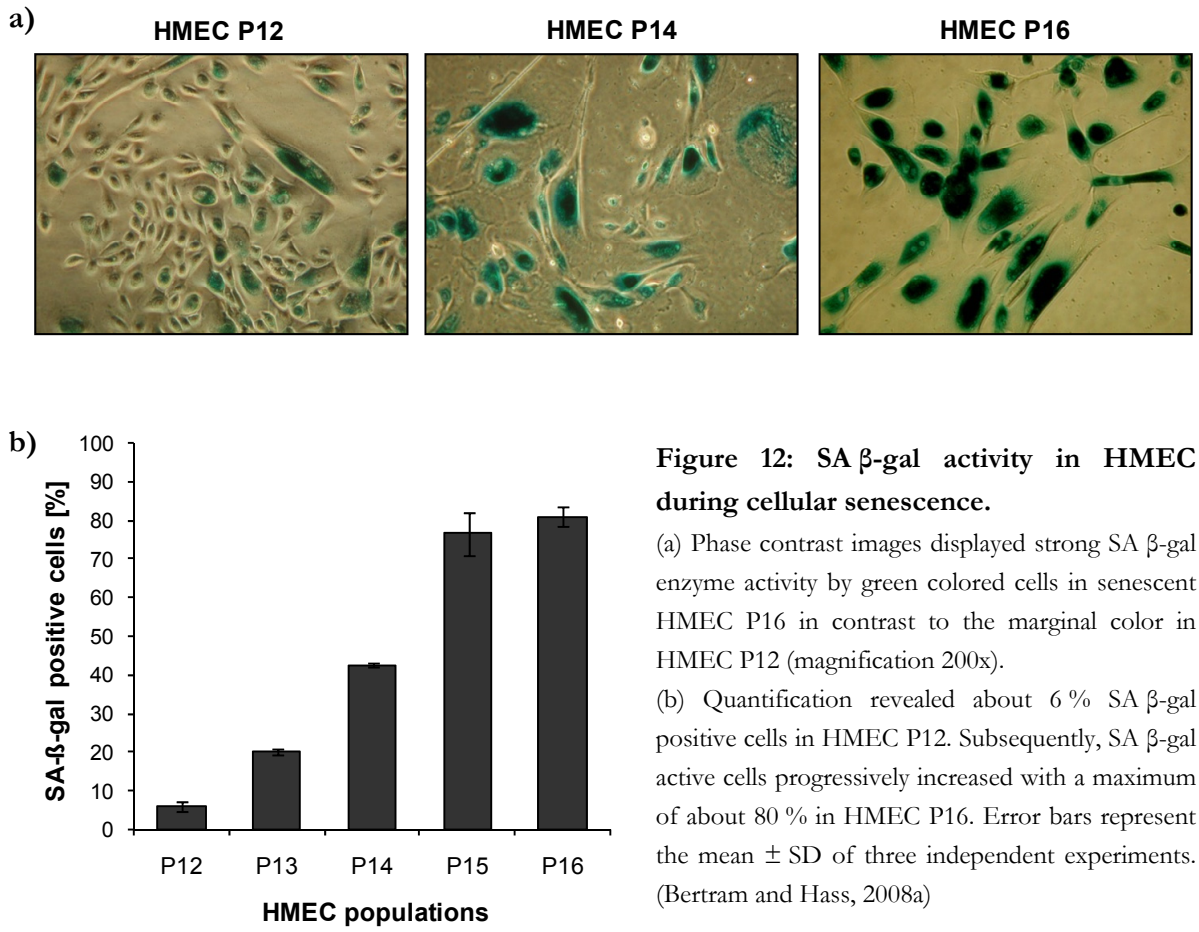

Figure 12: SA β-gal activity in HMEC during cellular senescence.

(a) Phase contrast images displayed strong SA β-gal enzyme activity by green colored cells in senescent HMEC P16 in contrast to the marginal color in HMEC P12 (magnification 200x).

(b) Quantification revealed about 6 % SA β-gal positive cells in HMEC P12. Subsequently, SA β-gal active cells progressively increased with a maximum of about 80 % in HMEC P16. Error bars represent the mean ± SD of three independent experiments. (Bertram and Hass, 2008a)

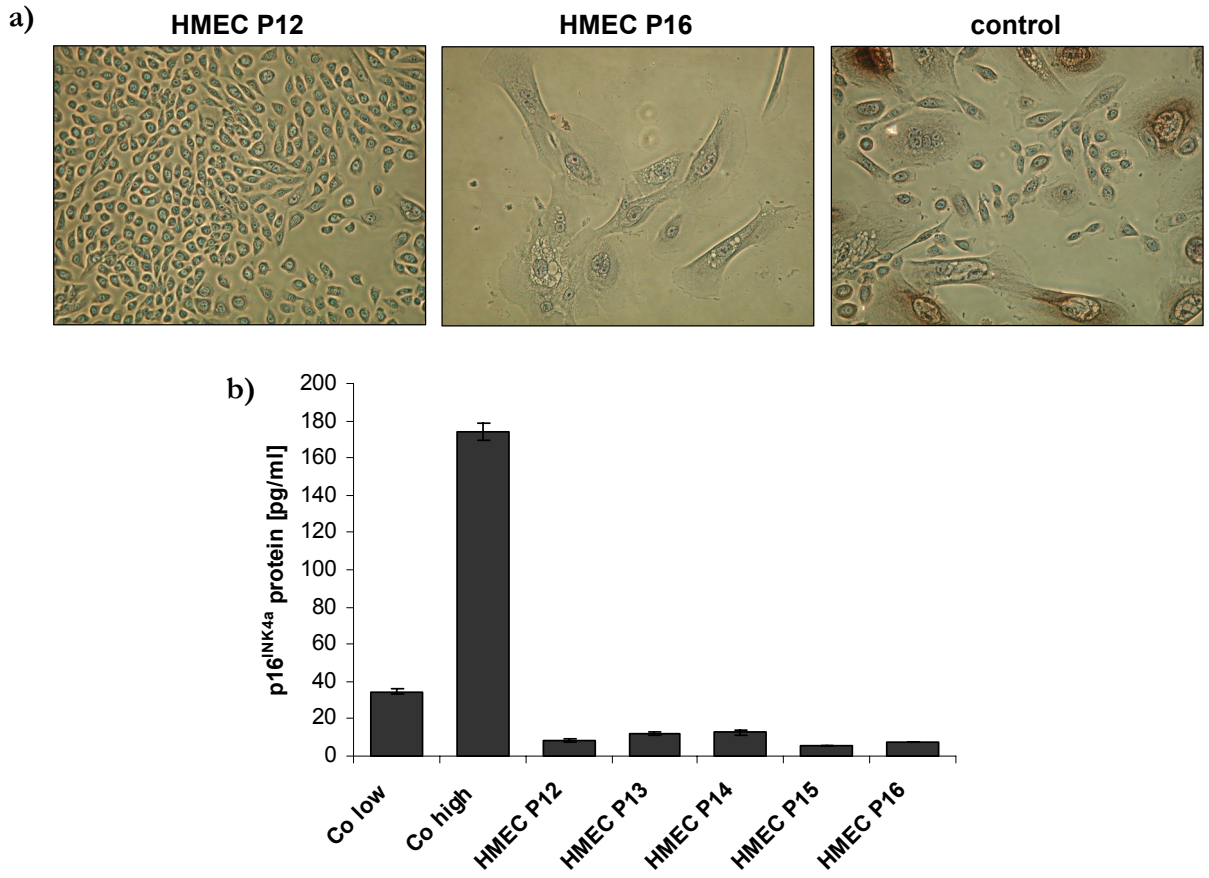

Figure 13: Expression of the cell cycle inhibitor p16^{INK4a} in HMEC.

(a) Cytological staining of HMEC P12 and P16 revealed no p16^{INK4a} protein expression in either HMEC passage. Primary breast epithelial cultures, obtained from a surgery, were used as a positive control and the p16^{INK4a} expression could be monitored by a brown staining in the enlarged, cell cycle-arrested cells. Cell nuclei were visualized by Haematoxylin staining (magnification 200x). (b) Quantitative determination of p16^{INK4a} protein by ELISA confirmed p16^{INK4a} levels below detection limit (Co low) in all HMEC populations. Accordingly, this characterizes the post-selection state of these HMEC populations (Huschtscha et al., 1998). Data represent the mean ± SD of three independent experiments.

However, an increased SA β-gal activity on its own cannot be accepted to prove senescence and requires additional verification. Thus, the senescent state of HMEC was further examined by expression analysis of the cell cycle inhibitor p16^{INK4a}. The growth phase of HMEC can be distinguished by discrete proliferation barriers, named stasis and agonescence. Whereas stasis is characterized by a significantly increasing expression of the cell cycle inhibitor p16^{INK4a}, HMEC overcoming this barrier by a selection process lack the expression of this CDK inhibitor. The expression status of p16^{INK4a} in HMEC was detected by a cytological immunostaining, demonstrating the presence of p16^{INK4a} by a brown color (Figure 13a). The cell nuclei were counterstained with Haematoxylin and primary breast epithelial cells, obtained from a surgery, were used as a positive control. Whereas in enlarged cell cycle-arrested control cells a strong brown color was exhibited, expression of the cell cycle inhibitor was not detectable in the small

dividing control population (Figure 13a, control). Cytological immunostaining of cultured HMEC between P12 and P16, however, revealed no detectable $p16^{INK4a}$ expression in either population (Figure 13a, HMEC P12 and HMEC P16). This was further substantiated using quantitative determination of $p16^{INK4a}$ protein expression by ELISA (Figure 13b). Control samples provided with the ELISA kit established the concentration range for low $p16^{INK4a}$ protein levels (Co low) and for high $p16^{INK4a}$ quantity (Co high) (Figure 13b). However, independent of their proliferative capacity and their aging state, all HMEC populations displayed a $p16^{INK4a}$ protein amount below the lowest control level (Figure 13b), validating the qualitative results from the cytological immunostaining (Figure 13a).

In conclusion, these results (3.1.1-3.1.3) allowed the characterization of HMEC P12 as young, proliferative post-selection HMEC and cells in P16 as senescent, cell cycle-arrested post-selection HMEC. In the following, every HMEC culture described and each experiment performed is always referred to post-selection HMEC, which finally encounter telomere-dependent agonescence.

3.2 Alterations of extracellular-associated proteins during cellular senescence of HMEC

Changes of proliferative capacity, cell morphology and cell attachment processes in senescent HMEC suggested further functional alterations correlated with the aging process of these cells. Initially, investigations were focused on molecules involved in cell-cell and cell-matrix interactions such as cell surface glycoproteins and certain matrix metalloproteinases (MMPs).

3.2.1 Cell surface proteins

Accordingly, a variety of surface adhesion molecules were examined during cellular senescence of HMEC and the human breast carcinoma cell line MCF-7 was used as a reference. Preferred cell surface proteins were represented by CD24, CD29, CD44 and CD227 (MUC1). Whereas the β_1-integrin family member CD29 was uniformly expressed in the cancer cell line as well as in young and senescent post-selection HMEC at about 100 %, expression levels of CD24 and CD44 were affected by the aging process of HMEC (Figure 14). The detected fluorescence intensity of nearly 100 % for CD24 and CD44 was similar in young HMEC and the immortalized MCF-7 cell line but was significantly reduced to 66 % and 61 % in senescent HMEC, respectively (Figure 14). CD227 protein levels, however, were already decreased when comparing primary HMEC P12 (81 %) with the MCF-7 tumor cell line (97 %) and further declined upon senescence (40 %) (Figure 14). Previous work has demonstrated alterations of certain protein levels upon long-term culture of MCF-7 (> P500) such as a loss of transforming growth factor-beta type II receptor (Wu et al., 1998; Wenger et al., 2004) or distinct surface proteins (Hand et al., 1983). The short-term passages of MCF-7 cells we used in our lab (P <150), however, demonstrated no alterations in surface marker expression caused by subculturing (data not shown).

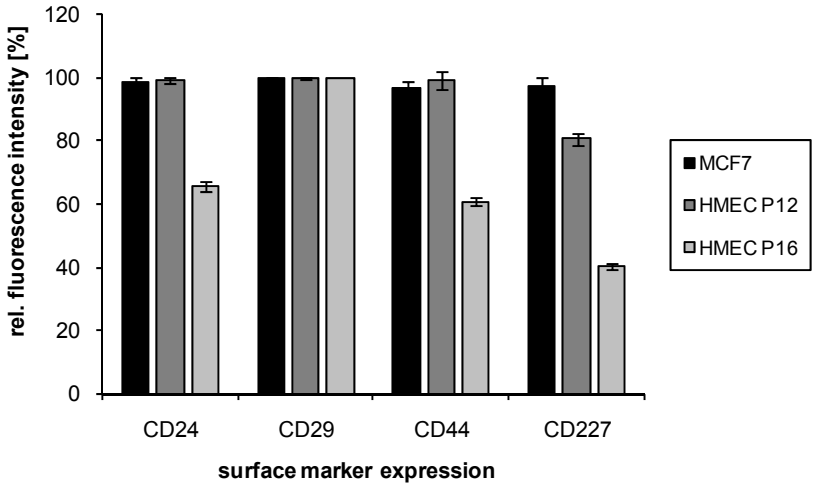

Figure 14: Analysis of cell surface proteins in HMEC and tumorigenic MCF-7 cells.
The β_1 integrin family member CD29 was uniformly expressed during the aging process of HMEC. However, CD24, CD44 as well as CD227 were significantly down-regulated in association with HMEC senescence. In contrast, tumorigenic MCF-7 exhibited these surface markers at about 100 %. Data represent the mean ± SD of three independent experiments. (Bertram and Hass, 2008a)

3.2.2 Matrix metalloproteinases (MMPs)

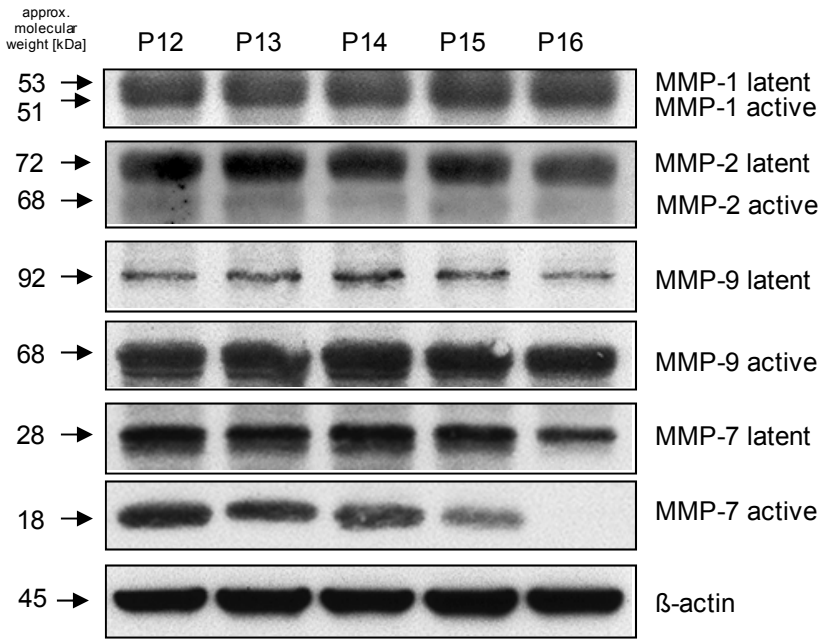

Figure 15: Expression analysis of MMPs during senescence of HMEC.
Both the latent progenitor form and the proteolytically active form of MMP-1, MMP-2 and MMP-9 were uniformly expressed in all passages of aging HMEC. However, the latent form of MMP-7 was slightly decreased after P15 and the active enzyme diminished below detection level in P16. The cytoskeletal protein β-actin was used as loading control. (Bertram and Hass, 2008a)

Matrix metalloproteinases comprise a strong proteolytic activity and thus are involved in ECM degradation and remodeling as well as modification of signaling molecules and activation of precursor proteins. Therefore, it was of interest to examine the expression pattern of certain MMPs during the process of cellular senescence in HMEC. Each MMP can be distinguished into its latent precursor form and its cleaved, active form, respectively. Thus, MMP-1, MMP-2 and MMP-9 demonstrated equal expression levels between P12 and P16 for both the latent and active form of these proteins and were not influenced by HMEC senescence (Figure 15). In contrast, latent MMP-7 exhibited a slight down-regulation between passage 15 and 16, which was even more pronounced by the active form. Active MMP-7 was significantly reduced after P14 and the protein quantity was below detection level in P16 (Figure 15), indicating a potential role of this extracellular protease during cellular senescence of HMEC.

3.3 The role of MMP-7 during cellular senescence of HMEC

In order to investigate a possible role of MMP-7 in the context of HMEC senescence, its expression was targeted by RNAi in HMEC P12. Accordingly, reduced MMP-7 protein levels in young HMEC induced by siRNA targeting could reveal potential implications of an impaired MMP-7 signaling associated with the HMEC senescence process.

3.3.1 Down-modulation of MMP-7 induced a premature senescence in young HMEC

Primary HMEC in passage 12 were initially transfected with pmaxGFP plasmid to verify the transfection method using the Nucleofector (amaxa). Thus, different manufacturer-recommended programs were tested and GFP expression was examined by fluorescence microscopy (data not shown). The program, resulting in the best balance between cell viability and transfection efficiency, represented by GFP expression (Figure 16a), was used for further transfection experiments. Additionally, non-silencing, green fluorescence-labeled siRNA-AF488 (FITC-siRNA) was used to analyze the transfection efficiency, when comparing FITC-labeled siRNA transfected HMEC with non-transfected HMEC by flow cytometry. This demonstrated about 80 % transfected cells using the nucleofector program X-005 (Figure 16b). Down-modulation of MMP-7 was performed by transfection of young HMEC P12 with two specific MMP-7 siRNAs and the appropriate control transfections were carried out using non-targeting AllStars Negative Control siRNA (neg. siRNA) (2.1.4 and 2.2.1.12). Following incubation for 24 h, 48 h and 72 h, respectively, the cells were harvested and MMP-7 protein levels were documented by Western blot analysis (Figure 16c). This demonstrated a significant down-modulation of both the latent and the active form of MMP-7 between 48 h and 72 h in contrast to unregulated protein levels in negative siRNA transfected HMEC, 24 h MMP-7 siRNA transfectants and pmaxGFP control transfectants (Figure 16c).

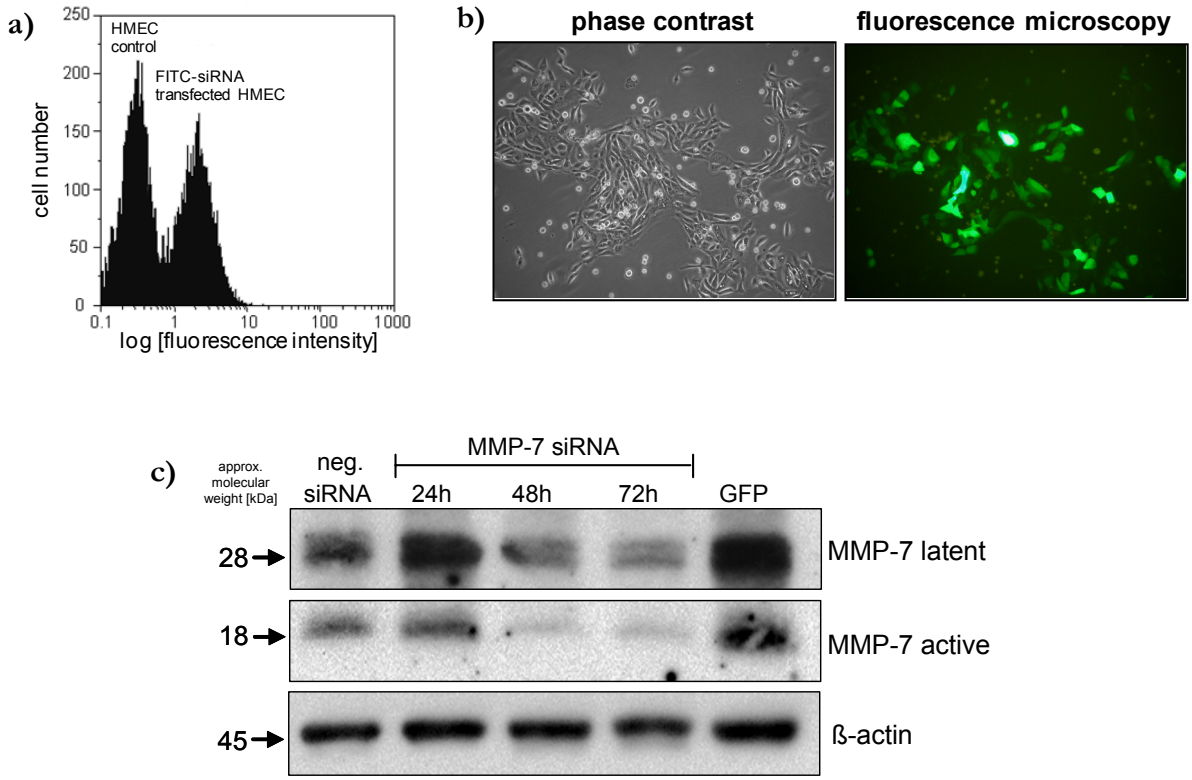

Figure 16: RNAi of MMP-7 in HMEC P12.

(a) HMEC (HMEC control) and HMEC transfected with green fluorescence-labeled siRNA-AF488 (FITC-siRNA-transfected HMEC) were analyzed by flow cytometry. The siRNA transfection using program X-005 of the Nucleofector II yielded in an efficiency of 80 %. (b) The pmaxGFP plasmid was provided with the HMEC nucleofector kit and served as a positive control. 48 h post transfection, pmaxGFP-transfected cells were visualized by phase contrast and fluorescence microscopy, respectively. (c) HMEC transfected with MMP-7 siRNA were harvested 24 h, 48 h and 72 h post transfection and Western blot analysis revealed a significant down-modulation of both the latent and active form of MMP-7 after 48 h and 72 h compared to control-transfected HMEC. Staining with anti-β-actin was used as a loading control. (Bertram and Hass, 2008a)

a)

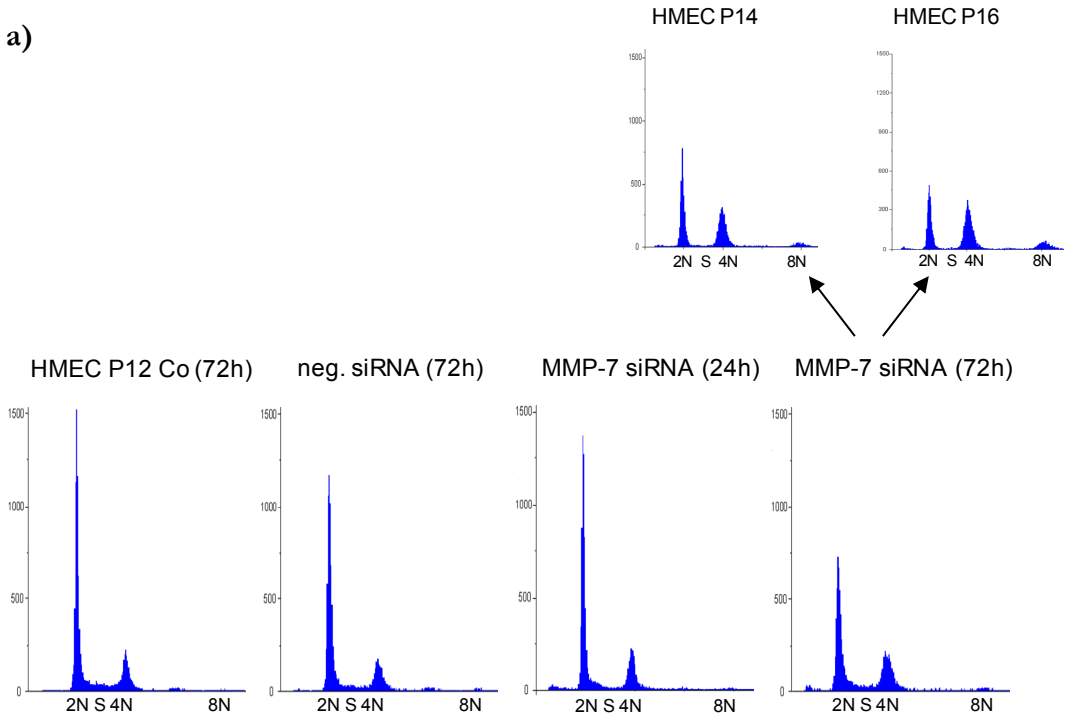

deg. DNA [%]	1	1	4	3
2N DNA [%]	61	61	60	48
S phase [%]	13	9	7	9
4N DNA [%]	18	18	20	26
8N DNA [%]	1	2	2	3

b)

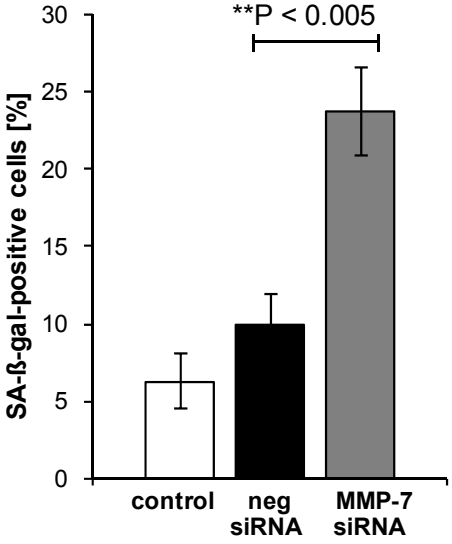

Figure 17: Functional analysis of young HMEC after down-modulation of MMP-7.

(a) Flow cytometry analysis revealed a cell cycle distribution of HMEC control cells, negative siRNA-transfected HMEC and 24 h MMP-7 siRNA transfectants similar to HMEC P12. However, after 72 h, the amount of 2N DNA cells decreased in MMP-7 siRNA-transfected HMEC (48 %). This was paralleled by a marked accumulation of cells with 4N DNA (26 %), resembling a cell cycle pattern of HMEC populations in about P14 before reaching senescence in P16. Deviations from a total of 100 % result due to mathematical rounding and cells excluded from the gating regions as they represent no numeral DNA content. (b) Determination of SA β-gal activity revealed an increased amount of senescent cells in 72 h MMP-7 siRNA transfectants (25 % ± 3.2 %) (**P < 0.005) compared to a 72 h populations of control HMEC (6 % ± 2.1 %) and negative siRNA transfectants (10 % ± 2.2 %), respectively. (Bertram and Hass, 2008a)

Subsequent functional investigations were performed by cell cycle analysis and SA β-gal assay to reveal potential effects on proliferation and senescence due to MMP-7 down-modulation in young HMEC. Flow cytometry analysis demonstrated a cell cycle distribution of negative siRNA transfected HMEC resembling the pattern of non-transfected control cells in passage 12 (Figure 17a), confirming that the transfection methods itself had no effect on the cell cycle. Moreover, 24 h MMP-7 siRNA transfected cells displayed a similar cell cycle as the control populations. However, down-modulation of MMP-7 for 72 h induced significant alterations of the cell cycle pattern in these cells. Whereas the amount of cells with 2N DNA was markedly reduced (from 60 % to 48 %), the 4N DNA population obviously increased from 18 % to 26 % (Figure 17a), suggesting an induced growth arrest upon decreased MMP-7 protein levels. When comparing the cell cycle distribution after MMP-7 RNAi with the different cell cycle patterns during cellular senescence, it became apparent that MMP-7 down-modulation provoked a cell cycle resembling that of aging HMEC in P14 before encountering senescence in P16 (Figure 17a).
These findings were further verified by staining for SA β-gal activity (Figure 17b). Thus, SA β-gal activity was significantly increased after MMP-7 RNAi and revealed 25 % ± 3.2 % senescent cells in the 72 h MMP-7 siRNA transfected HMEC population in contrast to 6 % ± 2.1 % and 10 % ± 2.2 % in 72 h non-transfected HMEC and negative siRNA transfectants, respectively (Figure 17b). These findings confirmed a premature senescence in HMEC P12 upon down-modulation of MMP-7.
Taken together, these results validated an important role of MMP-7 during cellular senescence of HMEC and demonstrated an accelerated aging process in young HMEC due to reduced protein levels of MMP-7.

3.3.2 MMP-7 RNAi in the breast cancer cell line MCF-7

The induced aging process as a consequence of down-modulated MMP-7 in primary normal HMEC was additionally evaluated in the breast cancer cell line MCF-7. Therefore, these immortalized cancer cells were transfected with MMP-7 siRNA and subsequently analyzed for alterations in MMP-7 protein expression, cell cycle distribution and SA β-gal activity (Figure 18). Successful down-modulation of MMP-7 was demonstrated for the latent precursor form as well as for the active protein form by Western blot analysis (Figure 18a). Cell cycle analysis of transfected MCF-7 cancer cells exhibited a slight increase of 2N DNA cells, whereas the amount of cells with 4N DNA decreased upon MMP-7 down-modulation (Figure 18b). Additionally, SA β-gal activity was slightly affected and increased upon MMP-7 siRNA transfection (Figure 18c). However, compared to negative siRNA transfected HMEC, statistical analysis showed no significance of these values, suggesting that genetic alterations in this artificial, immortalized cell line may interfere with a sufficient induction of senescence.

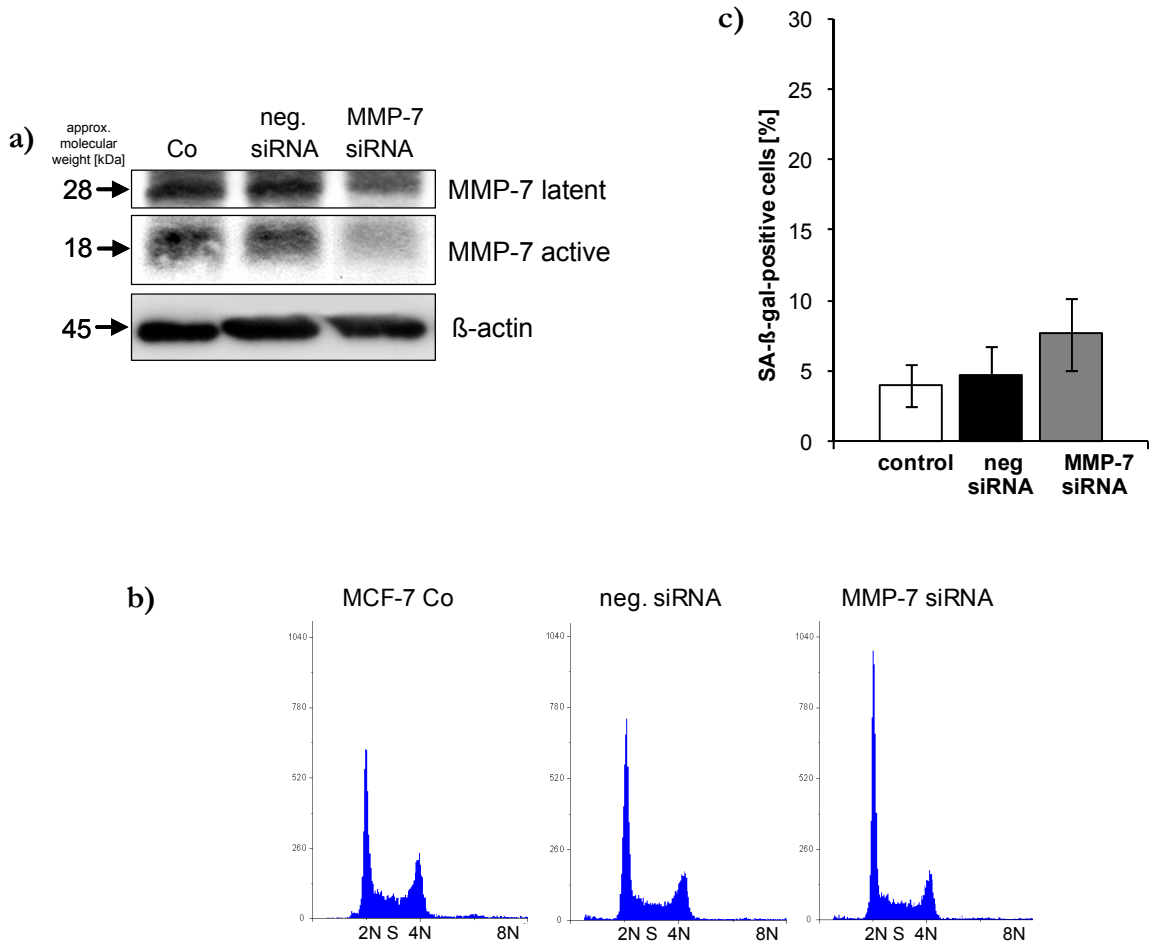

deg. DNA [%]	2	3	2
2N DNA [%]	42	48	52
S phase [%]	24	19	21
4N DNA [%]	27	27	19
8N DNA [%]	1	1	1

Figure 18: MMP-7 down-modulation in MCF-7.

MCF-7 breast cancer cells were transiently transfected with MMP-7 siRNA as compared to control cells and to negative siRNA transfected cells and harvested 48h post transfection. (a) Western blot analysis revealed a successful down-modulation of both the latent and active form of MMP-7 in the appropriately transfected MCF-7 population, whereby β-actin was used as loading control. (b) However, cell cycle distribution was not significantly affected by MMP-7 RNAi. Deviations from a total of 100 % result due to mathematical rounding and cells excluded from the gating regions as they represent no numeral DNA content. (c) The SA β-gal staining was increased in the MMP-7-transfected MCF-7 population, but the unpaired t-test revealed no statistical significance. Data represent mean ± SD of three independent experiments.

3.4 The role of the extracellular matrix (ECM) during cellular senescence of HMEC

3.4.1 The extracellular filaments

Cellular senescence of HMEC was associated with an enhanced formation of extracellular filaments. A stable network of fine characteristic structures became detectable in HMEC cultures after passage 14 and markedly increased in the senescent P16 population (Figure 19). These regular, well-organized fine fibers spread across the media surface of senescent HMEC, whereas no comparable structures were observed in HMEC between P12 and P14.

Immunofluorescence analysis of this extracellular filament allowed the detection of certain matrix proteins as compounds of these fibers, including fibrillin-1 and polymeric elastin (Figure 20). Immunostaining with a specific anti-elastin antibody revealed a fibrillar organization of this polymer, whereas the anti-fibrillin-1 antibody recognized a scattered pattern of structures with distinct localization (Figure 20). The merged fluorescence images demonstrated that these distinctive appearing fibrillin-1 structures co-localize with the fibrillar shape of elastin, suggesting the extracellular filament in senescent HMEC cultures to be composed of elastin-like structures. Control experiments confirmed the specificity of the secondary antibodies and immunostaining with these antibodies alone revealed no detectable fluorescence.

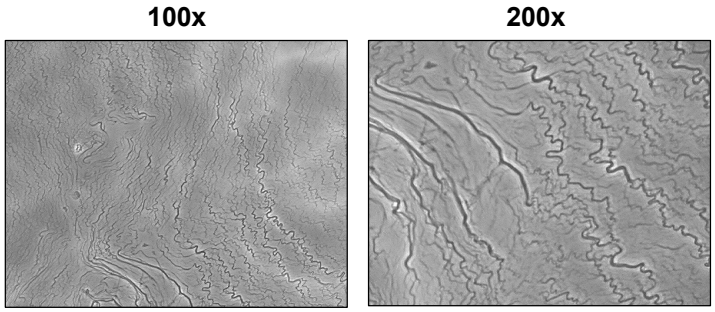

Figure 19: Extracellular fiber network in senescent HMEC cultures.

Phase contrast images showed a regular, well-organized network of distinct fibers in the senescent HMEC culture (magnification 100x and 200x). However, no comparable structures were visible in cultures of young, dividing HMEC in P12 to P14.

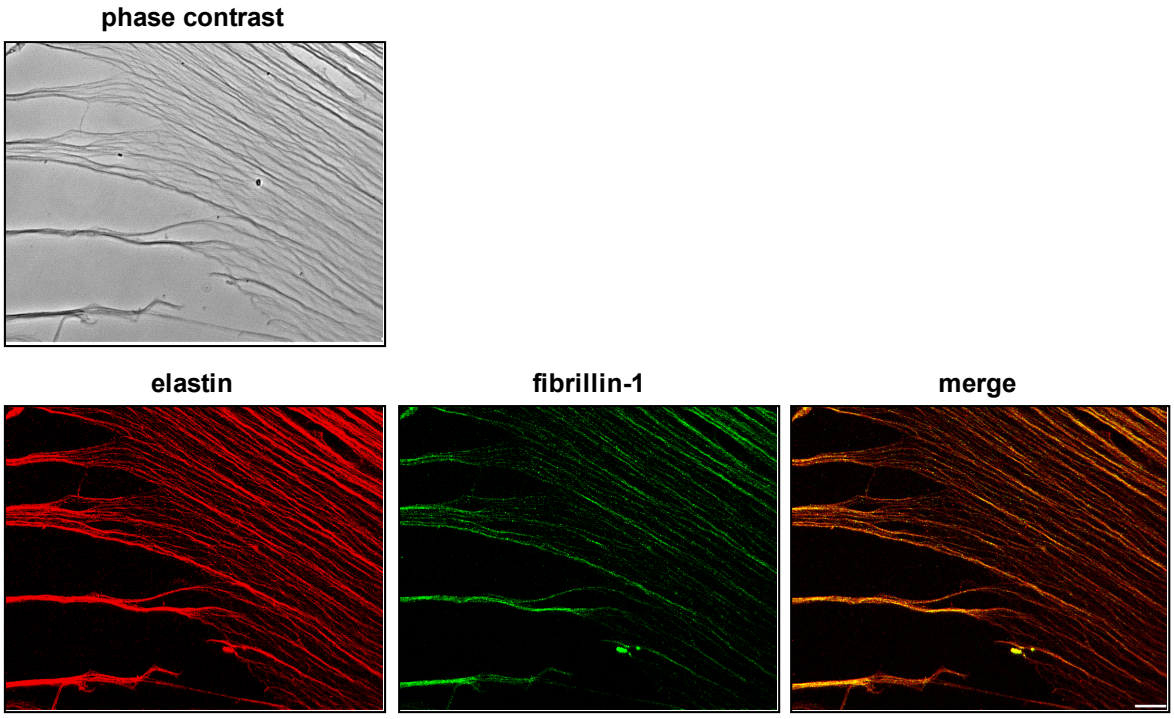

Figure 20: IF analysis of the extracellular filament in senescent HMEC cultures.
Immunofluorescence allowed the detection of the ECM proteins fibrillin-1 and polymeric elastin. While the anti-elastin antibody identified a fibrous network (red), the anti-fibrillin-1 antibody demonstrated a distinctive scattered pattern (green). The merged image showed an overlay of elastin with fibrillin-1, suggesting a filament composed of elastin-like structures in the senescent HMEC population (bar = 30 μm).

3.4.2 Fiber maturation during HMEC senescence is BAPN-dependent

Elastin fiber generation requires enzyme activity of lysyl oxidases (LOs). This enzyme family is responsible for cross-linking of the elastin precursor protein tropoelastin to form insoluble elastic filaments as part of the ECM (1.3.1.3). In order to verify the immunofluorescence detection of extracellular elastin in senescent HMEC cultures and to confirm the cellular origin of these elastin-like structures, LO activity was prevented by incubation with the synthetic LO inhibitor β-aminopropionitrile (BAPN). HMEC populations were cultured in the presence and absence of BAPN for 12 days with regular media changes (2.2.1.3). Whereas the untreated HMEC P16 populations generated elastin-like structures, no comparable extracellular fibers were detectable in HMEC P16 after BAPN incubation. Using immunofluorescence analysis, the anti-fibrillin-1 antibody revealed small aggregates at the cell surface of HMEC populations independent of BAPN treatment (Figure 21). In contrast, the anti-elastin antibody detected cell-associated aggregates at the HMEC controls, whereas little if any elastin could be detected after BAPN stimulation (Figure 21). Moreover, the merged fluorescence images displayed a co-localization of fibrillin-1 and elastin in the HMEC P16 control populations in cell-associated aggregates and fibers. These data demonstrated that the elastin-like fiber formation in senescent HMEC P16 was inhibited upon BAPN incubation and thus is dependent on LO activity.

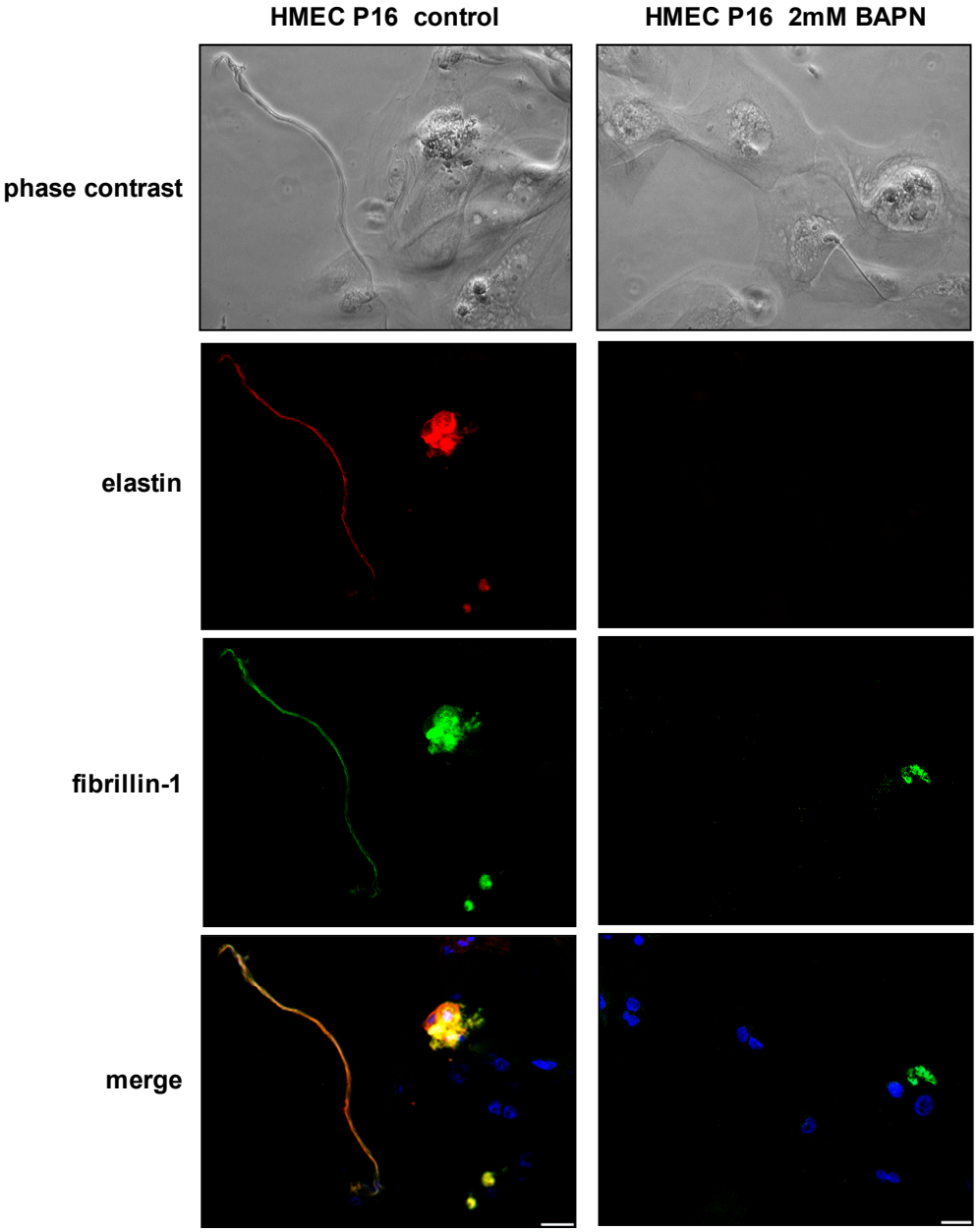

Figure 21: Cell-associated elastin-like fiber formation.

Immunofluorescence studies of senescent control HMEC P16 compared to senescent BAPN-treated HMEC P16 revealed the formation of cell-associated aggregates, consisting of elastin (red) and fibrillin-1 (green), at the cell surface of untreated HMEC populations. Moreover, the polymerization of extracellular elastin-like fibers could be observed in the controls. The BAPN-treated HMEC cultures demonstrated some cell-associated fibrillin-1; however, no elastin was detectable in these populations. The nuclei were stained using Hoechst 33258 (bar = 50 μm).

3.4.3 Lysyl oxidase expression and activity during cellular senescence of HMEC

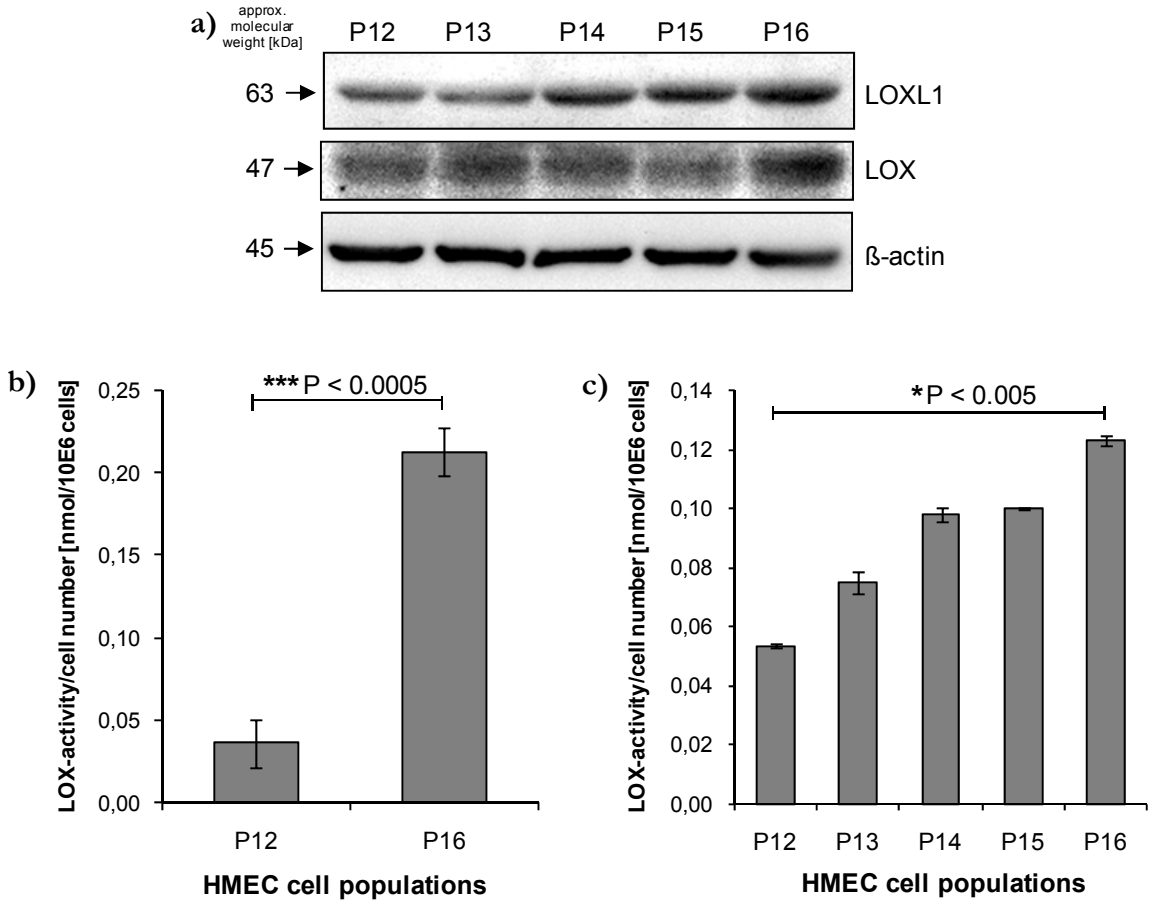

Figure 22: LO protein expression and enzyme activity during cellular senescence of HMEC.
(a) Protein expression of LOXL1, an important enzyme for cross-linking of elastin molecules, was gradually elevated during HMEC senescence and LOX demonstrated an increased expression in HMEC P16. (b) Enzyme activity measurements revealed a dramatic increase in extracellular LO activity in the conditioned media of senescent HMEC cultures P16 compared to the respective media of young HMEC P12 (***P < 0.0005). (c) Enzyme activity of cell-associated LO was determined in HMEC lysates, demonstrating a progressive increase during cellular senescence (P12 to P16). Comparing young, dividing HMEC P12 and senescent HMEC P16, LO activity was 2.5-fold elevated in the senescent population (**P < 0.005) when calculated based upon an equal amount of cells. This was in concert with the measurements in the conditioned media. Data represent mean ± SD of three independent experiments.

Subsequently, the question arose, whether this enhanced formation of extracellular structures in senescent HMEC cultures is accompanied by elevated LO protein levels and enhanced enzyme activities. Initially, intracellular expression levels of two distinct members of the LO enzyme family, LOX and LOXL1, were investigated during HMEC senescence, whereby LOXL1 is the enzyme predominantly involved in elastin polymerization. Expression of LOX was slightly affected by the aging process of HMEC and the protein levels were enhanced in passage 16

(Figure 22a). LOXL1 protein levels gradually increased after passage 13 and were significantly elevated in senescent HMEC P16 (Figure 22a).

Although these results implied a marked increase in lysyl oxidase occurrence, these enzymes require proteolytic activation, and thus, it remained unclear if senescence is actually associated with an enhanced LO activity. To address this question, enzyme activity was determined by substrate turnover and subsequent detection of fluorescence intensity (Figure 22b and c). While LO can oxidatively deaminate peptidyl lysine residues *in vivo*, these enzymes can also deaminate non-peptidyl amines *in vitro*, and thus, previous work has demonstrated that the 1,5-diaminopentane provides an optimal enzyme substrate in this assay (cp. 2.2.3.8) (Trackman et al., 1981). Moreover, the amine oxidation is accompanied by release of hydrogen peroxide, which in turn reacts with N-acetyl-3,7-dihydroxyphenoxazine (Amplex red) in the presence of horseradish peroxidase in a 1:1 stoichiometry to the fluorescent product 7-hydroxy-3H-phenoxazine-3-one (resorufin). To exclude other oxidase activities and ensure exclusive determination of lysyl oxidase activity, samples were additionally prepared while adding of LO inhibitor BAPN. The resulting difference in fluorescence intensity, and thus, substrate turnover, finally provides the particular LO enzyme activity. During cellular senescence of HMEC, LO activity was determined in the extracellular environment (Figure 22b) as well as cell-associated (Figure 22c). Extracellular activity of secreted LO was examined in the 72 h cell culture supernatant of young proliferating HMEC P12 and compared to senescent HMEC P16, respectively. Thus, the conditioned media of senescent P16 cells revealed a more than 6-fold higher LO activity (***$P < 0.0005$) as compared to young proliferating P12 HMEC (Figure 22b). Moreover, cellular-associated LO activity in HMEC whole cell lysates was measured during senescence and demonstrated an about 2.5-fold increased LO activity between P12 and P16 (*$P < 0.005$), when calculated based upon an equal amount of P12 and P16 cells (Figure 22c).

Together, the increased formation of elastin-like structures in senescent HMEC cultures was accompanied by an elevated LOX and LOXL1 protein expression which was paralleled by a significantly enhanced cellular-associated and extracellular LO enzyme activity.

3.5 Extracellular MMP-7 is linked to intracellular signal transduction pathways

The phenotypic alterations of the extracellular microenvironment in senescent HMEC populations, characterized by an increased maturation of elastin-like fibers, were substantiated by investigations at the post-translational level, including LO activity measurements and BAPN-dependence. However, little is known about regulation of the elastin precursor protein tropoelastin during senescence, which is required for the generation of elastic fibers. Thus, besides tropoelastin expression analysis, a potential link to the decreased MMP-7 levels during HMEC senescence was examined.

3.5.1 Expression pattern of tropoelastin during cellular senescence of HMEC

Tropoelastin protein levels were analyzed in whole cell lysates of different HMEC populations between P12 and P16 by Western blot. The expression data demonstrated an elevated intracellular production of the elastin precursor during HMEC senescence (Figure 23). Cell-associated human tropoelastin monomers increased in HMEC P14 and displayed maximal expression in P16 (Figure 23). As tropoelastin molecules covalently dimerize, a similar upregulation was observed for those dimers at an approximate molecular weight of 144 kDa (Figure 23). Remarkably, these data revealed inverse intracellular expression patterns for tropoelastin and the proteinase MMP-7 (cp. Figure 15 and Figure 23).

MMP-7 is known to be responsible for ectodomain shedding of numerous cytokines and growth factors (1.3.3.4). In this context, other work identified a membrane-anchored complex of MMP-7 with the heparin-binding epidermal growth factor-like growth factor (HB-EGF) to generate its soluble form sHB-EGF (Yu et al., 2002; Cheng et al., 2007; Lynch et al., 2007). Interestingly, expression of HB-EGF was detectable in young HMEC P12, but declined during senescence (Figure 23). Thus, the growth factor HB-EGF exhibited a similar protein regulation as MMP-7 during cellular senescence of HMEC, suggesting potential signaling correlations. In this context, downstream signal transduction by sHB-EGF involves the transcription factor Fra-1, which among others triggers regulation of tropoelastin expression. Immunoblot analysis demonstrated that Fra-1 was markedly expressed in young HMEC P12 and P13, whereas the protein levels gradually decreased with continuous passage number and were, eventually, significantly diminished in the senescent P16 populations (Figure 23).

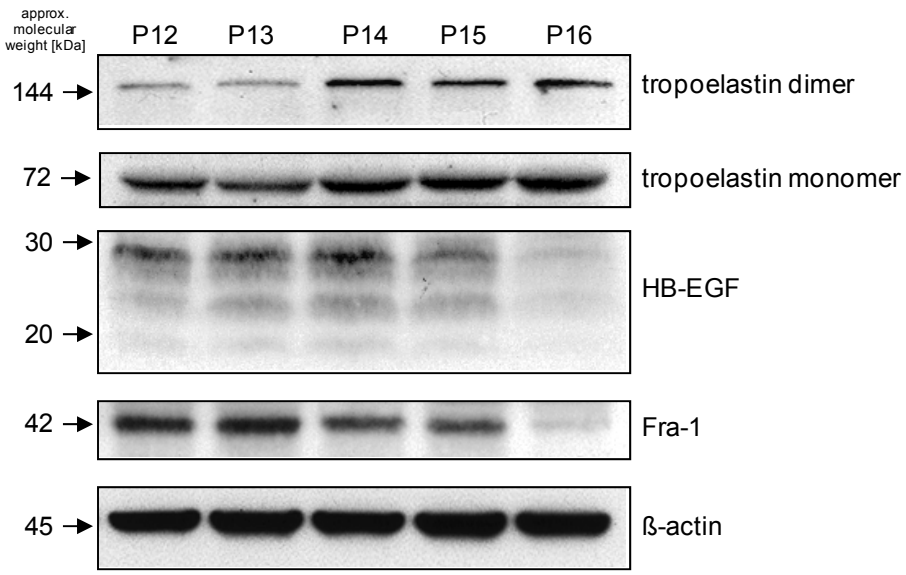

Figure 23: Expression of tropoelastin, HB-EGF and Fra-1 during cellular senescence of HMEC.
Western blot analysis of whole cell lysates during cellular senescence of HMEC demonstrated an increasing expression of both the monomeric as well as the dimeric form of the elastin precursor protein tropoelastin in HMEC after passage 13. This was paralleled by a down-regulation of HB-EGF. The transcription factor Fra-1 was previously shown to be involved in intracellular HB-EGF-mediated tropoelastin regulation and decreasing Fra-1 protein levels were observed during cellular senescence of HMEC. An equal loading control was performed using an anti-β-actin antibody.

3.5.2 Down-regulation of MMP-7 induced tropoelastin expression

Besides the direct effect of MMP-7 on the degradation and remodeling of ECM, the inverse expression pattern between MMP-7 and tropoelastin during HMEC senescence may indicate a possible relationship of MMP-7 to processing signaling molecules and modifying downstream signals. In addition to the induction of an accelerated aging of HMEC by MMP-7 down-regulation (see 3.3.1), the question arose, whether the decreased MMP-7 expression affects tropoelastin synthesis.

According to paragraph 3.3.1, young proliferating HMEC P12 were targeted by a MMP-7 RNAi approach and reduced MMP-7 protein levels were investigated in the context of potential effects on tropoelastin expression (Figure 24). As already elucidated in detail above, control transfections were performed with pmaxGFP plasmid and transfection with non-silencing, green fluorescence-labeled siRNA-AF488 revealed a transfection efficiency of approximately 75 %. In order to examine effects on downstream signaling pathways, MMP-7 down-regulation by RNAi was prolonged for 96 h. Thus, 48 h-transfected HMEC were harvested by trypsinization, submitted to a second siRNA transfection and incubated for another 48 h.

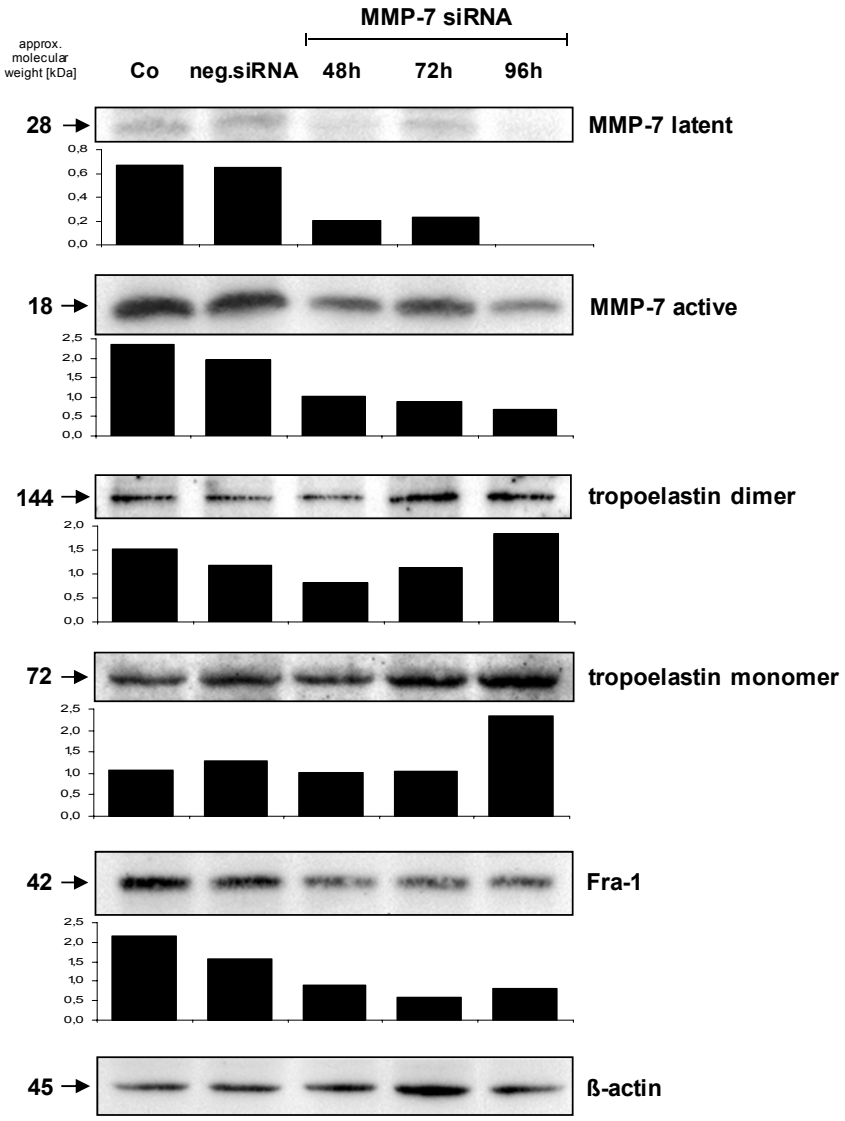

Figure 24: MMP-7 down-modulation affected tropoelastin expression.

Young HMEC P12 were transfected with MMP-7 siRNA and harvested 48 h, 72 h and 96 h post transfection. Western blot analysis revealed a successful down-modulation of both the latent and active form of MMP-7 in MMP-7 siRNA transfectants compared to control-transfected HMEC. The expression of tropoelastin was significantly affected by MMP-7 down-modulation. Reduced MMP-7 levels implicated about 1.5-fold elevated tropoelastin levels for both the monomer and the dimer of this protein in 96 h-MMP-7 siRNA transfected HMEC. Concerning potential signaling mechanisms, Fra-1 demonstrated a significant down-regulation in the MMP-7 RNAi transfectants after 48 h, which was maintained until 96 h post transfection. Normalization to β-actin protein levels was performed by densitometry and is indicated by arbitrary units in the y-axis (ImageJ).

Finally, whole cell lysates were separated by SDS-gel electrophoresis and immunoblot detection revealed a successful down-modulation of both latent and active form of MMP-7 in MMP-7 siRNA transfected HMEC as compared to non-transfected and negative siRNA-transfected controls (Figure 24). Normalization to β-actin protein levels by densitometry (ImageJ) confirmed these results. In contrast, MMP-7 down-modulation was accompanied by increasing expression of the elastin precursor protein tropoelastin. The monomeric form as well as the dimer displayed

about 1.5-fold elevated protein levels in MMP-7 siRNA-transfected HMEC after 96 h, when compared to negative siRNA transfectants (Figure 24). Following the initial hypothesis of an induced downstream signaling by MMP-7, including the transcription factor Fra-1, expression analysis revealed Fra-1 levels after 96 h-MMP-7 siRNA transfection to be reduced to about one third of the protein levels in the control populations (Figure 24).

Taken together, these data confirmed a direct link between MMP-7 down-regulation and an increased tropoelastin expression during cellular senescence of HMEC. Although the associated intracellular pathways that trigger an up-regulation of tropoelastin expression during HMEC senescence still remain unclear, HB-EGF signaling via Fra-1 could represent one possible piece in this puzzle.

3.5.3 MMP-7 affected HB-EGF signaling via Fra-1

In order to follow a possible role of HB-EGF-transduced signaling in the regulation of tropoelastin expression during HMEC senescence, HB-EGF was down-modulated by RNAi in HMEC P12. Subsequently, potential effects of an impaired HB-EGF expression in young HMEC were evaluated on cell growth and expression of affected signaling molecules. Moreover, LO enzyme activity measurements could verify further processing of a potentially induced tropoelastin amount.

Control experiments for successful transfection and transfection efficiency were performed as described above (3.3.1) and revealed similar results as indicated for MMP-7 RNAi (Figure 16). Suppression of HB-EGF mRNA translation by siRNA was maintained for 96 h by a second siRNA transfection after 48 h as indicated for MMP-7 RNAi (3.5.2). This ensured sufficient prevention of HB-EGF biosynthesis to allow investigation of interacting downstream signaling molecules. HB-EGF expression analysis demonstrated a successful down-modulation in HB-EGF siRNA transfected HMEC as compared to the non-transfected and negative siRNA transfected controls (Figure 25a). Similarly, Fra-1 protein was down-regulated in HB-EGF RNAi transfectants (Figure 25a). However, both tropoelastin monomers as well as tropoelastin dimers revealed enhanced protein levels in the HB-EGF RNAi transfectants (Figure 25a).

Functional studies of the transfectants by cell cycle analysis revealed a significant amount of cell death in HB-EGF siRNA-transfected HMEC as compared to the control cell groups (***$P < 0.0005$ and **$P < 0.01$, respectively), indicated by cell populations with degraded DNA (Figure 25b). Moreover, aberrant mitosis, as documented by the accumulation of cells with 8N DNA, was markedly elevated in 96 h-HB-EGF siRNA transfected HMEC in contrast to non-transfected (*$P < 0.05$) and negative siRNA transfected control cells (*$P < 0.05$) (Figure 25b).

Moreover, it was investigated if excessive tropoelastin levels due to HB-EGF down-modulation might interfere with extracellular LO enzyme activity. Indeed, cross-linking activity of lysyl oxidases considerably differed from the control transfected HMEC and was significantly elevated after HB-EGF down-modulation (*$P < 0.05$) (Figure 25c).

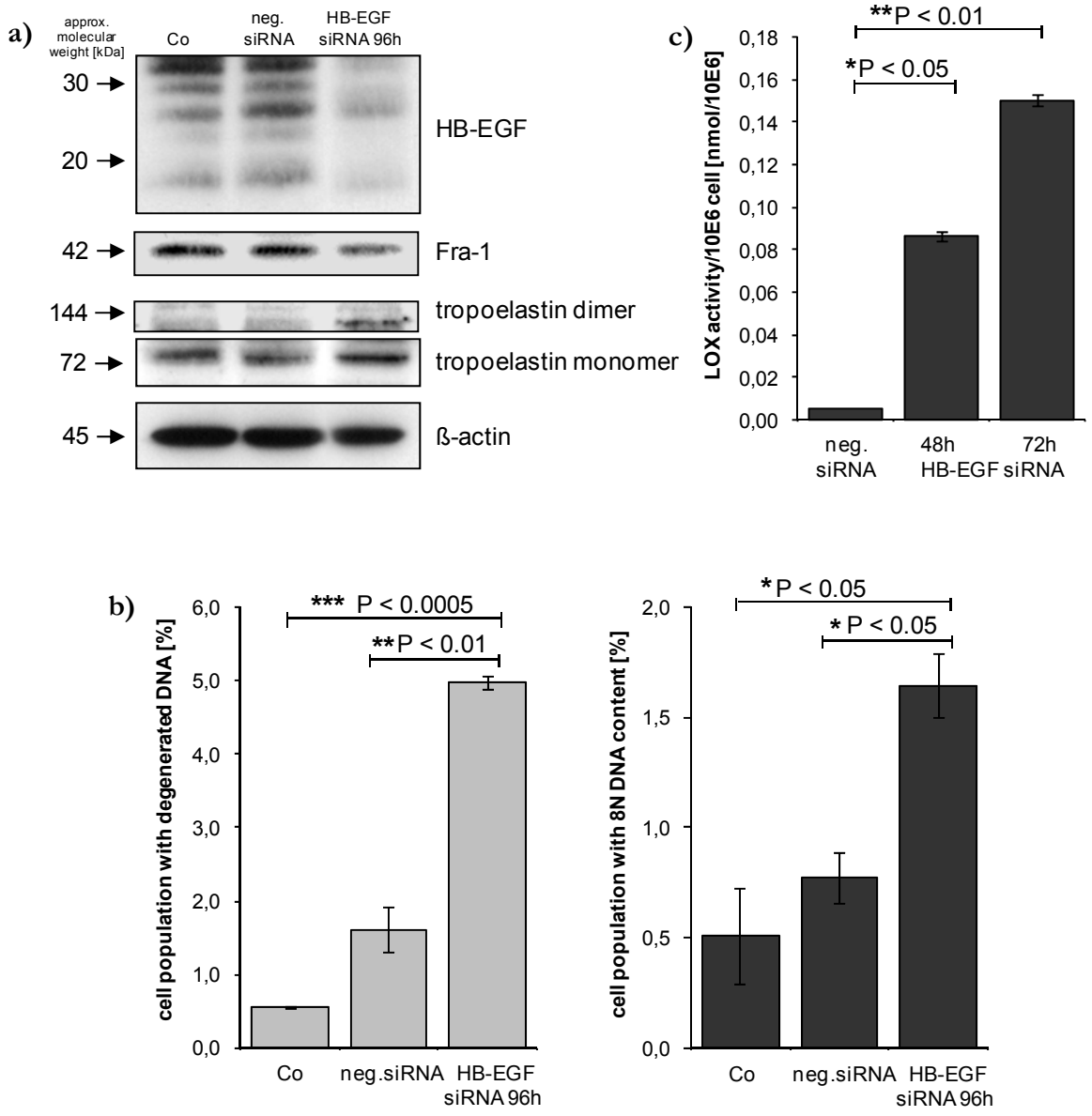

Figure 25: RNAi of HB-EGF in HMEC P12.

(a) HMEC P12 were transfected with HB-EGF siRNA and harvested 96 h post transfection. Western blot analysis revealed a successful down-modulation of HB-EGF protein levels in HB-EGF siRNA transfected HMEC compared to non-transfected and negative siRNA transfected cells. In addition, transcription factor Fra-1 protein levels were reduced in HB-EGF siRNA targeted HMEC. HB-EGF and Fra-1 down-modulation were paralleled by an increase in tropoelastin expression and both the tropoelastin monomer and dimer were elevated in HB-EGF RNAi HMEC. (b) The cell cycle distribution was evaluated in HMEC transfected with HB-EGF siRNA, non-transfected HMEC and negative siRNA-transfected cells. After 96 h, HB-EGF down-modulation was associated with a dramatic increase in cell death. The amount of apoptotic cells increased more than 2.5-fold compared to negative siRNA transfectants (**P < 0.01). Moreover, a marked accumulation of cells with 8N DNA indicated aberrant mitosis in HB-EGF siRNA transfected HMEC compared to negative siRNA transfectants (*P < 0.05). Data represent mean ± SD of three independent experiments. (c) Extracellular LO activity in the conditioned media of HB-EGF RNAi transfectants was significantly higher than in the respective media of negative siRNA transfected HMEC (*P < 0.05 and **P < 0.01), demonstrating elevated cross-linking activity after down-modulation of HB-EGF. Data represent mean ± SD of three independent experiments.

Thus, HB-EGF RNAi revealed the membrane-associated growth factor as an additional effector associated with downstream intracellular tropoelastin regulation in HMEC. Decreased HB-EGF signal transduction caused a reduced Fra-1 activation which in turn abolished inhibition of tropoelastin transcription in senescent HMEC.

3.5.4 Localization of MMP-7 and HB-EGF in HMEC

The present data suggested MMP-7 downstream signaling mechanisms via extracellular activation of the growth factor HB-EGF and subsequent intracellular Fra-1 induction. In order to verify this hypothesis, immunofluorescence analysis was used to reveal the cellular localization of the proteinase and the growth factor, depending on the age of the cells. HMEC were harvested in P12, P14 and P16 and processed for immunostaining. The DNA-intercalating dye Hoechst 33258 visualized the appropriate nuclei in each cell (Figure 26). In young HMEC P12, both MMP-7 as well as HB-EGF were predominantly concentrated around the cell body (Figure 26). Moreover, the merged fluorescence images confirmed a co-localization of MMP-7 and HB-EGF in small, proliferating HMEC, displaying a circled position at the rim of the cell body (Figure 26, arrows). HMEC P14 represented a mixed population of smaller cells and cells significantly increased in cell size compared to P12. Thus, MMP-7 and HB-EGF expression represented both the characteristic circled localization around the cell body in smaller cells, resembling the position in HMEC P12, and a more spread distribution on the cell surface of enlarged HMEC (Figure 26, arrowhead). This diffuse location of MMP-7 and HB-EGF was further strengthened in the senescent P16 population, demonstrating little if any co-localization of these two proteins (Figure 26, arrowheads). Furthermore, MMP-7 exhibited a distinct punctuate staining in the nuclear compartment of senescent HMEC P16 (Figure 26, double-headed arrows).

Cellular senescence of HMEC was accompanied by a decreasing MMP-7 expression. Induction of down-regulated MMP-7 protein levels in young HMEC triggered an accelerated aging in these cells, indicating the importance of this extracellular metalloproteinase for HMEC. Moreover, reduced MMP-7 involved an impaired HB-EGF downstream signaling via the transcription factor Fra-1 which in turn resulted in activation of tropoelastin mRNA transcription. Interaction of the proteinase MMP-7 with the membrane-bound growth factor HB-EGF was confirmed by immunofluorescence analysis in young HMEC, whereas co-localization vanished in senescent HMEC.

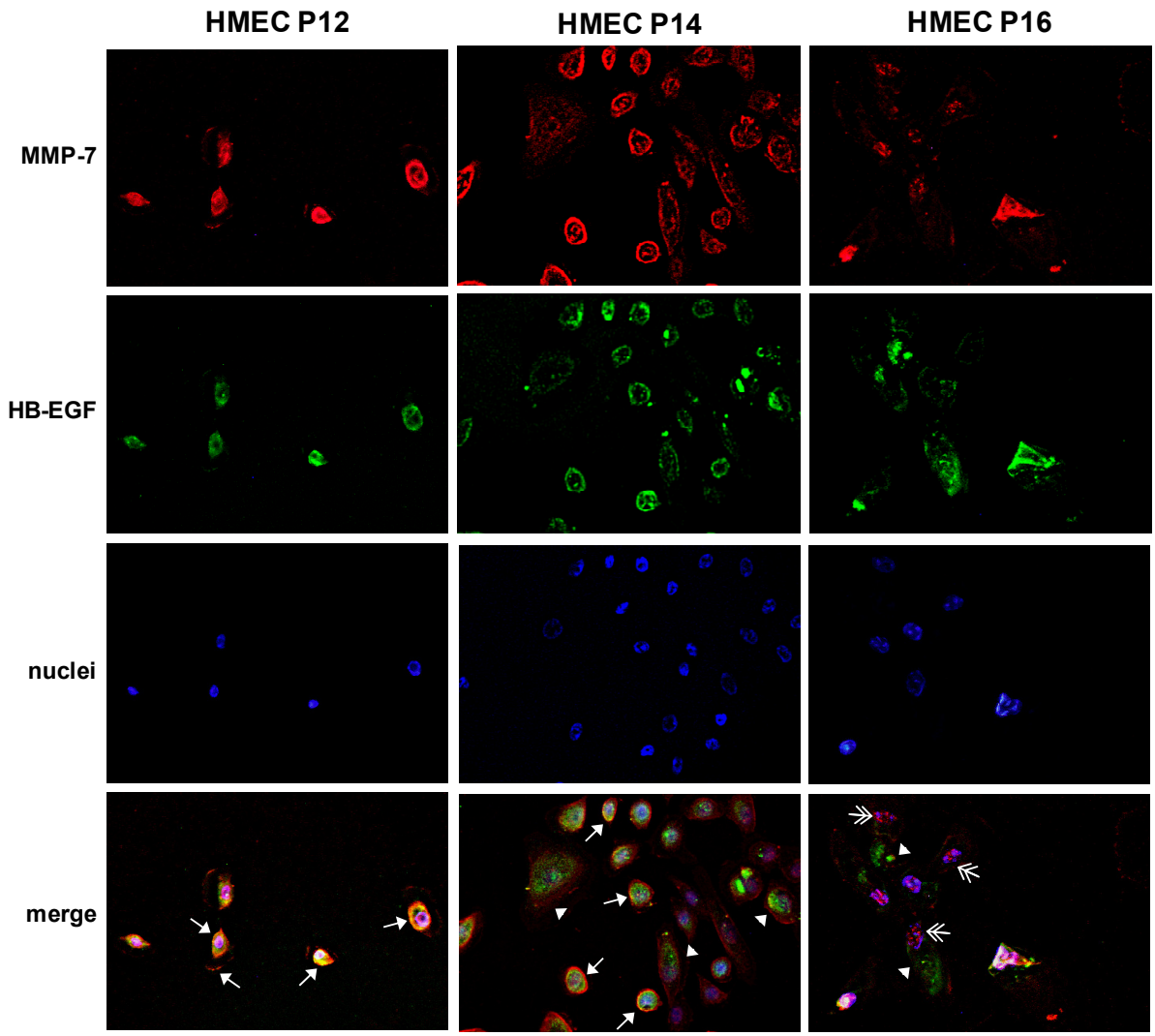

Figure 26: Co-localization of MMP-7 and the growth factor HB-EGF.

Immunofluorescence analysis during cellular senescence of HMEC P12, P14 and P16 exhibited a predominant localization of the proteinase MMP-7 and the growth factor HB-EGF at the plasma membrane of the cells. The nuclei became visual using Hoechst 33258 and MMP-7 and HB-EGF were detected by monoclonal mouse anti-MMP-7 (red) and polyclonal goat anti-HB-EGF (green), respectively. Whereas young, proliferating HMEC revealed a characteristic co-localization of these two proteins at the rim of the cell body (arrow), enlarged senescent HMEC demonstrated a diffuse pattern of MMP-7 and HB-EGF (arrowhead), indicating a reduced interaction of the proteinase with the growth factor. In addition, MMP-7 exhibited a distinct punctuate staining overlayed with the nuclear compartment (double-headed arrow) (magnification 200x).

4 Discussion

4.1 Post-selection HMEC encounter agonescence

Cultured primary HMEC have a limited number of cell divisions and acquire distinct morphological changes with increasing culture period. The formation of long cytoplasmic processes and a considerable increase in cell size are accompanied by substantial intra- and extracellular alterations. Qualitative and quantitative analysis of $p16^{INK4a}$ levels in different HMEC populations demonstrated that neither young proliferating HMEC P12 nor senescent HMEC P16 expressed this cell cycle inhibitor. This characterizes these populations to be in the post-selection phase (Yaswen and Stampfer, 2002). Activity of SA β-gal in these post-selection HMEC was dramatically intensified in HMEC P16 to more than 80%, suggesting HMEC P16 as senescent, growth-arrested populations which eventually encounter agonescence (Figure 3). For simplicity, in the following HMEC P12 are referred to as young HMEC and HMEC P16 are designated senescent HMEC.

As demonstrated by cell cycle analysis, cellular senescence of HMEC was associated with a gradually decreasing number of cells with 2N DNA but an accumulation of cells with 4N DNA. Besides cells arrested in the G_2 phase, these results could also indicate HMEC with a tetraploid DNA content that arrest in the G_1 phase (Sandhu et al., 2000). It was shown that cells exposed to DNA damage can overcome the G_2 control checkpoint and proceed into mitosis. Due to the high risk for cells entering the M-phase with damaged DNA such as double strand breaks, these cells try to avoid missegregation and omit cytokinesis, resulting in binucleated tetraploid cells which subsequently traverse into G_1 phase and are subjected to the G_1 checkpoint control, inhibiting further S phase transition (Andreassen et al., 2001). As binucleation could be observed as a natural process during cardiac development, senescent cells might utilize these mechanisms to terminate mitosis and traverse into G_1 phase (Soonpaa et al., 1996). The appearance of cells with an 8N DNA content in the senescent HMEC population suggested, at least for a few cells, further cell cycle progression. Probably owing to improper G_1 checkpoint functions, some tetraploid HMEC might overcome this control and start again DNA replication without cell division, which eventually leads to 8N DNA cells (Huang et al., 2005).

Whereas stasis, the first proliferation barrier in HMEC, is stress-associated and mediated by induction of the CDK-inhibitor $p16^{INK4a}$, the agonescent state is characterized by dysfunctional telomeres inducing the DNA damage response (Figure 2, Figure 3). In general, DNA damage stimulates p53 which in turn activates the expression of the CDK-inhibitor $p21^{Cip1}$ (Jackson and Pereira-Smith, 2006). However, previous studies demonstrated that senescent HMEC are not susceptible to p53-induced cell cycle inhibition by $p21^{Cip1}$, as HMEC reaching agonescence exhibit invariable expression levels of this inhibitor (Sandhu et al., 2000; Romanov et al., 2001). Moreover, post-selection HMEC lost expression of the CDK-inhibitor $p16^{INK4a}$, which as well contributes to an improper G_1 checkpoint control (Figure 1). In addition to the regulation through these inhibitory proteins, cell cycle progression and CDK activity are influenced by the

Cdc25 phosphatase family (Nilsson and Hoffmann, 2000). Indeed, inhibition and degradation of Cdc25A in senescent HMEC was shown to trigger CDK2/cyclin E inactivity at the G_1 checkpoint (Sandhu et al., 2000) and impaired CDK-dephosphorylation may contribute to the regulation of a cell cycle arrest in senescent HMEC.

Senescent HMEC cease proliferation but remain in a viable, active state and last in a permanent growth arrest. Moreover, several studies demonstrated that many cell types underlying senescence become resistant to various apoptotic signals, suggesting that certain cellular pathways regulate the decision about cell death and elimination or permanent exit from the cell cycle but inability to die (Chen et al., 2000; Marcotte et al., 2004; Murata et al., 2006). Functional alterations including interference with apoptotic pathways in senescent cells might confer upon them a reduced susceptibility to certain suicide signaling (Chen et al., 2000; Marcotte et al., 2004). Thus, resistance to apoptosis in senescent fibroblasts is probably associated with the lack of essential pro-apoptotic proteins such as caspase-3, while anti-apoptotic factors (e.g. Bcl-2) are maintained at high levels (Chen et al., 2000; Marcotte et al., 2004). Likewise, another mediator of apoptosis, the death-associated protein 3 (DAP3), demonstrated reduced levels in senescent cells, effecting resistance to oxidative stress (Murata et al., 2006). However, whereas senescent fibroblasts sustain a variety of apoptotic signals compared to the corresponding younger populations, senescent endothelial cells derived from the umbilical cord (HUVEC) are more prone to the induction of cell death and rather acquire a pro-apoptotic phenotype (Hampel et al., 2004). Thus, cellular senescence cannot be equated with resistance to apoptosis but might provide many cell types with functional alterations required to suppress distinct apoptotic signaling pathways and to maintain viability. The detailed mechanisms involved in an insusceptibility of HMEC to diverse cell death signals, causing long term viability and eventual accumulation in the organism, have to be elucidated.

4.2 Cell surface-associated proteins

Epithelial cells express a variety of cell surface proteins involved in cell-ECM adhesion, migration, intercellular communication, cytokine and growth factor presentation as well as intracellular downstream signal transduction. Interestingly, cellular senescence of HMEC was associated with significantly decreased levels of selected cell surface proteins (CD24, CD44, CD227) when comparing young versus senescent HMEC. Expression of the β_1-integrin family member CD29, however, appeared to be unrelated to the HMEC aging process.

The uniformly expressed CD29 functions as β_1-subunit of a variety of heterodimeric cell surface integrins. Together with the α_5-subunit, CD29 forms an essential cell surface receptor for fibronectin, required for fibronectin-matrix assembly and involved in cell migration processes (Zhang et al., 1993). Moreover, β_1-integrins can interact with the ECM proteins fibrillin-1 and EMILIN-1, thereby supporting microfibril formation but also relaying extracellular alterations to cell behavior and downstream intracellular signaling pathways (Bax et al., 2003; Spessotto et al., 2003). Other studies demonstrated a relation of an increased β_1-integrin expression to the MMP-

9-associated induction of senescence in medulloblastoma cells, but apparently this had no effect in the aging of mammary epithelial cells (Bhoopathi et al., 2008).

CD227 (MUC1) is aberrantly expressed on numerous epithelial malignancies, including breast cancer cells, and therefore is investigated as a new tumor marker and a potential therapeutic target (Singh and Bandyopadhyay, 2007). Indeed, about 100% of the MCF-7 breast cancer cells exhibited MUC1 expression in contrast to a significantly reduced population of young HMEC and a further decline during HMEC senescence. MUC1 belongs to the family of mucins and represents a large transmembrane protein with several isoforms due to multiple alternative splicing as well as different proteolytical cleavages. It is composed of a heavily glycosylated extracellular domain and a tyrosine-rich cytoplasmic tail, which is involved in a variety of intracellular signal transduction processes (Ahmad et al., 2007). In addition to the overexpression of MUC1 on tumor cells, the glycosylation pattern differs significantly from that on non-tumorigenic breast epithelial cells (Singh and Bandyopadhyay, 2007). Following ectodomain shedding and secretion, the extracellular part of MUC1 confers tumorigenic epithelial cells with an immune-suppressive function via growth inhibitory effects on T cells (Chan et al., 1999). MUC1 protects the EGF receptor ErbB1 against degradation and rather induces its recycling. This entails significantly increasing levels of cellular ErbB1 and might as well contribute to cell transformation (Pochampalli et al., 2007). Moreover, extracellular MUC1 can bind to ICAM-1 (intercellular adhesion molecule-1) on adjacent cells and induces an intracellular signaling cascade which triggers cytoskeleton reorganization and migration (Shen et al., 2008). The cytoplasmic domain of MUC1 plays a crucial role in NFκB-activation (Ahmad et al., 2007). Intracellular binding of MUC1 to IKK-β stimulates phosphorylation and degradation of the NFκB inhibitor IκB, thereby implicating release and activation of NFκB. Whereas under physiological conditions, MUC1 is an important regulator of IKK-β, overexpression of this glycoprotein causes persistent NFκB-activation and confers the malignant cells with an anti-apoptotic mechanism (Ahmad et al., 2007). Whereas overexpression of MUC1 on MCF-7 cells is in concert with the tumorigenic phenotype of these cells, reduced MUC1 levels in HMEC and a further down-regulation during senescence may demonstrate a decreased tumorigenic potential in the aging cells.

CD24, whose expression was reduced upon senescence in HMEC, is a small, heavily glycosylated, extracellular protein anchored by a GPI-link to the cell surface. This glycoprotein is typically expressed on B cells, but also represents an important function for a variety of epithelial tumors, including breast cancer (Lim, 2005; Schabath et al., 2006). CD24 is a known ligand of P-selectin, a cell adhesion molecule on endothelial cells and platelets, and thus, is suggested to enhance the metastatic potential of malignant cells by mediating rolling of tumor cells on endothelial cells (Friederichs et al., 2000; Lim, 2005). The metastasis promoting character of CD24 is augmented by its regulatory role concerning the function of the chemokine receptor CXCR4 (Schabath et al., 2006). Cellular migration mediated by the chemokine CXCL12 and subsequent activation of CXCR4 was significantly reduced when CD24 was expressed. Moreover, loss of CD24 in breast cancer cells induced an increased tumor formation in mice (Schabath et al., 2006). Whereas these data seem contrary claiming both abundant CD24 as well as low CD24 expression to be involved

in solid tumor formation and metastatic developments, recent studies identified breast cancer cells with a stem cell-like character, expressing low to undetectable CD24 levels (Ponti et al., 2005). This suggests that either high or negligible CD24 expression confers the cell with tumor-promoting functions, while normal occurrence of this cell adhesion molecule contributes to physiological conditions and might be associated with a non-malignant phenotype.
Similarly, protein levels of the CD44 cell adhesion molecule decreased in aging HMEC, whereas it was abundantly expressed on MCF-7 breast cancer cells. Interestingly, breast cancer cells displaying stem/progenitor cell properties are not only characterized as $CD24^{neg./low}$, but also express high levels of CD44 (Ponti et al., 2006; Liu et al., 2007). CD44 represents a group of multistructural and multifunctional transmembrane heparan sulfate proteoglycans (HSPG) generated due to alternative splicing and different glycosylations and glycosaminoglycations (Naor et al., 1997). These CD44 variants interact with a large number of extracellular and intracellular proteins and are implicated in diverse cellular processes. The specific isoform CD44v3 recruits MMP-7 to the cell surface of epithelial cells (Yu et al., 2002). Simultaneously, binding of HB-EGF to CD44 heparan sulfate chains ensures localization of the proteinase in close proximity to its substrate. Interference of CD44 with ErbB1 and ErbB4 eventually allows binding of the activated growth factor with its receptors and subsequent signal transduction (Yu et al., 2002). Thus, decreased expression of CD44 in senescent HMEC could affect the interaction between MMP-7 and HB-EGF and thus might as well be responsible for the impaired HB-EGF downstream signaling in this cell population. However, further investigations are necessary to determine the expression of specific CD44 isoforms at the cell surface of HMEC. Thus, a potential role of CD44 during the aging process of HMEC and dysfunctional MMP-7 signaling could be verified.
Cell surface receptors involved in cellular adhesion as well as inter- and intracellular communication may be crucial for the function and motility of both young proliferating HMEC as well as tumor cells, whereby decreased levels in the senescent HMEC population may reflect their transition to a growth-arrested state associated with an altered signal transduction.

4.3 MMP-7 is involved in the aging of HMEC

4.3.1 MMP-7 induces an accelerated senescence in HMEC

MMPs represent an important enzyme family of the extracellular compartment. Due to their versatile functionality, MMPs regulate several physiological processes; however, small interferences might implicate deleterious consequences for the cell itself and the surrounding tissue.
Investigation of MMP-1 (interstitial collagenase), MMP-2 (gelatinase A) and MMP-9 (gelatinase B) expression during cellular senescence of HMEC demonstrated that these proteases were not affected by the aging process and revealed unvarying protein levels of both their latent and active forms. However, proMMP-7 was slightly diminished in senescent HMEC and this was

even more pronounced by the active enzyme form, which was reduced below detection level in the senescent population, indicating a potential role of this extracellular proteinase during senescence of HMEC. Indeed, down-modulation of MMP-7 by RNAi had a strong impact on young HMEC and induced an accelerated aging in these cells. In contrast, MCF-7 breast cancer cells were unaffected by the reduced MMP-7 levels, suggesting that the immortalized cell line carries certain genetic manipulations that overcome MMP-7-induced senescence.

Besides its originally described function in degradation and remodeling of the ECM structure, MMP-7 acts upon several other extracellular matrix molecules involved in cellular reorganization and locomotion (Wilson and Matrisian, 1996). Thus, reduced MMP-7 levels in aging HMEC would conversely imply restrained cell motility. Due to its broad substrate specificity against ECM components (e.g. collagen, elastin, fibronectin, laminin and proteoglycans) MMP-7 prepares and allows penetration of cells through the matrix (Wilson and Matrisian, 1996). In addition, MMP-7 proteolysis can loose cellular aggregations and cell-matrix attachment to induce cell migration. Ectodomain shedding of E-cadherin by MMP-7 likewise impairs intercellular connections and promotes migration in association with both physiological wound healing but also metastasis and invasion (Noe et al., 2001; McGuire et al., 2003). Extracellular cleavage of E-cadherin by MMP-7 is additionally associated with an intracellular disruption of the E-cadherin/β-catenin complex, leading to release and nuclear translocation of β-catenin, which eventually transactivates the expression of diverse proteins, including MMP-7 (Crawford et al., 1999; Noe et al., 2001). Thus, decreased MMP-7 activity not only causes diminished cell motility but also results in less transcriptional activation of its own promoter region, which would potentiate MMP-7 down-regulation by a negative feedback loop. Consequently, down-modulation of MMP-7 by RNAi in young HMEC may inhibit essential intercellular and cell-ECM communications which are required for cellular growth and physiological functions.

Interestingly, mice deficient in MMP-7 demonstrated significantly decreased apoptotic events than the control group (Powell et al., 1999), which would be in concert with the restricted response to certain apoptotic signals in senescent cells, also observed in HMEC (cp. 4.1, Figure 11) (Yaswen and Stampfer, 2002). MMP-7 plays an essential role in extracellular cleavage of the Fas death receptor ligand FasL by generating soluble FasL (sFasL), and thereby, represents an important mediator of epithelial cell apoptosis (Powell et al., 1999; Vargo-Gogola et al., 2002a).

Besides cleavage of structural ECM, the probably most important function of MMP-7 is the capability of growth factor activation and release of signaling molecules. Consequently, decreased MMP-7 levels in senescent HMEC or rather down-modulation of MMP-7 by RNAi would implicate a significantly reduced frequency of growth factors, and thus, diminished cell growth, whereas no comparable effects were observed in the tumorigenic MCF-7 breast cancer cells. MMP-7 demonstrates strong proteolytic activity against all six known IGF-binding proteins (IGFBP), thereby regulating the bioavailability of IGFs in the microenvironment and stimulating cell proliferation and survival (Nakamura et al., 2005). Moreover, direct cleavage of PGs by MMP-7 interferes with the PG-binding capacity and provokes the release of signaling molecules (Wight et al., 1992). The PG decorin functions as an extracellular reservoir for TGF-β, whereas

MMP-7-mediated degradation of decorin enhances the activation of this cytokine (Imai et al., 1997). Involvement of TGF-β in cell cycle arrest and apoptosis suggests another possible mechanism that may support apoptotic resistance in senescent HMEC (Mimori et al., 2004). Furthermore, binding of MMP-7 to the HSPG CD44 anchors the proteinase on the cell surface and subsequently assists processing of the growth factor HB-EGF to its soluble active form (sHB-EGF) (Yu et al., 2002). Simultaneous recruitment of ErbB1 and ErbB4, respectively, brings the activated growth factor in close proximity to its receptors and ensures precise and efficient signal transduction in a non-diffusible manner. MMP-7-catalyzed release of HB-EGF and subsequent transactivation of ErbB4 and ErbB1 marks a crucial mechanism involved in cell proliferation as well as tumor cell growth (Yu et al., 2002; Cheng et al., 2007; Lynch et al., 2007; Xie et al., 2009) and might as well be influenced during cellular senescence of HMEC.
These MMP-7-associated mechanisms display only a selection of multiple pathways affected by this extracellular proteinase, which is even more potentiated by the ability of MMP-7 to activate other proteinases, including MMP-1, MMP-9 and ADAM28, resulting in the initiation of additional signaling cascades (Imai et al., 1995; Mochizuki et al., 2004; Page-McCaw et al., 2007). The involvement of this ECM protease in cellular senescence suggested an essential impact of extracellular signaling mechanisms and the surrounding microenvironment on the aging of HMEC. However, further investigations are required to identify the detailed mechanisms of MMP-7 activity and to eventually reveal its role in the aging process.

4.3.2 MMP-7/HB-EGF co-localization in young HMEC but nuclear localization of MMP-7 in the senescent HMEC population

Localization studies of MMP-7 and HB-EGF revealed a co-localization of both proteins in young HMEC, whereas cellular senescence was accompanied by a more diffuse spreading of HB-EGF which did not co-localize anymore with MMP-7. These findings indicated a possible interaction of MMP-7 with HB-EGF in young HMEC, which decreased in the senescent cells in conformity with the protein expression data. Furthermore, the senescent HMEC population displayed a defined intracellular localization of MMP-7 in close proximity to the nucleus. Whereas a specific role for intracellular or nuclear MMP-7, respectively, has not been described so far, MMP-2 and MMP-3 were also shown to localize to the nucleus and thereby confer a pro-apoptotic function (Kwan et al., 2004; Si-Tayeb et al., 2006). Both nuclear proteinases demonstrated catalytic activity and MMP-2 was suggested to be implicated in the degradation of PARP-1 (poly(ADP-ribose) polymerase-1), a protein involved in DNA repair and apoptosis (Kwan et al., 2004). As little if any cell death was detected in the senescent HMEC populations, this would exclude a similar role for nuclear MMP-7 during HMEC senescence. For MMP-3, an essential nuclear localization signal (NLS) was identified that ensures a directed MMP-3 transport into the nucleus (Si-Tayeb et al., 2006). Thus, the nuclear appearance of MMP-7 could also result from an unknown NLS that triggers the retrograde transport of MMP-7 from the ECM back into the cell. On the other hand, increased intracellular MMP-7 levels could arise from a diminished extracellular MMP-7 transfer

after protein synthesis. Thus, previous data verified the necessity of the MMP-7-binding CD44v3 for localization of the proteinase at the cell surface. Other CD44 isoforms incapable of MMP-7-anchorage, however, failed to direct the enzyme to the extracellular compartment and predominantly showed intracellular MMP-7 location (Yu et al., 2002). Thus, decreased presence of certain MMP-7-interacting cell surface proteins such as CD44 on senescent HMEC may contribute to diminished MMP-7 in the extracellular space. This is substantiated by the expression analysis of MMP-7 during cellular senescence, demonstrating only slightly reduced protein levels of latent MMP-7, whereas the active form of the enzyme, which is typically processed at the cell surface, dramatically decreased in the senescent population. The precise localization of MMP-7 in senescent HMEC and its specific function in the different cellular compartments needs further examination.

4.3.3 Down-regulation of MMP-7 and an impaired HB-EGF signaling are associated with elevated tropoelastin levels in senescent HMEC

As indicated by the crucial role of MMP-7 in HB-EGF growth factor activation (cp. 4.3.1) (Yu et al., 2002), expression analysis revealed significantly reduced levels of this growth factor during senescence of HMEC. Conversely, examination of proteins involved in ECM formation such as tropoelastin and lysyl oxidases demonstrated a markedly increased expression in senescent cells, which was in concert with the detection of an enhanced appearance of elastin-like structures.

In order to verify the potential relationship between the decreased expression of MMP-7 or HB-EGF and the enhanced tropoelastin levels during HMEC senescence, both signaling pathways were targeted by RNAi. Remarkably, upon down-modulation of MMP-7, young HMEC in P12 already exhibited an elevated tropoelastin expression when compared to the control cells. A similar effect was observed after siRNA targeting of HB-EGF in young HMEC, revealing increased tropoelastin levels in the transfectants. Expression analysis of the transcription factor Fra-1 revealed significantly diminished protein levels in senescent HMEC. Interestingly, down-regulated Fra-1 levels could also be mediated by impaired MMP-7 signaling as well as upon HB-EGF RNAi.

Previous work demonstrated Fra-1 up-regulation to be responsible for tropoelastin inhibition (Rich et al., 1999), suggesting downstream signaling via Fra-1 as one potential mechanism that triggers tropoelastin expression in HMEC. Fra-1, also termed FOSL1 (Fos-like antigen-1), is a leucine zipper protein and belongs to the Fos family of transcription factors. It can dimerize with members of the Jun transcription factor family to form one of the AP-1 heterodimers (Rich et al., 1999). Fra-1 can be induced upon EGF receptor signaling via downstream activation of the mitogen-activated protein (MAP) kinases cascade (Zhang et al., 2005). Thus, transactivation of the EGF receptor confers intracellular phosphorylation via the MAP kinases MEK1/2 and ERK1/2 (Figure 27). Activated ERK1/2 can directly phosphorylate Fra-1 in the cytosol or in the nucleus after ERK1/2 translocation. Phosphorylation of Fra-1 implicates a significant increase of its DNA-binding ability (Gruda et al., 1994) and together with a binding partner of the Jun

transcription factor family, Fra-1 forms an AP-1 transcription complex (Figure 27). This either induces autoactivation of the fra-1 gene or binds within the tropoelastin promoter and thereby inhibits tropoelastin transcription (Rich et al., 1999; Carreras et al., 2001). Another potential mechanism involves ERK1/2-mediated activation of the transcription factor Elk-1 that in turn binds the Fra-1 promoter and stimulates Fra-1 transcription (Carreras et al., 2001) (Figure 27). More recently, a similar mechanism, including ERK1/2 and Fra-1, was validated in response to sHB-EGF and the growth factor was shown to be responsible for reduced tropoelastin levels in pulmonary fibroblasts (Liu et al., 2003b). Conversely, an attenuated EGF receptor-mediated MAPK-signaling cascade was shown to be associated with an elevated tropoelastin expression and an up-regulated elastin formation (Rich et al., 1999).

Decreased amounts of enzymatically active MMP-7 at the cell surface of senescent HMEC would thus imply less shedding and release of active sHB-EGF which in turn suggests a diminished transactivation of ErbB4 and ErbB1, respectively (Figure 27). Consequently, inhibition of the receptor-associated downstream signaling reduces Fra-1 accumulation in the nucleus and may then allow transcription of the tropoelastin gene during cellular senescence of HMEC. Concomitant up-regulation of LOX and LOXL1 as well as a considerably increased LO enzyme activity in the senescent HMEC population could contribute to an increased elastin fiber formation during cellular senescence. Comparably, tropoelastin stimulation after HB-EGF down-modulation in young HMEC was accompanied by enhanced LO activity, indicating certain associations of induced tropoelastin precursor expression with an initiation of the maturation to elastin fibers.

In addition to the induction of tropoelastin transcription, hindered HB-EGF signal transduction following RNAi implicated aberrant mitosis and apoptosis-promoting effects. As demonstrated by cell cycle analysis, HB-EGF siRNA transfectants exhibited an elevated amount of cells with an 8N DNA content and a significant population that underwent DNA degeneration. Whereas overexpression of HB-EGF is associated with tumorigenesis and bears growth-inducing effects, down-regulation of HB-EGF causes restrained ErbB1 phosphorylation and a substantial increase of cell death in colon cancer cells (Ongusaha et al., 2004; Wang et al., 2007). Besides signal transduction via extracellular binding to ErbB4 and ErbB1, HB-EGF is capable of intracellular signaling involving its cytoplasmic C-terminal fragment (CTF) which bears cell cycle-promoting functions (Toki et al., 2005; Shimura et al., 2008). In order to verify a potential role of the CTF during HMEC senescence additional experiments have to address this question.

Taken together, the present findings substantiated the importance of MMP-7 for the aging process of HMEC and suggested ectodomain shedding of HB-EGF as one crucial mechanism to relay intracellular downstream signaling via Fra-1 to transcriptional regulation of tropoelastin. Attenuated HB-EGF signaling provoked decreased Fra-1 levels which acts as a transcriptional repressor of tropoelastin and in turn, allowed tropoelastin expression.

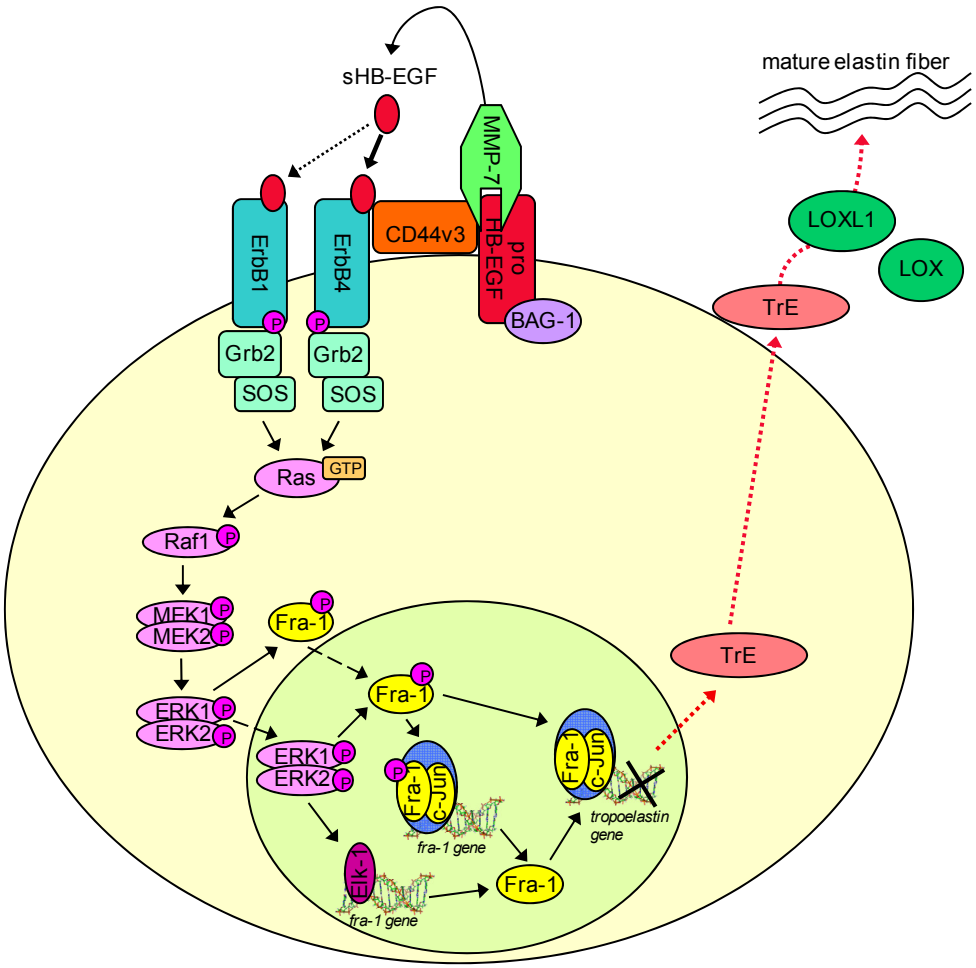

Figure 27: Schematic overview of a potential mechanism involved in MMP-7/HB-EGF-mediated tropoelastin regulation via Fra-1

Extracellular cleavage of proHB-EGF by MMP-7 generates active soluble sHB-EGF that in turn interacts either with ErbB4 or ErbB1. Autophosphorylation of the ErbB4/1 receptor transduces an intracellular signaling cascade implicating the MAP kinases MEK1/2 and ERK1/2. ERK1/2 can directly phosphorylate Fra-1 in the cytosol or after its translocation in the nucleus, which significantly improves Fra-1 DNA-binding activity. Fra-1 associates with a transcription factor of the Jun family to form one of the AP-1 heterodimers that either autoactivates the fra-1 gene or binds within the tropoelastin promoter and thereby inhibits tropoelastin transcription. In addition, ERK1/2 activates the transcription factor Elk-1 which as well induces gene transcription of Fra-1. However, attenuated MMP-7 activity in senescent HMEC would cause a decreased proHB-EGF shedding and thus less sHB-EGF. Restrained ErbB4/1 activation subsequently impedes MAP kinase signaling and prevents Fra-1 DNA-binding, which in turn allows access to the promoter region of the tropoelastin gene and leads to increased tropoelastin expression. (For a detailed scheme illustrating tropoelastin trafficking see Figure 4).

4.3.4 MMP-7 bears elastolytic enzyme activity

Apart from affecting downstream signaling pathways, MMP-7 has a broad substrate specificity against ECM components, including a potent elastolytic activity (Wilson and Matrisian, 1996). This suggested that reduced MMP-7 activity in senescent HMEC may hinder elastin degradation and thereby reinforces elastin occurrence. Indeed, MMP-7 represents one of the most effective metalloproteinases capable of elastin cleavage and for example confers macrophages with a proficient elastolytic system associated with physiological and pathological matrix degradation (Mecham et al., 1997; Filippov et al., 2003). In addition to its regulatory function related to tropoelastin gene transcription, diminished MMP-7 activity may also restrain degradation of the mature elastin fiber. However, further experiments are required to evaluate the elastolytic role of MMP-7 during cellular senescence of HMEC.

4.4 Impact of the ECM and alterations of the microenvironment on cellular behavior

4.4.1 Increased elastin formation in the senescent HMEC population contributes to an altered extracellular microenvironment

The extracellular microenvironment has an important impact on the development and function of a cell, which includes the initiation of extracellular-triggered signaling mechanisms as well as the composition of the extracellular matrix. The present study revealed that progression of cellular senescence in HMEC is accompanied by an increased intracellular tropoelastin expression followed by enhanced extracellular elastin fiber formation. Alterations in the biosynthesis of ECM macromolecules were shown to play a crucial role in biological aging and age-related disease as well as malignant transformation (Labat-Robert and Robert, 2007; Marastoni et al., 2008). In tissues such as lung, skin and blood vessels, elastin biosynthesis exclusively occurs early in life and the aging process is rather associated with progressive degeneration of the elastin matrix, causing dysfunctional tissue (Bouissou et al., 1988; Bruce and Honaker, 1998; Pezet et al., 2008). Whereas these effects may be tissue-specific, other work compared healthy breast tissue specimens of young and elderly women and revealed excessive elastin fibers predominantly around the ducts of more than 50% of women over age 50, whereas this phenomenon was not observed in young women (Farahmand and Cowan, 1991). According to these findings, a prominent appearance of elastic tissue in the breast was proposed to be involved in a precancerous development (Jackson and Orr, 1957; Azzopardi and Laurini, 1974). Whereas primary studies exclusively considered stromal cells to be capable of elastin formation (Lundmark, 1972; Tremblay, 1976), there is increasing evidence that epithelial cells themselves generate newly synthesized elastic fibers (McCullagh et al., 1980; Krishnan and Cleary, 1990) which is also supported by our results. Altered cell matrix interactions and modified ECM components have been proposed to play a crucial role in tumor formation and metastatic

developments (Labat-Robert and Robert, 2007; Ingber, 2008). Thus, it is notable that tumor cells not only affect normal ECM biosynthesis by stimulation of adjacent fibroblasts but themselves are able to produce elastic fibers (Kadar et al., 2002; Lapis and Timar, 2002). Considering an accumulation of senescent cells in the aging tissue, an increased elastin formation of senescent HMEC may thus provide a microenvironment in the aged breast which might favor malignant transformation. However, ECM formation, composition and architecture are determined by a complex interplay of a multifactorial regulatory system, whereof the particular mechanisms are still obscure. Additional investigations are required to assess the impact of the extracellular microenvironment and to understand influences of modified ECM components in relation to tumor formation and cancer progression.

4.4.2 Increased LOXL1 expression in senescent HMEC contributes to an enhanced elastic fiber formation

Post-translational processing by lysyl oxidases plays a key role in elastin fiber formation and provides structural shape to the ECM (Liu et al., 2004; Szauter et al., 2005). Lysyl oxidases are multifunctional proteins whose deregulation contributes to a variety of pathological developments including fibrotic processes, neurodegenerative disorders as well as tumor progression and metastasis (Rodriguez et al., 2008). Recent investigations revealed LOXL1 as an essential factor in normal elastin synthesis, and moreover, suggested an important role for this isoform in adult elastin maturation (Liu et al., 2004; Behmoaras et al., 2008), which is also supported by the present data. During cellular senescence of HMEC, the enhanced tropoelastin expression was accompanied by increased LOXL1 protein levels and an elevated lysyl oxidase activity, probably contributing to the high incidence of elastin fibers in senescent HMEC cultures. Furthermore, the direct involvement of LO enzyme activity in elastin formation during HMEC senescence was verified by inhibitor studies. These findings suggested an important function of LOXL1 to ensure further processing of the prevalent tropoelastin precursor molecules in senescent HMEC populations. LOXL1 knockout studies in mice substantiate an abnormal elastin polymerization and confirm an accumulation of dysfunctional tropoelastin aggregates (Liu et al., 2004). In addition to their cross-linking activity and certain scaffolding capacities, there is increasing evidence that lysyl oxidases are able to regulate transcriptional activation, migration and cell adhesion and in that way contribute to malignant cell transformation and cancer progression (Payne et al., 2007). Moreover, it was observed that LOX expression directly affects tropoelastin levels and was shown to interfere with tropoelastin promoter regulation (Oleggini et al., 2007). However, further experiments have to analyze the function of an increased LOXL1 expression with respect to potential intracellular alterations during cellular senescence of HMEC.

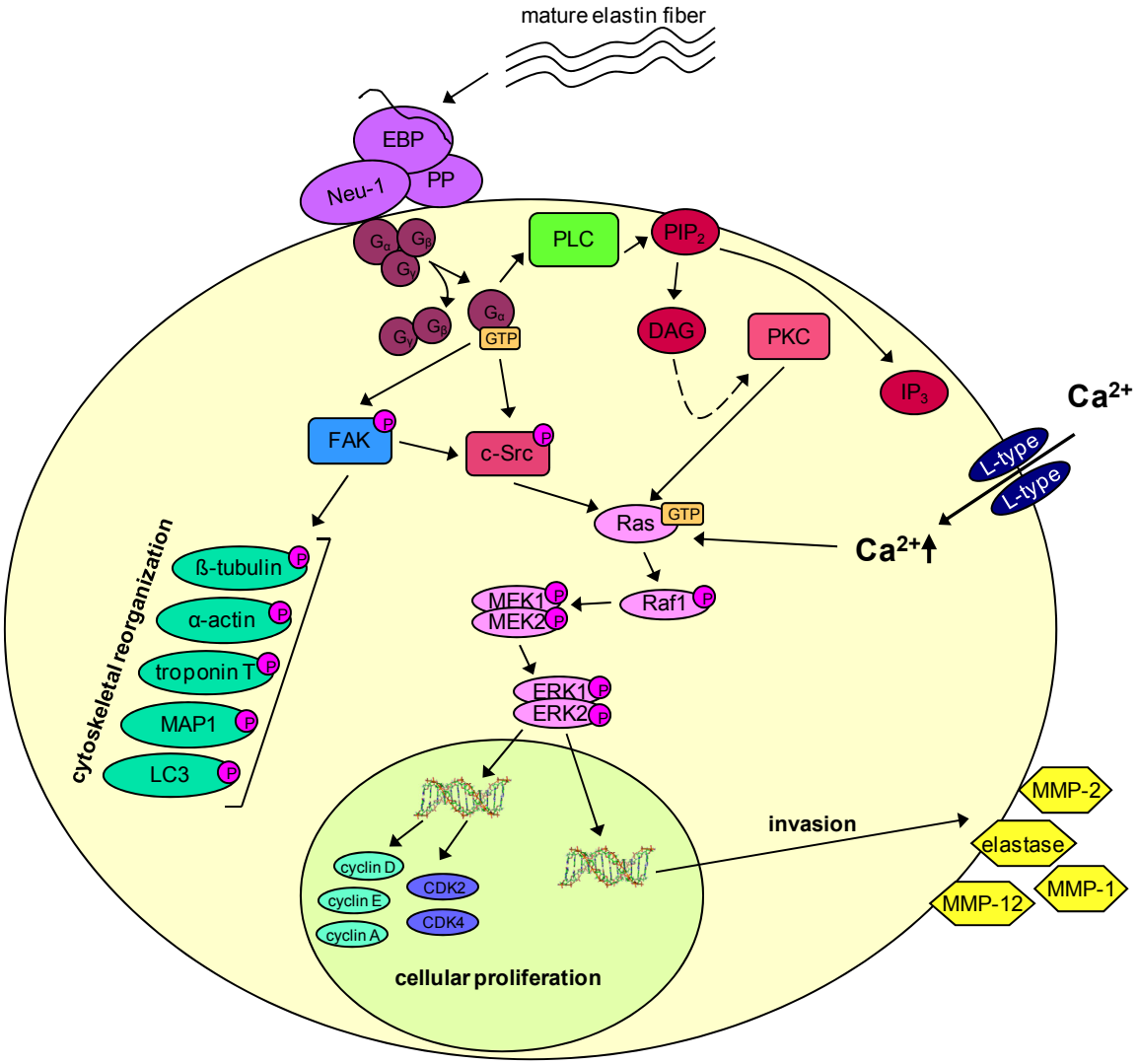

Figure 28: A schematic overview of elastin receptor signaling

Interaction of elastin with EBP stimulates Neu-1 activity and involves activation of intracellular G proteins that impart receptor signaling to a variety of cellular pathways. Phosphorylation of FAK induces reorganization of the cytoskeleton and ensures cell motility. An increasing invasiveness is moreover achieved by enhanced expression and extracellular secretion of degrading enzymes such as MMPs and elastase. The tyrosine kinase c-Src can be stimulated by FAK or via G proteins and relays phosphorylation signals downstream to ERK1/2. Activated PLC cleaves phosphatidylinositol biphosphate (PIP_2) in the plasma membrane and releases intracellular DAG and IP_3 followed by an elevation of cytoplasmic Ca^{2+} ions and translocation of PKC to the plasma membrane. Initiation of the MAP kinase cascade including the small GTPase Ras and ERK1/2 provokes activation of several transcription factors. The presence of other signaling molecules and the interaction with distinct binding-partners subsequently modulates transcriptional activation of genes such as CDKs and their associated cyclins or MMPs. In contrast, ERK1/2-activation upon sHB-EGF/ErbB4/1-binding stimulates transcription of the elastin precursor tropoelastin (cp. Figure 27). Thus, binding of elastin to the EBP at the cell surface can affect cellular proliferation, migration, invasion and chemotaxis, indicating crucial aspects involved in malignant transformation and metastatic developments. The scheme was adapted from (Mochizuki et al., 2002).

4.4.3 Elastin receptor signaling

Besides its structural function as a component of the ECM, elastin stimulates a variety of biological activities such as chemotaxis, proliferation and protease release (Duca et al., 2004). This suggests other potential mechanisms by which the senescent HMEC may influence susceptible adjacent cells and may favor a malignant transformation. Elastin peptides can specifically interact with surrounding cells via receptor-binding and thereby affect intracellular signal transduction pathways (Mochizuki et al., 2002). The same complex of elastin-binding protein (EBP) associated with neuraminidase-1 (Neu-1) and protective protein/cathepsin A (PP) can act on one hand as a molecular chaperone in tropoelastin trafficking (cp. 1.3.1.2 and Figure 4) (Hinek et al., 1995), and on the other hand, can function as a specific elastin receptor at the cell surface of a variety of cells types (Figure 28) (Fulop et al., 2001; Hinek et al., 2006). EBP represents a spliced variant of lysosomal β-galactosidase and is localized to the cell surface by membrane-bound Neu-1 and PP (Duca et al., 2007). Neu-1 is a member of sialidases that hydrolyze terminal sialic acid residues of glycoproteins, oligosaccharides and glycolipids. Whereas Neu-1 activity was essential for elastin peptide signaling, the serine protease activity of PP was not required and PP rather protects EBP and Neu-1 from proteasomal digestion (Duca et al., 2007). Elastin binding stimulates a variety of signal transduction pathways that provoke diverse effects; however, the mechanisms affected by elastin receptor activation vary greatly among different cell types (Figure 28). Thus, binding of elastin to EBP involves intracellular activation of pertussis toxin-sensitive G proteins, opening of L-type Ca^{2+}-channels and induction of several tyrosine kinases including c-Src, FAK, PDGF receptor kinase and the MAP kinase pathway (Figure 28) (Duca et al., 2004). G protein-mediated activation of phospholipase C (PLC) causes increase of the second messengers inositoltriphosphate (IP_3) and diacylglycerol (DAG) that in turn lead to intracellular Ca^{2+} elevation and protein kinase C (PKC) activation and eventually relay downstream signaling via Ras to the MAP kinase pathway (Fulop et al., 2001). The elastin receptor-mediated initiation of the MAP kinase phosphorylation cascade via Ras – Raf-1 – MEK1/2 – ERK1/2 subsequently triggers expression and release of proteases such as elastase, MMP-1, MMP-2 and MMP-12 which contribute to matrix degradation and invasion (Fulop et al., 2001; Duca et al., 2007; Coquerel et al., 2009). Remarkably, as shown before, the same signaling cascade can also activate Fra-1 which inhibits tropoelastin expression (Figure 27). However, the stimulation of these apparent contradictory effects might probably not be caused due to one distinct signal but rather depends on a complex interplay of a variety of interacting proteins. Thus, presence of other binding-partners and the implementation of certain threshold effects might be related to the preference of one or the other signaling outcome. Thus, activation of MAP kinases by c-Src and/or PDGF receptor was shown to be responsible for an induction of CDKs and their regulatory cyclins, thereby stimulating cellular proliferation (Mochizuki et al., 2002). The focal adhesion kinase (FAK) imparts elastin receptor transduction to phosphorylation of cytoskeleton-associated molecules such as β-tubulin, α-actin, microtubule-associated protein-1 light chain 3 (LC3), microtubule-associated protein 1 (MAP1) or troponin T, implicating

cytoskeletal reorganization (Mochizuki et al., 2002). Besides presence on non-tumorigenic cells, the elastin receptor was shown to be abundantly expressed on tumor cells and was related to the metastatic evolution of breast cancer, related to its role in migration and invasion (Fulop and Larbi, 2002; Lapis and Timar, 2002). Previous studies have demonstrated a progressive uncoupling of the elastin receptor to be reliant on age and suggested an important role in the development of age-associated diseases (Jacob et al., 1987; Fulop et al., 2001).
According to the diversity of biological functions affected by the elastin receptor, an increased elastin occurrence during cellular senescence of HMEC might as well imply potential effects on the senescent cell itself or through paracrine signaling on neighboring cells. However, extensive investigations are required to assess a possible role for the elastin receptor during senescence of HMEC.

4.5 Conclusion

The present data revealed significant alterations in the extracellular environment of senescent HMEC including down-regulation of the cell surface glycoproteins CD24, CD44 and CD227, an attenuated MMP-7 activity and an increased expression of tropoelastin that may contribute to an enhanced elastic fiber generation in the senescent HMEC population. Down-modulation of MMP-7 in young HMEC induced an accelerated aging, and thus, verified a direct involvement of this metalloproteinase in the aging process of HMEC. Besides extracellular effects due to reduced matrix degradation, MMP-7 down-regulation can affect a variety of intracellular signaling mechanisms. Localization studies revealed a co-localization of MMP-7 with the growth factor HB-EGF in young HMEC but a diffuse distribution in the senescent population. The reduced interaction between MMP-7 and HB-EGF could be related to the decreased expression of CD44 at the cell surface of senescent HMEC. However, supplementary analyses that specify the different CD44 variants, particularly variant 3, are required to evaluate a potential role of CD44 in MMP-7/HB-EGF cell surface anchorage.
Further experiments demonstrated that reduced MMP-7 and diminished HB-EGF affected downstream signals that caused decreased levels of the transcription factor Fra-1, which resulted in an increased tropoelastin transcription. Moreover, the activation of tropoelastin expression may favor the LO-dependent elastin maturation in the extracellular matrix of senescent HMEC. Examination of the elastin receptor status at the cell surface of senescent HMEC populations would be interesting to consider a potential role of elastin receptor-associated signaling pathways in aging HMEC. In this context, it may be speculated that an increased interaction between elastin and its receptor during senescence could induce expression of proliferation-promoting genes (e.g. CDKs and cyclins; cp. Figure 28), which in turn would contribute to an aberrant cell cycle progression and the generation of senescent 8N DNA HMEC. However, the particular signaling mechanisms and their complex interplay that regulates the cell cycle during cellular senescence of HMEC need to be elucidated.

The inhibited cell division and the enlarged cell morphology of senescent HMEC represented characteristics of a non-malignant cell, which was in concert with the reduced levels of the tumor-associated CD227 (MUC1) during senescence. Conversely, an increased presence of elastin was related to a potential breast cancer development. To unravel this apparent contradiction, the *in vivo* situation has to be considered. In the aging organism, senescent HMEC accumulate in the breast tissue, and thus, the predicted effects of elastin may not only influence the senescent cells themselves, but rather act on susceptible adjacent cells, whose signaling mechanisms are affected by additional cancer-promoting deregulations which favor their malignant transformation.

5 Table of figures

6 List of abbreviations

53BP1	p53-binding protein
ADAM	a desintegrin and metalloproteinase
ADAMTS	a desintegrin and metalloproteinase with thrombospondin motif
ATM	ataxia telangiectasia mutated
AP-1	activator protein-1
BAPN	β-aminopropionitrile
BiP5	heat shock 70kDa protein 5
BMP-1	bone morphogenetic protein-1
CD	cluster of differentiation
Cdc25	cell division cycle 25
CDK	cyclin-dependent kinase
C/EBP-ß	CCAAT/enhancer binding protein-ß
cEGF	Ca^{2+}-binding epidermal growth factor
CHK1	checkpoint kinase 1
CHK2	checkpoint kinase 2
CIP	CDK-interacting protein
CRE	cAMP response element
c-Src	cellular Src (tyrosine kinase), similar to v-src gene of Rous sarcoma virus
ddH_2O	double distilled water
DMEM	Dulbecco's Modified Eagle Medium
DMSO	dimethyl sulfoxide
DP	dimerization partner
DSB	double strand break
EBP	elastin binding protein
ECM	extracellular matrix
EDTA	ethylene diamine tetraacetic acid
EGTA	ethylene glycol tetraacetic acid
EGF	epidermal growth factor
Elk-1	E26 like protein-1 (Ets domain transcription factor, TCF subfamily)
EMILIN-1	elastin-microfibril-interface located protein-1
EMMPRIN	extracellular matrix metalloproteinase inducer
ErbB1	avian v-erb-a erythroblastic leukemia viral oncogene homolog 1
ErbB4	avian v-erb-a erythroblastic leukemia viral oncogene homolog 4
ERK1/2	extracelluar signal-related kinase 1/2
Ets-1	erythroblastosis twenty six (erythroblastosis virus E26 oncogene homolog 1)
FAK	focal adhesion kinase
FCS	fetal calf serum

FGF	fibroblast growth factor
Fib-1	fibrillin-1
FKBP65	FK506 binding protein
Fra-1	Fos-related antigen-1
GPI	glycosylphosphatidylinositol
HB-EGF	heparin-binding epidermal growth factor-like growth factor
HMEC	human mammary epithelial cells
HSP47	heat shock protein 47
HSPG	heparan sulfate proteoglycan
hTERC	human telomerase RNA component
hTERT	human telomerase reverse transcriptase
Id-1	inhibitor of DNA binding 1
IGF	insulin growth factor
IGFBP	insulin growth factor binding protein
INF-β	interferon-β
INK4a	polypeptide inhibitors of CDK4 and CDK6
kbp	kilo basepairs
KGF	keratinocyte growth factor
KIP	kinase inhibitor protein
LC3	microtubule-associated protein-1 light chain 3
LO	lysyl oxidase (enzyme family)
LOX	lysyl oxidase
LOXL1	lysyl oxidase-like 1
LTQ	lysyl tyrosylquinon
MAP1	microtubule-associated protein 1
MAGP	matrix-associated glycoprotein-1
MDM2	mouse double minute 2 homolog
MMP	matrix metalloproteinase
MT1-MMP	membrane type 1 matrix metalloproteinase
MRE11	meiotic recombination 11
NBS1	Nijmegen breakage syndrome 1
Neu-1	neuraminidase-1
NF-*x*B	nuclear factor kappa B
NLS	nuclear localization signal
P	phosphorylation
PARP-1	poly(ADP-ribose) polymerase-1
PBS	phosphate buffered saline
PBST	phosphate buffered saline and Tween
PD	population doublings

PDGF	platelet-derived growth factor
PEA3	polyoma enhancer activator 3
PG	proteoglycans
PP	protective protein/cathepsin A
PP1	protein phosphatase 1
pRb	retinoblastoma protein
ROS	reactive oxygen species
RNAi	RNA interference
SA β-gal	senescence associated β-galactosidase
SD	standard deviation
sHB-EGF	soluble heparin-binding epidermal growth factor
siRNA	small interfering RNA
SP	specificity protein
stasis	stress or aberrant signaling-inducing senescence
TB	TGF-β-binding
TBS	tris buffered saline
TGF-β	transforming growth factor-β
TIMP	tissue inhibitor of metalloproteinases
TNF-α	tumor necrosis factor-α
TNS	trypsin neutralization solution
VEGF	vascular endothelial growth factor

7 References

Ahmad, R., Raina, D., Trivedi, V., Ren, J., Rajabi, H., Kharbanda, S., Kufe, D. (2007) MUC1 oncoprotein activates the IkappaB kinase beta complex and constitutive NF-kappaB signalling. Nat Cell Biol 9, 1419-1427.

Alani, R.M., Young, A.Z., Shifflett, C.B. (2001) Id1 regulation of cellular senescence through transcriptional repression of p16/Ink4a. Proc Natl Acad Sci U S A 98, 7812-7816.

Andreassen, P.R., Lacroix, F.B., Lohez, O.D., Margolis, R.L. (2001) Neither p21WAF1 nor 14-3-3sigma prevents G2 progression to mitotic catastrophe in human colon carcinoma cells after DNA damage, but p21WAF1 induces stable G1 arrest in resulting tetraploid cells. Cancer Res 61, 7660-7668.

Andreassi, M.G. (2008) DNA damage, vascular senescence and atherosclerosis. J Mol Med 86, 1033-1043.

Arellano, M., Moreno, S. (1997) Regulation of CDK/cyclin complexes during the cell cycle. Int J Biochem Cell Biol 29, 559-573.

Ashworth, J.L., Kelly, V., Rock, M.J., Shuttleworth, C.A., Kielty, C.M. (1999) Regulation of fibrillin carboxy-terminal furin processing by N-glycosylation, and association of amino- and carboxy-terminal sequences. J Cell Sci 112 (Pt 22), 4163-4171.

Aviv, A., Levy, D., Mangel, M. (2003) Growth, telomere dynamics and successful and unsuccessful human aging. Mech Ageing Dev 124, 829-837.

Bajorath, J., Greenfield, B., Munro, S.B., Day, A.J., Aruffo, A. (1998) Identification of CD44 residues important for hyaluronan binding and delineation of the binding site. J Biol Chem 273, 338-343.

Bakkenist, C.J., Kastan, M.B. (2003) DNA damage activates ATM through intermolecular autophosphorylation and dimer dissociation. Nature 421, 499-506.

Bax, D.V., Bernard, S.E., Lomas, A., Morgan, A., Humphries, J., Shuttleworth, C.A., Humphries, M.J., Kielty, C.M. (2003) Cell adhesion to fibrillin-1 molecules and microfibrils is mediated by alpha 5 beta 1 and alpha v beta 3 integrins. J Biol Chem 278, 34605-34616.

Behmoaras, J., Slove, S., Seve, S., Vranckx, R., Sommer, P., Jacob, M.P. (2008) Differential expression of lysyl oxidases LOXL1 and LOX during growth and aging suggests specific roles in elastin and collagen fiber remodeling in rat aorta. Rejuvenation Res 11, 883-889.

Belkin, A.M., Akimov, S.S., Zaritskaya, L.S., Ratnikov, B.I., Deryugina, E.I., Strongin, A.Y. (2001) Matrix-dependent proteolysis of surface transglutaminase by membrane-type metalloproteinase regulates cancer cell adhesion and locomotion. J Biol Chem 276, 18415-18422.

Bernfield, M., Kokenyesi, R., Kato, M., Hinkes, M.T., Spring, J., Gallo, R.L., Lose, E.J. (1992) Biology of the syndecans: a family of transmembrane heparan sulfate proteoglycans. Annu Rev Cell Biol 8, 365-393.

Bertram, C., Hass, R. (2008a) MMP-7 is involved in the aging of primary human mammary epithelial cells (HMEC). Exp Gerontol 43, 209-217.

Bertram, C., Hass, R. (2008b) Cellular responses to reactive oxygen species-induced DNA damage and aging. Biol Chem 389, 211-220.

Bhoopathi, P., Chetty, C., Kunigal, S., Vanamala, S.K., Rao, J.S., Lakka, S.S. (2008) Blockade of tumor growth due to matrix metalloproteinase-9 inhibition is mediated by sequential activation of beta1-integrin, ERK, and NF-kappaB. J Biol Chem 283, 1545-1552.

Blackburn, E.H., Greider, C.W., Henderson, E., Lee, M.S., Shampay, J., Shippen-Lentz, D. (1989) Recognition and elongation of telomeres by telomerase. Genome 31, 553-560.

Blackburn, E.H. (1991) Structure and function of telomeres. Nature 350, 569-573.

Bode, W., Gomis-Ruth, F.X., Stockler, W. (1993) Astacins, serralysins, snake venom and matrix metalloproteinases exhibit identical zinc-binding environments (HEXXHXXGXXH and

Met-turn) and topologies and should be grouped into a common family, the 'metzincins'. FEBS Lett 331, 134-140.

Bode, W., Maskos, K. (2003) Structural basis of the matrix metalloproteinases and their physiological inhibitors, the tissue inhibitors of metalloproteinases. Biol Chem 384, 863-872.

Bollinger, J.A., Brown, D.E., Dooley, D.M. (2005) The Formation of lysine tyrosylquinone (LTQ) is a self-processing reaction. Expression and characterization of a Drosophila lysyl oxidase. Biochemistry 44, 11708-11714.

Bosman, F.T., Stamenkovic, I. (2003) Functional structure and composition of the extracellular matrix. J Pathol 200, 423-428.

Bouissou, H., Pieraggi, M.T., Julian, M., Savit, T. (1988) The elastic tissue of the skin. A comparison of spontaneous and actinic (solar) aging. Int J Dermatol 27, 327-335.

Brenner, A.J., Stampfer, M.R., Aldaz, C.M. (1998) Increased p16 expression with first senescence arrest in human mammary epithelial cells and extended growth capacity with p16 inactivation. Oncogene 17, 199-205.

Bressan, G.M., Daga-Gordini, D., Colombatti, A., Castellani, I., Marigo, V., Volpin, D. (1993) Emilin, a component of elastic fibers preferentially located at the elastin-microfibrils interface. J Cell Biol 121, 201-212.

Broekelmann, T.J., Kozel, B.A., Ishibashi, H., Werneck, C.C., Keeley, F.W., Zhang, L., Mecham, R.P. (2005) Tropoelastin interacts with cell-surface glycosaminoglycans via its COOH-terminal domain. J Biol Chem 280, 40939-40947.

Broekelmann, T.J., Ciliberto, C.H., Shifren, A., Mecham, R.P. (2008) Modification and functional inactivation of the tropoelastin carboxy-terminal domain in cross-linked elastin. Matrix Biol 27, 631-639.

Brown-Augsburger, P., Broekelmann, T., Rosenbloom, J., Mecham, R.P. (1996) Functional domains on elastin and microfibril-associated glycoprotein involved in elastic fibre assembly. Biochem J 318 (Pt 1), 149-155.

Bruce, M.C., Honaker, C.E. (1998) Transcriptional regulation of tropoelastin expression in rat lung fibroblasts: changes with age and hyperoxia. Am J Physiol 274, L940-950.

Busino, L., Chiesa, M., Draetta, G.F., Donzelli, M. (2004) Cdc25A phosphatase: combinatorial phosphorylation, ubiquitylation and proteolysis. Oncogene 23, 2050-2056.

Campisi, J., d'Adda di Fagagna, F. (2007) Cellular senescence: when bad things happen to good cells. Nat Rev Mol Cell Biol 8, 729-740.

Carreras, I., Rich, C.B., Jaworski, J.A., Dicamillo, S.J., Panchenko, M.P., Goldstein, R., Foster, J.A. (2001) Functional components of basic fibroblast growth factor signaling that inhibit lung elastin gene expression. Am J Physiol Lung Cell Mol Physiol 281, L766-775.

Chan, A.K., Lockhart, D.C., von Bernstorff, W., Spanjaard, R.A., Joo, H.G., Eberlein, T.J., Goedegebuure, P.S. (1999) Soluble MUC1 secreted by human epithelial cancer cells mediates immune suppression by blocking T-cell activation. Int J Cancer 82, 721-726.

Chaturvedi, P., Eng, W.K., Zhu, Y., Mattern, M.R., Mishra, R., Hurle, M.R., Zhang, X., Annan, R.S., Lu, Q., Faucette, L.F., Scott, G.F., Li, X., Carr, S.A., Johnson, R.K., Winkler, J.D., Zhou, B.B. (1999) Mammalian Chk2 is a downstream effector of the ATM-dependent DNA damage checkpoint pathway. Oncogene 18, 4047-4054.

Chen, Q.M., Liu, J., Merrett, J.B. (2000) Apoptosis or senescence-like growth arrest: influence of cell-cycle position, p53, p21 and bax in H2O2 response of normal human fibroblasts. Biochem J 347, 543-551.

Cheng, K., Xie, G., Raufman, J.P. (2007) Matrix metalloproteinase-7-catalyzed release of HB-EGF mediates deoxycholyltaurine-induced proliferation of a human colon cancer cell line. Biochem Pharmacol 73, 1001-1012.

Choi, D.S., Kim, J.H., Ryu, H.S., Kim, H.C., Han, J.H., Lee, J.S., Min, C.K. (2007) Syndecan-1, a key regulator of cell viability in endometrial cancer. Int J Cancer 121, 741-750.

Choi, J., Bergdahl, A., Zheng, Q., Starcher, B., Yanagisawa, H., Davis, E.C. (2009) Analysis of dermal elastic fibers in the absence of fibulin-5 reveals potential roles for fibulin-5 in elastic fiber assembly. Matrix Biol.

Cleary, E.G., Gibson, M.A. (1983) Elastin-associated microfibrils and microfibrillar proteins. Int Rev Connect Tissue Res 10, 97-209.

Connell-Crowley, L., Harper, J.W., Goodrich, D.W. (1997) Cyclin D1/Cdk4 regulates retinoblastoma protein-mediated cell cycle arrest by site-specific phosphorylation. Mol Biol Cell 8, 287-301.

Cooper, S., Yu, C., Shayman, J.A. (1999) Phosphorylation-dephosphorylation of retinoblastoma protein not necessary for passage through the mammalian cell division cycle. IUBMB Life 48, 225-230.

Coppe, J.P., Kauser, K., Campisi, J., Beausejour, C.M. (2006) Secretion of vascular endothelial growth factor by primary human fibroblasts at senescence. J Biol Chem 281, 29568-29574.

Coquerel, B., Poyer, F., Torossian, F., Dulong, V., Bellon, G., Dubus, I., Reber, A., Vannier, J.P. (2009) Elastin-derived peptides: Matrikines critical for glioblastoma cell aggressiveness in a 3-D system. Glia.

Couillard, J., Demers, M., Lavoie, G., St-Pierre, Y. (2006) The role of DNA hypomethylation in the control of stromelysin gene expression. Biochem Biophys Res Commun 342, 1233-1239.

Crawford, H.C., Fingleton, B.M., Rudolph-Owen, L.A., Goss, K.J., Rubinfeld, B., Polakis, P., Matrisian, L.M. (1999) The metalloproteinase matrilysin is a target of beta-catenin transactivation in intestinal tumors. Oncogene 18, 2883-2891.

Cristofalo, V.J., Allen, R.G., Pignolo, R.J., Martin, B.G., Beck, J.C. (1998) Relationship between donor age and the replicative lifespan of human cells in culture: a reevaluation. Proc Natl Acad Sci U S A 95, 10614-10619.

Cronshaw, A.D., Fothergill-Gilmore, L.A., Hulmes, D.J. (1995) The proteolytic processing site of the precursor of lysyl oxidase. Biochem J 306 (Pt 1), 279-284.

Csiszar, K. (2001) Lysyl oxidases: a novel multifunctional amine oxidase family. Prog Nucleic Acid Res Mol Biol 70, 1-32.

d'Adda di Fagagna, F., Reaper, P.M., Clay-Farrace, L., Fiegler, H., Carr, P., Von Zglinicki, T., Saretzki, G., Carter, N.P., Jackson, S.P. (2003) A DNA damage checkpoint response in telomere-initiated senescence. Nature 426, 194-198.

d'Adda di Fagagna, F. (2008) Living on a break: cellular senescence as a DNA-damage response. Nat Rev Cancer 8, 512-522.

Danielson, K.G., Baribault, H., Holmes, D.F., Graham, H., Kadler, K.E., Iozzo, R.V. (1997) Targeted disruption of decorin leads to abnormal collagen fibril morphology and skin fragility. J Cell Biol 136, 729-743.

Datta, A., Nicot, C. (2008) Telomere attrition induces a DNA double-strand break damage signal that reactivates p53 transcription in HTLV-I leukemic cells. Oncogene 27, 1135-1141.

Davis, E.C., Broekelmann, T.J., Ozawa, Y., Mecham, R.P. (1998) Identification of tropoelastin as a ligand for the 65-kD FK506-binding protein, FKBP65, in the secretory pathway. J Cell Biol 140, 295-303.

Davis, E.C., Mecham, R.P. (1998) Intracellular trafficking of tropoelastin. Matrix Biol 17, 245-254.

Dimri, G.P., Lee, X., Basile, G., Acosta, M., Scott, G., Roskelley, C., Medrano, E.E., Linskens, M., Rubelj, I., Pereira-Smith, O., et al. (1995) A biomarker that identifies senescent human cells in culture and in aging skin in vivo. Proc Natl Acad Sci U S A 92, 9363-9367.

Downing, A.K., Knott, V., Werner, J.M., Cardy, C.M., Campbell, I.D., Handford, P.A. (1996) Solution structure of a pair of calcium-binding epidermal growth factor-like domains: implications for the Marfan syndrome and other genetic disorders. Cell 85, 597-605.

Duca, L., Floquet, N., Alix, A.J., Haye, B., Debelle, L. (2004) Elastin as a matrikine. Crit Rev Oncol Hematol 49, 235-244.

Duca, L., Blanchevoye, C., Cantarelli, B., Ghoneim, C., Dedieu, S., Delacoux, F., Hornebeck, W., Hinek, A., Martiny, L., Debelle, L. (2007) The elastin receptor complex transduces signals through the catalytic activity of its Neu-1 subunit. J Biol Chem 282, 12484-12491.

Edwards, D.R., 2001. The tissue inhibitors of metalloproteinases (TIMPs), in: Clendeninn, N.J., Appelt, K. (Eds.), Matrix Metalloproteinase Inhibitors in Cancer Therapy. Humana, Totowa, NJ, pp. 67–84.

El-Hallous, E., Sasaki, T., Hubmacher, D., Getie, M., Tiedemann, K., Brinckmann, J., Batge, B., Davis, E.C., Reinhardt, D.P. (2007) Fibrillin-1 interactions with fibulins depend on the first hybrid domain and provide an adaptor function to tropoelastin. J Biol Chem 282, 8935-8946.

Eyre, D.R., Paz, M.A., Gallop, P.M. (1984) Cross-linking in collagen and elastin. Annu Rev Biochem 53, 717-748.

Fahling, M., Steege, A., Perlewitz, A., Nafz, B., Mrowka, R., Persson, P.B., Thiele, B.J. (2005) Role of nucleolin in posttranscriptional control of MMP-9 expression. Biochim Biophys Acta 1731, 32-40.

Farahmand, S., Cowan, D.F. (1991) Elastosis in the normal aging breast. A histopathologic study of 140 cases. Arch Pathol Lab Med 115, 1241-1246.

Farhadian, F., Contard, F., Corbier, A., Barrieux, A., Rappaport, L., Samuel, J.L. (1995) Fibronectin expression during physiological and pathological cardiac growth. J Mol Cell Cardiol 27, 981-990.

Ferbeyre, G., de Stanchina, E., Lin, A.W., Querido, E., McCurrach, M.E., Hannon, G.J., Lowe, S.W. (2002) Oncogenic ras and p53 cooperate to induce cellular senescence. Mol Cell Biol 22, 3497-3508.

Fernandes, R.J., Hirohata, S., Engle, J.M., Colige, A., Cohn, D.H., Eyre, D.R., Apte, S.S. (2001) Procollagen II amino propeptide processing by ADAMTS-3. Insights on dermatosparaxis. J Biol Chem 276, 31502-31509.

Filippov, S., Caras, I., Murray, R., Matrisian, L.M., Chapman, H.A., Jr., Shapiro, S., Weiss, S.J. (2003) Matrilysin-dependent elastolysis by human macrophages. J Exp Med 198, 925-935.

Fini, M.E., Cook, J.R., Mohan, R., Brinckerhoff, C.E., 1998. Regulation of matrix metalloproteinase gene expression, in: Parks, W.C., Mecham, R.P. (Eds.), Matrix Metalloproteinases. Academic, New York, pp. 299–356.

Flanary, B.E., Sammons, N.W., Nguyen, C., Walker, D., Streit, W.J. (2007) Evidence that aging and amyloid promote microglial cell senescence. Rejuvenation Res 10, 61-74.

Fogelgren, B., Polgar, N., Szauter, K.M., Ujfaludi, Z., Laczko, R., Fong, K.S., Csiszar, K. (2005) Cellular fibronectin binds to lysyl oxidase with high affinity and is critical for its proteolytic activation. J Biol Chem 280, 24690-24697.

Fowlkes, J.L., Thrailkill, K.M., Serra, D.M., Suzuki, K., Nagase, H. (1995) Matrix metalloproteinases as insulin-like growth factor binding protein-degrading proteinases. Prog Growth Factor Res 6, 255-263.

Friederichs, J., Zeller, Y., Hafezi-Moghadam, A., Grone, H.J., Ley, K., Altevogt, P. (2000) The CD24/P-selectin binding pathway initiates lung arrest of human A125 adenocarcinoma cells. Cancer Res 60, 6714-6722.

Fulop, T., Larbi, A. (2002) Putative role of 67 kDa elastin-laminin receptor in tumor invasion. Semin Cancer Biol 12, 219-229.

Fulop, T., Jr., Douziech, N., Jacob, M.P., Hauck, M., Wallach, J., Robert, L. (2001) Age-related alterations in the signal transduction pathways of the elastin-laminin receptor. Pathol Biol (Paris) 49, 339-348.

Garbe, J.C., Holst, C.R., Bassett, E., Tlsty, T., Stampfer, M.R. (2007) Inactivation of p53 function in cultured human mammary epithelial cells turns the telomere-length dependent senescence barrier from agonescence into crisis. Cell Cycle 6, 1927-1936.

Ghajar, C.M., Bissell, M.J. (2008) Extracellular matrix control of mammary gland morphogenesis and tumorigenesis: insights from imaging. Histochem Cell Biol 130, 1105-1118.

Giampuzzi, M., Oleggini, R., Di Donato, A. (2003) Demonstration of in vitro interaction between tumor suppressor lysyl oxidase and histones H1 and H2: definition of the regions involved. Biochim Biophys Acta 1647, 245-251.

Giannelli, G., Falk-Marzillier, J., Schiraldi, O., Stetler-Stevenson, W.G., Quaranta, V. (1997) Induction of cell migration by matrix metalloprotease-2 cleavage of laminin-5. Science 277, 225-228.

Gibson, M.A., Leavesley, D.I., Ashman, L.K. (1999) Microfibril-associated glycoprotein-2 specifically interacts with a range of bovine and human cell types via alphaVbeta3 integrin. J Biol Chem 274, 13060-13065.

Goldstein, S. (1990) Replicative senescence: the human fibroblast comes of age. Science 249, 1129-1133.

Golubnitschaja, O. (2007) Cell cycle checkpoints: the role and evaluation for early diagnosis of senescence, cardiovascular, cancer, and neurodegenerative diseases. Amino Acids 32, 359-371.

Gray, W.R., Sandberg, L.B., Foster, J.A. (1973) Molecular model for elastin structure and function. Nature 246, 461-466.

Griffith, J.D., Comeau, L., Rosenfield, S., Stansel, R.M., Bianchi, A., Moss, H., de Lange, T. (1999) Mammalian telomeres end in a large duplex loop. Cell 97, 503-514.

Gruda, M.C., Kovary, K., Metz, R., Bravo, R. (1994) Regulation of Fra-1 and Fra-2 phosphorylation differs during the cell cycle of fibroblasts and phosphorylation in vitro by MAP kinase affects DNA binding activity. Oncogene 9, 2537-2547.

Hampel, B., Malisan, F., Niederegger, H., Testi, R., Jansen-Durr, P. (2004) Differential regulation of apoptotic cell death in senescent human cells. Exp Gerontol 39, 1713-1721.

Hand, P.H., Nuti, M., Colcher, D., Schlom, J. (1983) Definition of antigenic heterogeneity and modulation among human mammary carcinoma cell populations using monoclonal antibodies to tumor-associated antigens. Cancer Res 43, 728-735.

Handford, P.A., Downing, A.K., Reinhardt, D.P., Sakai, L.Y. (2000) Fibrillin: from domain structure to supramolecular assembly. Matrix Biol 19, 457-470.

Hao, L., Du, M., Lopez-Campistrous, A., Fernandez-Patron, C. (2004) Agonist-induced activation of matrix metalloproteinase-7 promotes vasoconstriction through the epidermal growth factor-receptor pathway. Circ Res 94, 68-76.

Hara, E., Smith, R., Parry, D., Tahara, H., Stone, S., Peters, G. (1996) Regulation of p16CDKN2 expression and its implications for cell immortalization and senescence. Mol Cell Biol 16, 859-867.

Harendza, S., Lovett, D.H., Panzer, U., Lukacs, Z., Kuhnl, P., Stahl, R.A. (2003) Linked common polymorphisms in the gelatinase a promoter are associated with diminished transcriptional response to estrogen and genetic fitness. J Biol Chem 278, 20490-20499.

Harley, C.B., Futcher, A.B., Greider, C.W. (1990) Telomeres shorten during ageing of human fibroblasts. Nature 345, 458-460.

Harper, J.W., Adami, G.R., Wei, N., Keyomarsi, K., Elledge, S.J. (1993) The p21 Cdk-interacting protein Cip1 is a potent inhibitor of G1 cyclin-dependent kinases. Cell 75, 805-816.

Hayflick, L., Moorhead, P.S. (1961) The serial cultivation of human diploid cell strains. Exp Cell Res 25, 585-621.

Hayflick, L. (1965) The Limited in Vitro Lifetime of Human Diploid Cell Strains. Exp Cell Res 37, 614-636.

He, G., Siddik, Z.H., Huang, Z., Wang, R., Koomen, J., Kobayashi, R., Khokhar, A.R., Kuang, J. (2005) Induction of p21 by p53 following DNA damage inhibits both Cdk4 and Cdk2 activities. Oncogene 24, 2929-2943.

Heldin, P., Karousou, E., Bernert, B., Porsch, H., Nishitsuka, K., Skandalis, S.S. (2008) Importance of hyaluronan-CD44 interactions in inflammation and tumorigenesis. Connect Tissue Res 49, 215-218.

Henderson, M., Polewski, R., Fanning, J.C., Gibson, M.A. (1996) Microfibril-associated glycoprotein-1 (MAGP-1) is specifically located on the beads of the beaded-filament structure for fibrillin-containing microfibrils as visualized by the rotary shadowing technique. J Histochem Cytochem 44, 1389-1397.

Henningsson, F., Hergeth, S., Cortelius, R., Abrink, M., Pejler, G. (2006) A role for serglycin proteoglycan in granular retention and processing of mast cell secretory granule components. Febs J 273, 4901-4912.

Herbert, G.S., Sohn, V.Y., Mulcahy, M.J., Champeaux, A.L., Brown, T.A. (2007) Prognostic significance of reactivation of telomerase in breast core biopsy specimens. Am J Surg 193, 547-550; discussion 550.

Herbig, U., Jobling, W.A., Chen, B.P., Chen, D.J., Sedivy, J.M. (2004) Telomere shortening triggers senescence of human cells through a pathway involving ATM, p53, and p21(CIP1), but not p16(INK4a). Mol Cell 14, 501-513.

Hinek, A., Keeley, F.W., Callahan, J. (1995) Recycling of the 67-kDa elastin binding protein in arterial myocytes is imperative for secretion of tropoelastin. Exp Cell Res 220, 312-324.

Hinek, A., Pshezhetsky, A.V., von Itzstein, M., Starcher, B. (2006) Lysosomal sialidase (neuraminidase-1) is targeted to the cell surface in a multiprotein complex that facilitates elastic fiber assembly. J Biol Chem 281, 3698-3710.

Holst, C.R., Nuovo, G.J., Esteller, M., Chew, K., Baylin, S.B., Herman, J.G., Tlsty, T.D. (2003) Methylation of p16(INK4a) promoters occurs in vivo in histologically normal human mammary epithelia. Cancer Res 63, 1596-1601.

Hornsby, P.J. (2007) Senescence as an anticancer mechanism. J Clin Oncol 25, 1852-1857.

Huang, X., Tran, T., Zhang, L., Hatcher, R., Zhang, P. (2005) DNA damage-induced mitotic catastrophe is mediated by the Chk1-dependent mitotic exit DNA damage checkpoint. Proc Natl Acad Sci U S A 102, 1065-1070.

Hughes, K.A., Reynolds, R.M. (2005) Evolutionary and mechanistic theories of aging. Annu Rev Entomol 50, 421-445.

Huschtscha, L.I., Noble, J.R., Neumann, A.A., Moy, E.L., Barry, P., Melki, J.R., Clark, S.J., Reddel, R.R. (1998) Loss of p16INK4 expression by methylation is associated with lifespan extension of human mammary epithelial cells. Cancer Res 58, 3508-3512.

Huveneers, S., Truong, H., Danen, H.J. (2007) Integrins: signaling, disease, and therapy. Int J Radiat Biol 83, 743-751.

Huwiler, A., Akool el, S., Aschrafi, A., Hamada, F.M., Pfeilschifter, J., Eberhardt, W. (2003) ATP potentiates interleukin-1 beta-induced MMP-9 expression in mesangial cells via recruitment of the ELAV protein HuR. J Biol Chem 278, 51758-51769.

Imai, K., Yokohama, Y., Nakanishi, I., Ohuchi, E., Fujii, Y., Nakai, N., Okada, Y. (1995) Matrix metalloproteinase 7 (matrilysin) from human rectal carcinoma cells. Activation of the precursor, interaction with other matrix metalloproteinases and enzymic properties. J Biol Chem 270, 6691-6697.

Imai, K., Hiramatsu, A., Fukushima, D., Pierschbacher, M.D., Okada, Y. (1997) Degradation of decorin by matrix metalloproteinases: identification of the cleavage sites, kinetic analyses and transforming growth factor-beta1 release. Biochem J 322 (Pt 3), 809-814.

Ingber, D.E. (2008) Can cancer be reversed by engineering the tumor microenvironment? Semin Cancer Biol 18, 356-364.

Irelan, J.T., Gutierrez Del Arroyo, A., Gutierrez, A., Peters, G., Quon, K.C., Miraglia, L., Chanda, S.K. (2009) A functional screen for regulators of CKDN2A reveals MEOX2 as a transcriptional activator of INK4a. PLoS ONE 4, e5067.

Jackson, J.G., Pereira-Smith, O.M. (2006) p53 is preferentially recruited to the promoters of growth arrest genes p21 and GADD45 during replicative senescence of normal human fibroblasts. Cancer Res 66, 8356-8360.

Jacob, M.P., Fulop, T., Jr., Foris, G., Robert, L. (1987) Effect of elastin peptides on ion fluxes in mononuclear cells, fibroblasts, and smooth muscle cells. Proc Natl Acad Sci U S A 84, 995-999.

Jacobs, J.J., de Lange, T. (2004) Significant role for p16INK4a in p53-independent telomere-directed senescence. Curr Biol 14, 2302-2308.

Jacobs, J.J., de Lange, T. (2005) p16INK4a as a second effector of the telomere damage pathway. Cell Cycle 4, 1364-1368.

Jeffrey, P.D., Russo, A.A., Polyak, K., Gibbs, E., Hurwitz, J., Massague, J., Pavletich, N.P. (1995) Mechanism of CDK activation revealed by the structure of a cyclinA-CDK2 complex. Nature 376, 313-320.

Jensen, S.A., Reinhardt, D.P., Gibson, M.A., Weiss, A.S. (2001) Protein interaction studies of MAGP-1 with tropoelastin and fibrillin-1. J Biol Chem 276, 39661-39666.

Jeyapalan, J.C., Ferreira, M., Sedivy, J.M., Herbig, U. (2007) Accumulation of senescent cells in mitotic tissue of aging primates. Mech Ageing Dev 128, 36-44.

Jeyapalan, J.C., Sedivy, J.M. (2008) Cellular senescence and organismal aging. Mech Ageing Dev 129, 467-474.

Kadar, A., Tokes, A.M., Kulka, J., Robert, L. (2002) Extracellular matrix components in breast carcinomas. Semin Cancer Biol 12, 243-257.

Kadler, K.E., Holmes, D.F., Trotter, J.A., Chapman, J.A. (1996) Collagen fibril formation. Biochem J 316 (Pt 1), 1-11.

Kadler, K.E., Hill, A., Canty-Laird, E.G. (2008) Collagen fibrillogenesis: fibronectin, integrins, and minor collagens as organizers and nucleators. Curr Opin Cell Biol 20, 495-501.

Kagan, H.M., Williams, M.A., Williamson, P.R., Anderson, J.M. (1984) Influence of sequence and charge on the specificity of lysyl oxidase toward protein and synthetic peptide substrates. J Biol Chem 259, 11203-11207.

Kajita, M., Itoh, Y., Chiba, T., Mori, H., Okada, A., Kinoh, H., Seiki, M. (2001) Membrane-type 1 matrix metalloproteinase cleaves CD44 and promotes cell migration. J Cell Biol 153, 893-904.

Kang, J., Chen, W., Xia, J., Li, Y., Yang, B., Chen, B., Sun, W., Song, X., Xiang, W., Wang, X., Wang, F., Bi, Z., Wan, Y. (2008) Extracellular matrix secreted by senescent fibroblasts induced by UVB promotes cell proliferation in HaCaT cells through PI3K/AKT and ERK signaling pathways. Int J Mol Med 21, 777-784.

Kessler, E., Takahara, K., Biniaminov, L., Brusel, M., Greenspan, D.S. (1996) Bone morphogenetic protein-1: the type I procollagen C-proteinase. Science 271, 360-362.

Kielty, C.M., Sherratt, M.J., Marson, A., Baldock, C. (2005) Fibrillin microfibrils. Adv Protein Chem 70, 405-436.

Kim, Y., Lee, Y.S., Choe, J., Lee, H., Kim, Y.M., Jeoung, D. (2008) CD44-epidermal growth factor receptor interaction mediates hyaluronic acid-promoted cell motility by activating protein kinase C signaling involving Akt, Rac1, Phox, reactive oxygen species, focal adhesion kinase, and MMP-2. J Biol Chem 283, 22513-22528.

Kirkpatrick, K.L., Ogunkolade, W., Elkak, A.E., Bustin, S., Jenkins, P., Ghilchick, M., Newbold, R.F., Mokbel, K. (2003) hTERT expression in human breast cancer and non-cancerous breast tissue: correlation with tumour stage and c-Myc expression. Breast Cancer Res Treat 77, 277-284.

Kozel, B.A., Rongish, B.J., Czirok, A., Zach, J., Little, C.D., Davis, E.C., Knutsen, R.H., Wagenseil, J.E., Levy, M.A., Mecham, R.P. (2006) Elastic fiber formation: a dynamic view of extracellular matrix assembly using timer reporters. J Cell Physiol 207, 87-96.

Kresse, H., Schonherr, E. (2001) Proteoglycans of the extracellular matrix and growth control. J Cell Physiol 189, 266-274.

Krishnamurthy, J., Torrice, C., Ramsey, M.R., Kovalev, G.I., Al-Regaiey, K., Su, L., Sharpless, N.E. (2004) Ink4a/Arf expression is a biomarker of aging. J Clin Invest 114, 1299-1307.

Krishnan, R., Cleary, E.G. (1990) Elastin gene expression in elastotic human breast cancers and epithelial cell lines. Cancer Res 50, 2164-2171.

Krtolica, A., Parrinello, S., Lockett, S., Desprez, P.Y., Campisi, J. (2001) Senescent fibroblasts promote epithelial cell growth and tumorigenesis: a link between cancer and aging. Proc Natl Acad Sci U S A 98, 12072-12077.

Kunz, J. (2007) Matrix metalloproteinases and atherogenesis in dependence of age. Gerontology 53, 63-73.

Kwan, J.A., Schulze, C.J., Wang, W., Leon, H., Sariahmetoglu, M., Sung, M., Sawicka, J., Sims, D.E., Sawicki, G., Schulz, R. (2004) Matrix metalloproteinase-2 (MMP-2) is present in the nucleus of cardiac myocytes and is capable of cleaving poly (ADP-ribose) polymerase (PARP) in vitro. Faseb J 18, 690-692.

Kyriakides, T.R., Wulsin, D., Skokos, E.A., Fleckman, P., Pirrone, A., Shipley, J.M., Senior, R.M., Bornstein, P. (2009) Mice that lack matrix metalloproteinase-9 display delayed wound healing associated with delayed reepithelization and disordered collagen fibrillogenesis. Matrix Biol 28, 65-73.

Labat-Robert, J., Robert, L. (2007) The effect of cell-matrix interactions and aging on the malignant process. Adv Cancer Res 98, 221-259.

Laemmli, U.K. (1970) Cleavage of structural proteins during the assembly of the head of bacteriophage T4. Nature 227, 680-685.

Lamande, S.R., Bateman, J.F. (1999) Procollagen folding and assembly: the role of endoplasmic reticulum enzymes and molecular chaperones. Semin Cell Dev Biol 10, 455-464.

Lang, R., Kocourek, A., Braun, M., Tschesche, H., Huber, R., Bode, W., Maskos, K. (2001) Substrate specificity determinants of human macrophage elastase (MMP-12) based on the 1.1 A crystal structure. J Mol Biol 312, 731-742.

Lapis, K., Timar, J. (2002) Role of elastin-matrix interactions in tumor progression. Semin Cancer Biol 12, 209-217.

Larsen, M., Artym, V.V., Green, J.A., Yamada, K.M. (2006) The matrix reorganized: extracellular matrix remodeling and integrin signaling. Curr Opin Cell Biol 18, 463-471.

Leake, R. (1996) The cell cycle and regulation of cancer cell growth. Ann N Y Acad Sci 784, 252-262.

Lee, B.Y., Han, J.A., Im, J.S., Morrone, A., Johung, K., Goodwin, E.C., Kleijer, W.J., DiMaio, D., Hwang, E.S. (2006) Senescence-associated beta-galactosidase is lysosomal beta-galactosidase. Aging Cell 5, 187-195.

Lee, S., Jilani, S.M., Nikolova, G.V., Carpizo, D., Iruela-Arispe, M.L. (2005) Processing of VEGF-A by matrix metalloproteinases regulates bioavailability and vascular patterning in tumors. J Cell Biol 169, 681-691.

Levi, E., Fridman, R., Miao, H.Q., Ma, Y.S., Yayon, A., Vlodavsky, I. (1996) Matrix metalloproteinase 2 releases active soluble ectodomain of fibroblast growth factor receptor 1. Proc Natl Acad Sci U S A 93, 7069-7074.

Lim, S.C. (2005) CD24 and human carcinoma: tumor biological aspects. Biomed Pharmacother 59 Suppl 2, S351-354.

Liu, B.Y., Kim, Y.C., Leatherberry, V., Cowin, P., Alexander, C.M. (2003a) Mammary gland development requires syndecan-1 to create a beta-catenin/TCF-responsive mammary epithelial subpopulation. Oncogene 22, 9243-9253.

Liu, D., Hornsby, P.J. (2007) Senescent human fibroblasts increase the early growth of xenograft tumors via matrix metalloproteinase secretion. Cancer Res 67, 3117-3126.

Liu, J., Rich, C.B., Buczek-Thomas, J.A., Nugent, M.A., Panchenko, M.P., Foster, J.A. (2003b) Heparin-binding EGF-like growth factor regulates elastin and FGF-2 expression in pulmonary fibroblasts. Am J Physiol Lung Cell Mol Physiol 285, L1106-1115.

Liu, R., Wang, X., Chen, G.Y., Dalerba, P., Gurney, A., Hoey, T., Sherlock, G., Lewicki, J., Shedden, K., Clarke, M.F. (2007) The prognostic role of a gene signature from tumorigenic breast-cancer cells. N Engl J Med 356, 217-226.

Liu, X., Zhao, Y., Gao, J., Pawlyk, B., Starcher, B., Spencer, J.A., Yanagisawa, H., Zuo, J., Li, T. (2004) Elastic fiber homeostasis requires lysyl oxidase-like 1 protein. Nat Genet 36, 178-182.

Lolli, G., Lowe, E.D., Brown, N.R., Johnson, L.N. (2004) The crystal structure of human CDK7 and its protein recognition properties. Structure 12, 2067-2079.

Lories, V., Cassiman, J.J., Van den Berghe, H., David, G. (1992) Differential expression of cell surface heparan sulfate proteoglycans in human mammary epithelial cells and lung fibroblasts. J Biol Chem 267, 1116-1122.

Lucero, H.A., Kagan, H.M. (2006) Lysyl oxidase: an oxidative enzyme and effector of cell function. Cell Mol Life Sci 63, 2304-2316.

Lundin, M., Nordling, S., Lundin, J., Isola, J., Wiksten, J.P., Haglund, C. (2005) Epithelial syndecan-1 expression is associated with stage and grade in colorectal cancer. Oncology 68, 306-313.

Lundmark, C. (1972) Breast cancer and elastosis. Cancer 30, 1195-1201.

Lynch, C.C., Vargo-Gogola, T., Martin, M.D., Fingleton, B., Crawford, H.C., Matrisian, L.M. (2007) Matrix metalloproteinase 7 mediates mammary epithelial cell tumorigenesis through the ErbB4 receptor. Cancer Res 67, 6760-6767.

Ma, Z., Shah, R.C., Chang, M.J., Benveniste, E.N. (2004) Coordination of cell signaling, chromatin remodeling, histone modifications, and regulator recruitment in human matrix metalloproteinase 9 gene transcription. Mol Cell Biol 24, 5496-5509.

Mackay, C.R., Terpe, H.J., Stauder, R., Marston, W.L., Stark, H., Gunthert, U. (1994) Expression and modulation of CD44 variant isoforms in humans. J Cell Biol 124, 71-82.

Maiti, B., Li, J., de Bruin, A., Gordon, F., Timmers, C., Opavsky, R., Patil, K., Tuttle, J., Cleghorn, W., Leone, G. (2005) Cloning and characterization of mouse E2F8, a novel mammalian E2F family member capable of blocking cellular proliferation. J Biol Chem 280, 18211-18220.

Maki, J.M., Sormunen, R., Lippo, S., Kaarteenaho-Wiik, R., Soininen, R., Myllyharju, J. (2005) Lysyl oxidase is essential for normal development and function of the respiratory system and for the integrity of elastic and collagen fibers in various tissues. Am J Pathol 167, 927-936.

Marastoni, S., Ligresti, G., Lorenzon, E., Colombatti, A., Mongiat, M. (2008) Extracellular matrix: a matter of life and death. Connect Tissue Res 49, 203-206.

Marcotte, R., Lacelle, C., Wang, E. (2004) Senescent fibroblasts resist apoptosis by downregulating caspase-3. Mech Ageing Dev 125, 777-783.

Massova, I., Kotra, L.P., Fridman, R., Mobashery, S. (1998) Matrix metalloproteinases: structures, evolution, and diversification. Faseb J 12, 1075-1095.

Matsuda, K., Maruyama, H., Guo, F., Kleeff, J., Itakura, J., Matsumoto, Y., Lander, A.D., Korc, M. (2001) Glypican-1 is overexpressed in human breast cancer and modulates the mitogenic effects of multiple heparin-binding growth factors in breast cancer cells. Cancer Res 61, 5562-5569.

Matsuoka, S., Huang, M., Elledge, S.J. (1998) Linkage of ATM to cell cycle regulation by the Chk2 protein kinase. Science 282, 1893-1897.

Mbeunkui, F., Johann, D.J., Jr. (2009) Cancer and the tumor microenvironment: a review of an essential relationship. Cancer Chemother Pharmacol 63, 571-582.

McCullagh, K.G., Barnard, K., Davies, J.D., Partridge, S.M. (1980) Newly synthesized elastin is associated with neoplastic epithelial cells in human mammary carcinoma. Experientia 36, 1315-1316.

McGuire, J.K., Li, Q., Parks, W.C. (2003) Matrilysin (matrix metalloproteinase-7) mediates E-cadherin ectodomain shedding in injured lung epithelium. Am J Pathol 162, 1831-1843.

McQuibban, G.A., Gong, J.H., Wong, J.P., Wallace, J.L., Clark-Lewis, I., Overall, C.M. (2002) Matrix metalloproteinase processing of monocyte chemoattractant proteins generates CC chemokine receptor antagonists with anti-inflammatory properties in vivo. Blood 100, 1160-1167.

Mecham, R.P., Broekelmann, T., Davis, E.C., Gibson, M.A., Brown-Augsburger, P. (1995) Elastic fibre assembly: macromolecular interactions. Ciba Found Symp 192, 172-181; discussion 181-174.

Mecham, R.P., Broekelmann, T.J., Fliszar, C.J., Shapiro, S.D., Welgus, H.G., Senior, R.M. (1997) Elastin degradation by matrix metalloproteinases. Cleavage site specificity and mechanisms of elastolysis. J Biol Chem 272, 18071-18076.

Mielgo, A., van Driel, M., Bloem, A., Landmann, L., Gunthert, U. (2006) A novel antiapoptotic mechanism based on interference of Fas signaling by CD44 variant isoforms. Cell Death Differ 13, 465-477.

Millis, A.J., Hoyle, M., McCue, H.M., Martini, H. (1992) Differential expression of metalloproteinase and tissue inhibitor of metalloproteinase genes in aged human fibroblasts. Exp Cell Res 201, 373-379.

Mimori, K., Yamashita, K., Ohta, M., Yoshinaga, K., Ishikawa, K., Ishii, H., Utsunomiya, T., Barnard, G.F., Inoue, H., Mori, M. (2004) Coexpression of matrix metalloproteinase-7 (MMP-7) and epidermal growth factor (EGF) receptor in colorectal cancer: an EGF receptor tyrosine kinase inhibitor is effective against MMP-7-expressing cancer cells. Clin Cancer Res 10, 8243-8249.

Mithieux, S.M., Weiss, A.S. (2005) Elastin. Adv Protein Chem 70, 437-461.

Mochizuki, S., Brassart, B., Hinek, A. (2002) Signaling pathways transduced through the elastin receptor facilitate proliferation of arterial smooth muscle cells. J Biol Chem 277, 44854-44863.

Mochizuki, S., Shimoda, M., Shiomi, T., Fujii, Y., Okada, Y. (2004) ADAM28 is activated by MMP-7 (matrilysin-1) and cleaves insulin-like growth factor binding protein-3. Biochem Biophys Res Commun 315, 79-84.

Morgan, D.O. (1995) Principles of CDK regulation. Nature 374, 131-134.

Morgunova, E., Tuuttila, A., Bergmann, U., Isupov, M., Lindqvist, Y., Schneider, G., Tryggvason, K. (1999) Structure of human pro-matrix metalloproteinase-2: activation mechanism revealed. Science 284, 1667-1670.

Murata, Y., Wakoh, T., Uekawa, N., Sugimoto, M., Asai, A., Miyazaki, T., Maruyama, M. (2006) Death-associated protein 3 regulates cellular senescence through oxidative stress response. FEBS Lett 580, 6093-6099.

Myllyharju, J. (2003) Prolyl 4-hydroxylases, the key enzymes of collagen biosynthesis. Matrix Biol 22, 15-24.

Nagase, H., Woessner, J.F., Jr. (1999) Matrix metalloproteinases. J Biol Chem 274, 21491-21494.

Nakamura, M., Miyamoto, S., Maeda, H., Ishii, G., Hasebe, T., Chiba, T., Asaka, M., Ochiai, A. (2005) Matrix metalloproteinase-7 degrades all insulin-like growth factor binding proteins and facilitates insulin-like growth factor bioavailability. Biochem Biophys Res Commun 333, 1011-1016.

Naor, D., Sionov, R.V., Ish-Shalom, D. (1997) CD44: structure, function, and association with the malignant process. Adv Cancer Res 71, 241-319.

Narita, M., Nunez, S., Heard, E., Narita, M., Lin, A.W., Hearn, S.A., Spector, D.L., Hannon, G.J., Lowe, S.W. (2003) Rb-mediated heterochromatin formation and silencing of E2F target genes during cellular senescence. Cell 113, 703-716.

National Center for Biotechnology Information (NCBI), Entrez Protein,
http://www.ncbi.nlm.nih.gov/protein/116861?ordinalpos=1&itool=EntrezSystem2.PEntrez.Sequence.Sequence_ResultsPanel.Sequence_RVDocSum.

Nellaiappan, K., Risitano, A., Liu, G., Nicklas, G., Kagan, H.M. (2000) Fully processed lysyl oxidase catalyst translocates from the extracellular space into nuclei of aortic smooth-muscle cells. J Cell Biochem 79, 576-582.

Neptune, E.R., Frischmeyer, P.A., Arking, D.E., Myers, L., Bunton, T.E., Gayraud, B., Ramirez, F., Sakai, L.Y., Dietz, H.C. (2003) Dysregulation of TGF-beta activation contributes to pathogenesis in Marfan syndrome. Nat Genet 33, 407-411.

Nilsson, I., Hoffmann, I. (2000) Cell cycle regulation by the Cdc25 phosphatase family. Prog Cell Cycle Res 4, 107-114.

Noe, V., Fingleton, B., Jacobs, K., Crawford, H.C., Vermeulen, S., Steelant, W., Bruyneel, E., Matrisian, L.M., Mareel, M. (2001) Release of an invasion promoter E-cadherin fragment by matrilysin and stromelysin-1. J Cell Sci 114, 111-118.

Nonaka, R., Onoue, S., Wachi, H., Sato, F., Urban, Z., Starcher, B.C., Seyama, Y. (2009) DANCE/fibulin-5 promotes elastic fiber formation in a tropoelastin isoform-dependent manner. Clin Biochem.

Ohtani, N., Zebedee, Z., Huot, T.J., Stinson, J.A., Sugimoto, M., Ohashi, Y., Sharrocks, A.D., Peters, G., Hara, E. (2001) Opposing effects of Ets and Id proteins on p16INK4a expression during cellular senescence. Nature 409, 1067-1070.

Oleggini, R., Gastaldo, N., Di Donato, A. (2007) Regulation of elastin promoter by lysyl oxidase and growth factors: cross control of lysyl oxidase on TGF-beta1 effects. Matrix Biol 26, 494-505.

Ongusaha, P.P., Kwak, J.C., Zwible, A.J., Macip, S., Higashiyama, S., Taniguchi, N., Fang, L., Lee, S.W. (2004) HB-EGF is a potent inducer of tumor growth and angiogenesis. Cancer Res 64, 5283-5290.

Ottani, V., Raspanti, M., Ruggeri, A. (2001) Collagen structure and functional implications. Micron 32, 251-260.

Overholtzer, M., Mailleux, A.A., Mouneimne, G., Normand, G., Schnitt, S.J., King, R.W., Cibas, E.S., Brugge, J.S. (2007) A nonapoptotic cell death process, entosis, that occurs by cell-in-cell invasion. Cell 131, 966-979.

Pagano, M. (1997) Cell cycle regulation by the ubiquitin pathway. Faseb J 11, 1067-1075.

Page-McCaw, A., Ewald, A.J., Werb, Z. (2007) Matrix metalloproteinases and the regulation of tissue remodelling. Nat Rev Mol Cell Biol 8, 221-233.

Palamakumbura, A.H., Trackman, P.C. (2002) A fluorometric assay for detection of lysyl oxidase enzyme activity in biological samples. Anal Biochem 300, 245-251.

Palmero, I., Serrano, M. (2001) Induction of senescence by oncogenic Ras. Methods Enzymol 333, 247-256.

Panchenko, M.V., Stetler-Stevenson, W.G., Trubetskoy, O.V., Gacheru, S.N., Kagan, H.M. (1996) Metalloproteinase activity secreted by fibrogenic cells in the processing of prolysyl oxidase. Potential role of procollagen C-proteinase. J Biol Chem 271, 7113-7119.

Parks, W.C., Secrist, H., Wu, L.C., Mecham, R.P. (1988) Developmental regulation of tropoelastin isoforms. J Biol Chem 263, 4416-4423.

Parrinello, S., Coppe, J.P., Krtolica, A., Campisi, J. (2005) Stromal-epithelial interactions in aging and cancer: senescent fibroblasts alter epithelial cell differentiation. J Cell Sci 118, 485-496.

Patterson, C.E., Abrams, W.R., Wolter, N.E., Rosenbloom, J., Davis, E.C. (2005) Developmental regulation and coordinate reexpression of FKBP65 with extracellular matrix proteins

after lung injury suggest a specialized function for this endoplasmic reticulum immunophilin. Cell Stress Chaperones 10, 285-295.

Payne, S.L., Hendrix, M.J., Kirschmann, D.A. (2007) Paradoxical roles for lysyl oxidases in cancer--a prospect. J Cell Biochem 101, 1338-1354.

Pei, D., Weiss, S.J. (1995) Furin-dependent intracellular activation of the human stromelysin-3 zymogen. Nature 375, 244-247.

Pezet, M., Jacob, M.P., Escoubet, B., Gheduzzi, D., Tillet, E., Perret, P., Huber, P., Quaglino, D., Vranckx, R., Li, D.Y., Starcher, B., Boyle, W.A., Mecham, R.P., Faury, G. (2008) Elastin haploinsufficiency induces alternative aging processes in the aorta. Rejuvenation Res 11, 97-112.

Piccard, H., Van den Steen, P.E., Opdenakker, G. (2007) Hemopexin domains as multifunctional liganding modules in matrix metalloproteinases and other proteins. J Leukoc Biol 81, 870-892.

Pines, J. (1994) The cell cycle kinases. Semin Cancer Biol 5, 305-313.

Pochampalli, M.R., el Bejjani, R.M., Schroeder, J.A. (2007) MUC1 is a novel regulator of ErbB1 receptor trafficking. Oncogene 26, 1693-1701.

Ponta, H., Wainwright, D., Herrlich, P. (1998) The CD44 protein family. Int J Biochem Cell Biol 30, 299-305.

Ponti, D., Costa, A., Zaffaroni, N., Pratesi, G., Petrangolini, G., Coradini, D., Pilotti, S., Pierotti, M.A., Daidone, M.G. (2005) Isolation and in vitro propagation of tumorigenic breast cancer cells with stem/progenitor cell properties. Cancer Res 65, 5506-5511.

Ponti, D., Zaffaroni, N., Capelli, C., Daidone, M.G. (2006) Breast cancer stem cells: an overview. Eur J Cancer 42, 1219-1224.

Powell, W.C., Fingleton, B., Wilson, C.L., Boothby, M., Matrisian, L.M. (1999) The metalloproteinase matrilysin proteolytically generates active soluble Fas ligand and potentiates epithelial cell apoptosis. Curr Biol 9, 1441-1447.

Price, L.S., Roos, P.J., Shively, V.P., Sandberg, L.B. (1993) Valyl-alanyl-prolyl-glycine (VAPG) serves as a quantitative marker for human elastins. Matrix 13, 307-311.

Pupa, S.M., Menard, S., Forti, S., Tagliabue, E. (2002) New insights into the role of extracellular matrix during tumor onset and progression. J Cell Physiol 192, 259-267.

Qian, R.Q., Glanville, R.W. (1997) Alignment of fibrillin molecules in elastic microfibrils is defined by transglutaminase-derived cross-links. Biochemistry 36, 15841-15847.

Reinhardt, D.P., Sasaki, T., Dzamba, B.J., Keene, D.R., Chu, M.L., Gohring, W., Timpl, R., Sakai, L.Y. (1996) Fibrillin-1 and fibulin-2 interact and are colocalized in some tissues. J Biol Chem 271, 19489-19496.

Ren, S., Rollins, B.J. (2004) Cyclin C/cdk3 promotes Rb-dependent G0 exit. Cell 117, 239-251.

Rich, C.B., Fontanilla, M.R., Nugent, M., Foster, J.A. (1999) Basic fibroblast growth factor decreases elastin gene transcription through an AP1/cAMP-response element hybrid site in the distal promoter. J Biol Chem 274, 33433-33439.

Ritty, T.M., Broekelmann, T., Tisdale, C., Milewicz, D.M., Mecham, R.P. (1999) Processing of the fibrillin-1 carboxyl-terminal domain. J Biol Chem 274, 8933-8940.

Ritty, T.M., Broekelmann, T.J., Werneck, C.C., Mecham, R.P. (2003) Fibrillin-1 and -2 contain heparin-binding sites important for matrix deposition and that support cell attachment. Biochem J 375, 425-432.

Rock, M.J., Cain, S.A., Freeman, L.J., Morgan, A., Mellody, K., Marson, A., Shuttleworth, C.A., Weiss, A.S., Kielty, C.M. (2004) Molecular basis of elastic fiber formation. Critical interactions and a tropoelastin-fibrillin-1 cross-link. J Biol Chem 279, 23748-23758.

Rodriguez, C., Rodriguez-Sinovas, A., Martinez-Gonzalez, J. (2008) Lysyl oxidase as a potential therapeutic target. Drug News Perspect 21, 218-224.

Romanov, S.R., Kozakiewicz, B.K., Holst, C.R., Stampfer, M.R., Haupt, L.M., Tlsty, T.D. (2001) Normal human mammary epithelial cells spontaneously escape senescence and acquire genomic changes. Nature 409, 633-637.

Rosenbloom, J., Abrams, W.R., Indik, Z., Yeh, H., Ornstein-Goldstein, N., Bashir, M.M. (1995) Structure of the elastin gene. Ciba Found Symp 192, 59-74; discussion 74-80.

Rydziel, S., Delany, A.M., Canalis, E. (2004) AU-rich elements in the collagenase 3 mRNA mediate stabilization of the transcript by cortisol in osteoblasts. J Biol Chem 279, 5397-5404.

Sabatier, L., Chen, D., Fagotto-Kaufmann, C., Hubmacher, D., McKee, M.D., Annis, D.S., Mosher, D.F., Reinhardt, D.P. (2009) Fibrillin assembly requires fibronectin. Mol Biol Cell 20, 846-858.

Saha, P., Eichbaum, Q., Silberman, E.D., Mayer, B.J., Dutta, A. (1997) p21CIP1 and Cdc25A: competition between an inhibitor and an activator of cyclin-dependent kinases. Mol Cell Biol 17, 4338-4345.

Sanchez, Y., Wong, C., Thoma, R.S., Richman, R., Wu, Z., Piwnica-Worms, H., Elledge, S.J. (1997) Conservation of the Chk1 checkpoint pathway in mammals: linkage of DNA damage to Cdk regulation through Cdc25. Science 277, 1497-1501.

Sandhu, C., Donovan, J., Bhattacharya, N., Stampfer, M., Worland, P., Slingerland, J. (2000) Reduction of Cdc25A contributes to cyclin E1-Cdk2 inhibition at senescence in human mammary epithelial cells. Oncogene 19, 5314-5323.

Schabath, H., Runz, S., Joumaa, S., Altevogt, P. (2006) CD24 affects CXCR4 function in pre-B lymphocytes and breast carcinoma cells. J Cell Sci 119, 314-325.

Schagger, H. (2006) Tricine-SDS-PAGE. Nat Protoc 1, 16-22.

Schonherr, E., Hausser, H.J. (2000) Extracellular matrix and cytokines: a functional unit. Dev Immunol 7, 89-101.

Serrano, M., Blasco, M.A. (2001) Putting the stress on senescence. Curr Opin Cell Biol 13, 748-753.

Severino, J., Allen, R.G., Balin, S., Balin, A., Cristofalo, V.J. (2000) Is beta-galactosidase staining a marker of senescence in vitro and in vivo? Exp Cell Res 257, 162-171.

Shay, J.W., Wright, W.E. (2007) Hallmarks of telomeres in ageing research. J Pathol 211, 114-123.

Shelton, D.N., Chang, E., Whittier, P.S., Choi, D., Funk, W.D. (1999) Microarray analysis of replicative senescence. Curr Biol 9, 939-945.

Shen, Q., Rahn, J.J., Zhang, J., Gunasekera, N., Sun, X., Shaw, A.R., Hendzel, M.J., Hoffman, P., Bernier, A., Hugh, J.C. (2008) MUC1 initiates Src-CrkL-Rac1/Cdc42-mediated actin cytoskeletal protrusive motility after ligating intercellular adhesion molecule-1. Mol Cancer Res 6, 555-567.

Sherratt, M.J., Wess, T.J., Baldock, C., Ashworth, J., Purslow, P.P., Shuttleworth, C.A., Kielty, C.M. (2001) Fibrillin-rich microfibrils of the extracellular matrix: ultrastructure and assembly. Micron 32, 185-200.

Sheu, B.C., Hsu, S.M., Ho, H.N., Lien, H.C., Huang, S.C., Lin, R.H. (2001) A novel role of metalloproteinase in cancer-mediated immunosuppression. Cancer Res 61, 237-242.

Shimura, T., Kataoka, H., Ogasawara, N., Kubota, E., Sasaki, M., Tanida, S., Joh, T. (2008) Suppression of proHB-EGF carboxy-terminal fragment nuclear translocation: a new molecular target therapy for gastric cancer. Clin Cancer Res 14, 3956-3965.

Si-Tayeb, K., Monvoisin, A., Mazzocco, C., Lepreux, S., Decossas, M., Cubel, G., Taras, D., Blanc, J.F., Robinson, D.R., Rosenbaum, J. (2006) Matrix metalloproteinase 3 is present in the cell nucleus and is involved in apoptosis. Am J Pathol 169, 1390-1401.

Siegel, R.C. (1974) Biosynthesis of collagen crosslinks: increased activity of purified lysyl oxidase with reconstituted collagen fibrils. Proc Natl Acad Sci U S A 71, 4826-4830.

Singh, R., Bandyopadhyay, D. (2007) MUC1: a target molecule for cancer therapy. Cancer Biol Ther 6, 481-486.

Smith-Mungo, L.I., Kagan, H.M. (1998) Lysyl oxidase: properties, regulation and multiple functions in biology. Matrix Biol 16, 387-398.

Smith, T., Ferreira, L.R., Hebert, C., Norris, K., Sauk, J.J. (1995) Hsp47 and cyclophilin B traverse the endoplasmic reticulum with procollagen into pre-Golgi intermediate vesicles. A role for Hsp47 and cyclophilin B in the export of procollagen from the endoplasmic reticulum. J Biol Chem 270, 18323-18328.

Song, Y.S., Lee, B.Y., Hwang, E.S. (2005) Dinstinct ROS and biochemical profiles in cells undergoing DNA damage-induced senescence and apoptosis. Mech Ageing Dev 126, 580-590.

Soonpaa, M.H., Kim, K.K., Pajak, L., Franklin, M., Field, L.J. (1996) Cardiomyocyte DNA synthesis and binucleation during murine development. Am J Physiol 271, H2183-2189.

Spessotto, P., Cervi, M., Mucignat, M.T., Mungiguerra, G., Sartoretto, I., Doliana, R., Colombatti, A. (2003) beta 1 Integrin-dependent cell adhesion to EMILIN-1 is mediated by the gC1q domain. J Biol Chem 278, 6160-6167.

Sprenger, C.C., Drivdahl, R.H., Woodke, L.B., Eyman, D., Reed, M.J., Carter, W.G., Plymate, S.R. (2008) Senescence-induced alterations of laminin chain expression modulate tumorigenicity of prostate cancer cells. Neoplasia 10, 1350-1361.

Starcher, B., d'Azzo, A., Keller, P.W., Rao, G.K., Nadarajah, D., Hinek, A. (2008) Neuraminidase-1 is required for the normal assembly of elastic fibers. Am J Physiol Lung Cell Mol Physiol 295, L637-647.

Stein, G.H., Drullinger, L.F., Soulard, A., Dulic, V. (1999) Differential roles for cyclin-dependent kinase inhibitors p21 and p16 in the mechanisms of senescence and differentiation in human fibroblasts. Mol Cell Biol 19, 2109-2117.

Sternlicht, M.D., Werb, Z. (2001) How matrix metalloproteinases regulate cell behavior. Annu Rev Cell Dev Biol 17, 463-516.

Strongin, A.Y., Collier, I., Bannikov, G., Marmer, B.L., Grant, G.A., Goldberg, G.I. (1995) Mechanism of cell surface activation of 72-kDa type IV collagenase. Isolation of the activated form of the membrane metalloprotease. J Biol Chem 270, 5331-5338.

Su, G., Blaine, S.A., Qiao, D., Friedl, A. (2007) Shedding of syndecan-1 by stromal fibroblasts stimulates human breast cancer cell proliferation via FGF2 activation. J Biol Chem 282, 14906-14915.

Suske, G. (1999) The Sp-family of transcription factors. Gene 238, 291-300.

Szauter, K.M., Cao, T., Boyd, C.D., Csiszar, K. (2005) Lysyl oxidase in development, aging and pathologies of the skin. Pathol Biol (Paris) 53, 448-456.

Taipale, J., Keski-Oja, J. (1997) Growth factors in the extracellular matrix. Faseb J 11, 51-59.

Takai, H., Smogorzewska, A., de Lange, T. (2003) DNA damage foci at dysfunctional telomeres. Curr Biol 13, 1549-1556.

Tamrakar, S., Rubin, E., Ludlow, J.W. (2000) Role of pRB dephosphorylation in cell cycle regulation. Front Biosci 5, D121-137.

Taylor, W.R., Stark, G.R. (2001) Regulation of the G2/M transition by p53. Oncogene 20, 1803-1815.

Tiedemann, K., Batge, B., Muller, P.K., Reinhardt, D.P. (2001) Interactions of fibrillin-1 with heparin/heparan sulfate, implications for microfibrillar assembly. J Biol Chem 276, 36035-36042.

Timofeev, O., Cizmecioglu, O., Hu, E., Orlik, T., Hoffmann, I. (2009) Human Cdc25A phosphatase has a non-redundant function in G2 phase by activating Cyclin A-dependent kinases. FEBS Lett 583, 841-847.

Timpl, R., Sasaki, T., Kostka, G., Chu, M.L. (2003) Fibulins: a versatile family of extracellular matrix proteins. Nat Rev Mol Cell Biol 4, 479-489.

Tlsty, T.D., Romanov, S.R., Kozakiewicz, B.K., Holst, C.R., Haupt, L.M., Crawford, Y.G. (2001) Loss of chromosomal integrity in human mammary epithelial cells subsequent to escape from senescence. J Mammary Gland Biol Neoplasia 6, 235-243.

Toki, F., Nanba, D., Matsuura, N., Higashiyama, S. (2005) Ectodomain shedding of membrane-anchored heparin-binding EGF like growth factor and subcellular localization of the C-terminal fragment in the cell cycle. J Cell Physiol 202, 839-848.

Toonkool, P., Jensen, S.A., Maxwell, A.L., Weiss, A.S. (2001) Hydrophobic domains of human tropoelastin interact in a context-dependent manner. J Biol Chem 276, 44575-44580.

Trackman, P.C., Zoski, C.G., Kagan, H.M. (1981) Development of a peroxidase-coupled fluorometric assay for lysyl oxidase. Anal Biochem 113, 336-342.

Trask, B.C., Broekelmann, T., Ritty, T.M., Trask, T.M., Tisdale, C., Mecham, R.P. (2001) Posttranslational modifications of microfibril associated glycoprotein-1 (MAGP-1). Biochemistry 40, 4372-4380.

Trask, T.M., Trask, B.C., Ritty, T.M., Abrams, W.R., Rosenbloom, J., Mecham, R.P. (2000) Interaction of tropoelastin with the amino-terminal domains of fibrillin-1 and fibrillin-2 suggests a role for the fibrillins in elastic fiber assembly. J Biol Chem 275, 24400-24406.

Tremblay, G. (1976) Ultrastructure of elastosis in scirrhous carcinoma of the breast. Cancer 37, 307-316.

Tsirpanlis, G. (2008) Cellular senescence, cardiovascular risk, and CKD: a review of established and hypothetical interconnections. Am J Kidney Dis 51, 131-144.

Tsuruga, E., Sato, A., Ueki, T., Nakashima, K., Nakatomi, Y., Ishikawa, H., Yajima, T., Sawa, Y. (2009) Integrin alphavbeta3 regulates microfibril assembly in human periodontal ligament cells. Tissue Cell 41, 85-89.

Van Wart, H.E., Birkedal-Hansen, H. (1990) The cysteine switch: a principle of regulation of metalloproteinase activity with potential applicability to the entire matrix metalloproteinase gene family. Proc Natl Acad Sci U S A 87, 5578-5582.

Vargo-Gogola, T., Crawford, H.C., Fingleton, B., Matrisian, L.M. (2002a) Identification of novel matrix metalloproteinase-7 (matrilysin) cleavage sites in murine and human Fas ligand. Arch Biochem Biophys 408, 155-161.

Vargo-Gogola, T., Fingleton, B., Crawford, H.C., Matrisian, L.M. (2002b) Matrilysin (matrix metalloproteinase-7) selects for apoptosis-resistant mammary cells in vivo. Cancer Res 62, 5559-5563.

Vijayachandra, K., Lee, J., Glick, A.B. (2003) Smad3 regulates senescence and malignant conversion in a mouse multistage skin carcinogenesis model. Cancer Res 63, 3447-3452.

Villacanas, O., Perez, J.J., Rubio-Martinez, J. (2002) Structural analysis of the inhibition of Cdk4 and Cdk6 by p16(INK4a) through molecular dynamics simulations. J Biomol Struct Dyn 20, 347-358.

Vincenti, M.P., Brinckerhoff, C.E. (2007) Signal transduction and cell-type specific regulation of matrix metalloproteinase gene expression: can MMPs be good for you? J Cell Physiol 213, 355-364.

Vojta, P.J., Barrett, J.C. (1995) Genetic analysis of cellular senescence. Biochim Biophys Acta 1242, 29-41.

Vu, T.H., Shipley, J.M., Bergers, G., Berger, J.E., Helms, J.A., Hanahan, D., Shapiro, S.D., Senior, R.M., Werb, Z. (1998) MMP-9/gelatinase B is a key regulator of growth plate angiogenesis and apoptosis of hypertrophic chondrocytes. Cell 93, 411-422.

Wagenseil, J.E., Mecham, R.P. (2007) New insights into elastic fiber assembly. Birth Defects Res C Embryo Today 81, 229-240.

Wang, F., Liu, R., Lee, S.W., Sloss, C.M., Couget, J., Cusack, J.C. (2007) Heparin-binding EGF-like growth factor is an early response gene to chemotherapy and contributes to chemotherapy resistance. Oncogene 26, 2006-2016.

Wang, S.X., Mure, M., Medzihradszky, K.F., Burlingame, A.L., Brown, D.E., Dooley, D.M., Smith, A.J., Kagan, H.M., Klinman, J.P. (1996) A crosslinked cofactor in lysyl oxidase: redox function for amino acid side chains. Science 273, 1078-1084.

Wenger, S.L., Senft, J.R., Sargent, L.M., Bamezai, R., Bairwa, N., Grant, S.G. (2004) Comparison of established cell lines at different passages by karyotype and comparative genomic hybridization. Biosci Rep 24, 631-639.

Wess, T.J., Purslow, P.P., Sherratt, M.J., Ashworth, J., Shuttleworth, C.A., Kielty, C.M. (1998) Calcium determines the supramolecular organization of fibrillin-rich microfibrils. J Cell Biol 141, 829-837.

Wight, T.N., Kinsella, M.G., Qwarnstrom, E.E. (1992) The role of proteoglycans in cell adhesion, migration and proliferation. Curr Opin Cell Biol 4, 793-801.

Willenbrock, F., Murphy, G. (1994) Structure-function relationships in the tissue inhibitors of metalloproteinases. Am J Respir Crit Care Med 150, S165-170.

Williams, G.C. (1957) Pleiotropy, Natural Selection, and the Evolution of Senescence. Evolution 11, 398-411.

Williamson, P.R., Kagan, H.M. (1986) Reaction pathway of bovine aortic lysyl oxidase. J Biol Chem 261, 9477-9482.

Williamson, P.R., Kagan, H.M. (1987) Alpha-proton abstraction and carbanion formation in the mechanism of action of lysyl oxidase. J Biol Chem 262, 8196-8201.

Wilson, C.L., Matrisian, L.M. (1996) Matrilysin: an epithelial matrix metalloproteinase with potentially novel functions. Int J Biochem Cell Biol 28, 123-136.

Wise, S.G., Weiss, A.S. (2009) Tropoelastin. Int J Biochem Cell Biol 41, 494-497.

Woessner, J.F., Jr. (1991) Matrix metalloproteinases and their inhibitors in connective tissue remodeling. Faseb J 5, 2145-2154.

Wu, G., Fan, R.S., Li, W., Srinivas, V., Brattain, M.G. (1998) Regulation of transforming growth factor-beta type II receptor expression in human breast cancer MCF-7 cells by vitamin D3 and its analogues. J Biol Chem 273, 7749-7756.

Xie, G., Cheng, K., Shant, J., Raufman, J.P. (2009) Acetylcholine-induced activation of M3 muscarinic receptors stimulates robust matrix metalloproteinase gene expression in human colon cancer cells. Am J Physiol Gastrointest Liver Physiol 296, G755-763.

Xu, J., Rodriguez, D., Petitclerc, E., Kim, J.J., Hangai, M., Moon, Y.S., Davis, G.E., Brooks, P.C. (2001) Proteolytic exposure of a cryptic site within collagen type IV is required for angiogenesis and tumor growth in vivo. J Cell Biol 154, 1069-1079.

Yan, C., Boyd, D.D. (2007) Regulation of matrix metalloproteinase gene expression. J Cell Physiol 211, 19-26.

Yanagisawa, H., Davis, E.C., Starcher, B.C., Ouchi, T., Yanagisawa, M., Richardson, J.A., Olson, E.N. (2002) Fibulin-5 is an elastin-binding protein essential for elastic fibre development in vivo. Nature 415, 168-171.

Yanagishita, M., Podyma-Inoue, K.A., Yokoyama, M. (2008) Extraction and separation of proteoglycans. Glycoconj J.

Yang, H.Y., Wen, Y.Y., Chen, C.H., Lozano, G., Lee, M.H. (2003) 14-3-3 sigma positively regulates p53 and suppresses tumor growth. Mol Cell Biol 23, 7096-7107.

Yang, N.C., Hu, M.L. (2005) The limitations and validities of senescence associated-beta-galactosidase activity as an aging marker for human foreskin fibroblast Hs68 cells. Exp Gerontol 40, 813-819.

Yaswen, P., Stampfer, M.R. (2002) Molecular changes accompanying senescence and immortalization of cultured human mammary epithelial cells. Int J Biochem Cell Biol 34, 1382-1394.

Ye, S. (2000) Polymorphism in matrix metalloproteinase gene promoters: implication in regulation of gene expression and susceptibility of various diseases. Matrix Biol 19, 623-629.

Yu, Q., Stamenkovic, I. (2000) Cell surface-localized matrix metalloproteinase-9 proteolytically activates TGF-beta and promotes tumor invasion and angiogenesis. Genes Dev 14, 163-176.

Yu, W.H., Woessner, J.F., Jr., McNeish, J.D., Stamenkovic, I. (2002) CD44 anchors the assembly of matrilysin/MMP-7 with heparin-binding epidermal growth factor precursor and ErbB4 and regulates female reproductive organ remodeling. Genes Dev 16, 307-323.

Zanetti, M., Braghetta, P., Sabatelli, P., Mura, I., Doliana, R., Colombatti, A., Volpin, D., Bonaldo, P., Bressan, G.M. (2004) EMILIN-1 deficiency induces elastogenesis and vascular cell defects. Mol Cell Biol 24, 638-650.

Zhang, H., Pan, K.H., Cohen, S.N. (2003) Senescence-specific gene expression fingerprints reveal cell-type-dependent physical clustering of up-regulated chromosomal loci. Proc Natl Acad Sci U S A 100, 3251-3256.

Zhang, Q., Adiseshaiah, P., Reddy, S.P. (2005) Matrix metalloproteinase/epidermal growth factor receptor/mitogen-activated protein kinase signaling regulate fra-1 induction by cigarette smoke in lung epithelial cells. Am J Respir Cell Mol Biol 32, 72-81.

Zhang, Z., Morla, A.O., Vuori, K., Bauer, J.S., Juliano, R.L., Ruoslahti, E. (1993) The alpha v beta 1 integrin functions as a fibronectin receptor but does not support fibronectin matrix assembly and cell migration on fibronectin. J Cell Biol 122, 235-242.

Zhu, Q., Safavi, K.E., Spangberg, L.S. (1998) Integrin expression in human dental pulp cells and their role in cell attachment on extracellular matrix proteins. J Endod 24, 641-644.

Zhu, Y., Spitz, M.R., Lei, L., Mills, G.B., Wu, X. (2001) A single nucleotide polymorphism in the matrix metalloproteinase-1 promoter enhances lung cancer susceptibility. Cancer Res 61, 7825-7829.

8 List of publications

Original contributions:

The differentiation/retrodifferentiation program of human U937 leukemia cells is accompanied by changes of VCP/p97.
Bertram, C., von Neuhoff, N., Skawran, B., Steinemann, D., Schlegelberger, B., Hass, R. (2008)
BMC Cell Biol 9, 12.

MMP-7 is involved in the aging of primary human mammary epithelial cells (HMEC).
Bertram, C., Hass, R. (2008)
Exp Gerontol 43, 209-217.

Matrix metalloproteinase-7 and the 20S proteasome contribute to cellular senescence.
Bertram ,C., Hass, R. (2008)
Sci Signal. 1, pt1.

Cellular senescence of human mammary epithelial cells (HMEC) is associated with an altered MMP-7/HB-EGF signaling and increased formation of elastin-like structures.
Bertram, C., Hass, R.
Submitted

Human breast cancer epithelial cells (HBCEC) derived from long term culture of tumor biopsies exhibit tumor cell-like properties with response to chemotherapeutic agents.
Bertram, C., Hass, R.
Submitted

Reviews:

Cellular responses to reactive oxygen species-induced DNA damage and aging.
Bertram C, Hass R. (2008)
Biol Chem 389, 211-220.

Contributions to congresses:

Poster presentation:

The differentiation/retrodifferentiation program of human U937 leukemia cells is accompanied by changes of VCP/p97. „Receptors, Mediators and Genes" - Meeting of the Signal Transduction Society (STS), Weimar (2006).

MMP-7 is involved in the aging of primary human mammary epithelial cells (HMEC). Summer School „Signaling and Immunity" - Hannover Biomedical Research School (HBRS), Goslar (2008).

Cellular senescence of human mammary epithelial cells is accompanied by an increased elastin formation. „Receptors, Mediators and Genes" - Meeting of the Signal Transduction Society (STS), Weimar (2008).

Oral presentation:

Cellular senescence of U937 leukemia cells compared to normal human mammary epithelial cells. „Receptors, Mediators and Genes" - Meeting of the Signal Transduction Society (STS), Weimar (2007).

Curriculum vitae

Persönliche Daten

Name:	Catharina Bertram
Geburtsdatum:	08. Mai 1982
Geburtsort:	Göttingen

Promotion

seit 01/2007	Medizinische Hochschule Hannover Forschungszentrum Frauenklinik, Biochemie und Tumorbiologie Thema: The matrix metalloproteinase-7 (MMP-7) is involved in cellular senescence of human mammary epithelial cells (HMEC) and induces an increased tropoelastin expression via HB-EGF signal transduction

Berufserfahrung

08-12/2006	Medizinische Hochschule Hannover Institut für Zell- und Molekularpathologie Wissenschaftliche Hilfskraft Fortführung der wissenschaftlichen Arbeit des Diplomprojektes

Studium

10/2001 - 08/2006	Gottfried Wilhelm Leibniz Universität Hannover Studium der Biochemie
02-08/2006	Anfertigung der Diplomarbeit Medizinischen Hochschule Hannover, Arbeitsgruppe Biochemie und Tumorbiologie in Kooperation mit dem Institut für Zell- und Molekularpathologie Thema: Untersuchung des ‚Valosin-containing protein' (VCP) während der Retrodifferenzierung der humanen leukämischen U937 Zelllinie Abschluss: Diplom-Biochemikerin

Schulausbildung

1994-2001	Eichsfeld Gymnasium, Duderstadt, Abitur
1992-1994	Christian-Morgenstern-Schule, Gieboldehausen
1988-1992	Grundschule, Gieboldehausen